
# BRNO UNIVERSITY OF TECHNOLOGY
VYSOKÉ UČENÍ TECHNICKÉ V BRNĚ

## FACULTY OF MECHANICAL ENGINEERING
FAKULTA STROJNÍHO INŽENÝRSTVÍ

## INSTITUTE OF PHYSICAL ENGINEERING
ÚSTAV FYZIKÁLNÍHO INŽENÝRSTVÍ


# EXCHANGE BIAS IN METAMAGNETIC HETEROSTRUCTURES
VÝMĚNNÁ ANIZOTROPIE V METAMAGNETICKÝCH HETEROSTRUKTURÁCH

**MASTER'S THESIS**
DIPLOMOVÁ PRÁCE


**AUTHOR** — **Bc. Oleksii Zadorozhnii**
AUTOR PRÁCE

**SUPERVISOR** — **Ing. Vojtěch Uhlíř, Ph.D.**
VEDOUCÍ PRÁCE



**BRNO 2021**

VYSOKÉ UČENÍ TECHNICKÉ V BRNĚ
FAKULTA STROJNÍHO INŽENÝRSTVÍ

# Zadání diplomové práce

| | |
|---|---|
| Ústav: | Ústav fyzikálního inženýrství |
| Student: | **Bc. Oleksii Zadorozhnii** |
| Studijní program: | Fyzikální inženýrství a nanotechnologie |
| Studijní obor: | bez specializace |
| Vedoucí práce: | **Ing. Vojtěch Uhlíř, Ph.D.** |
| Akademický rok: | 2020/21 |

Ředitel ústavu Vám v souladu se zákonem č.111/1998 o vysokých školách a se Studijním a zkušebním řádem VUT v Brně určuje následující téma diplomové práce:

## Výměnná anizotropie v metamagnetických heterostrukturách

**Stručná charakteristika problematiky úkolu:**

Výměnná anizotropie se vyskytuje na rozhraní antiferomagnetického (AF) a feromagnetického (FM) uspořádání, což je běžně realizováno pomocí kombinace AF a FM tenkých vrstev. Pro objasnění fyzikální podstaty výměnné anizotropie a využití této interakce pro ovládání AF konfigurací v nanoměřítku budou prozkoumány různé přístupy pro vytvoření dobře definovaného rozhraní mezi AF a FM uspořádáním, a to pomocí fázové separace v nanostrukturách a iontovou iradiací metamagnetických vrstev.

**Cíle diplomové práce:**

1. Příprava metamagnetických heterostruktur ve formě AF–FM dvojvrstev.
2. Příprava struktur s laterálně definovanými rozhraními AF a FM.
3. Analýza výměnné anizotropie pomocí magneto–optických měření.

**Seznam doporučené literatury:**

COEY, J. M. D., Magnetism and magnetic materials. Cambridge University Press, Cambridge, (2009).

HELLMAN, F. et al., Interface-induced phenomena in magnetism. Reviews of Modern Physics, vol. 89(2), pp. 025006, DOI: 10.1103/RevModPhys.89.025006, (2017).

MIGLIORINI, A. et al., Spontaneous exchange bias formation driven by a structural phase transition in the antiferromagnetic material. Nature Materials, vol. 17(1), pp. 28-35, DOI: 10.1038/nmat5030, (2018).

Termín odevzdání diplomové práce je stanoven časovým plánem akademického roku 2020/21

V Brně, dne

L. S.

| | |
|---|---|
| prof. RNDr. Tomáš Šikola, CSc.<br>ředitel ústavu | doc. Ing. Jaroslav Katolický, Ph.D.<br>děkan fakulty |

**Abstrakt**

Výměnná anizotropie je zajímavý fyzikální jev vznikající na rozhraní antiferomagnetických (AF) a feromagnetických (FM) materiálů, který již je široce používán v elektronickém průmyslu a magnetickém záznamu. Přestože byl tento jev dlouhou dobu intenzivně studován, jeho přesný mechanizmus zatím nebyl uspokojivě vysvětlen. V této práci je představen přehled studií dokumentujících výměnnou anizotropii v tenkých dvojvrstvách, včetně experimentálních výsledků a teoretických modelů. Experimentální úkoly této diplomové práce zahrnovaly jak výrobu, tak měření různých modelových systémů vykazujících výměnnou anizotropii. Dvojvrstva Fe/FeRh, kde vrstva FeRh prochází fázovou přeměnou z AF fáze na FM fázi při 360 K, poskytuje možnost nastavení parametrů výměnné anizotropie. Dále byly zkoumány účinky výměnné anizotropie a tvarové anizotropie v mikrostrukturách Fe/FeRh. Konečně, přítomnost výměnné anizotropie byla zkoumána mezi FM a AF fází koexistujícími během fázové přeměny v nanodrátech FeRh. Vzorky byly vyrobeny pomocí magnetronového naprašování a elektronové litografie. Všechny prezentované systémy byly analyzovány pomocí magnetooptické Kerrovy mikroskopie. Výměnná anizotropie byla úspěšně nalezena v systému Fe/FeRh, přičemž její velikost byla téměř identická co do rozsahu i orientace s výsledky v literatuře, přestože námi vyrobená dvojvrstva měla horší kvalitu FM-AF rozhraní. Bylo také prokázáno, že v tomto systému existuje tzv. tréninkový efekt (Training effect), což je výrazným důkazem existence výměnné anizotropie. U nanodrátů bylo změřena významná výměnná anizotropie mezi koexistujícími fázemi FM a AF během fázové přeměny.

**Summary**

Exchange bias is an intriguing physical phenomenon occuring at the interface of antiferromagnet (AF) and ferromagnet (FM) materials, which has already been widely applied in electronics and magnetic recording industry. Despite being intensely studied for a long time, the exact mechanism behind it remains an unsettled matter. This work presents an overview of the relevant studies documenting exchange bias in thin film bilayer systems, including both experimental evidence and theoretical models developed. The experimental tasks of this diploma thesis covered both manufacturing and measurement of different exchange bias model systems. An Fe/FeRh bilayer (here the FeRh layer features a phase transition from AF to FM at 360K), provides convenient tunability of the exchange bias. Next, the exchange bias and shape anisotropy effects were investigated in Fe/FeRh microstructures. Lastly, the presence of exchange bias was investigated between the coexisting FM and AF phases in submicron FeRh nanowires. The samples were fabricated using magnetron sputtering and E-beam lithography. All the presented systems were analyzed using Magneto-Optical Kerr Effect microscopy. Exchange bias was successfully found in the Fe/FeRh system nearly identical in magnitude and orientation to the results in literature, having an inferior FM-AF interface quality. Training effect as well as rotational asymmetry were also proven to exist within this system, solidifying the presence of exchange bias. In nanowires, significant exchange bias was measured between the coexisting FM and AF phases during cooling from the FM phase to the AF phase.

**Klíčová slova**
výměnná anizotropie, FeRh, metamagnetický, nanodráty, dvojvrstvy, tenké vrstvy, koexistence fází

**Keywords**
exchange bias, exchange anisotropy, unidirectional anisotropy, training effect, FeRh, metamagnetic, nanowires, bilayers, thin film, magnetism, phase coexistence

ZADOROZHNII, O. *Výměnná anizotropie v metamagnetických heterostrukturách.* Brno: Vysoké učení technické v Brně, Fakulta strojního inženýrství, 2021. 81 s. Vedoucí Ing. Vojtěch Uhlíř, Ph.D.

I proclaim that this work is my own. Where applicable, source material has been properly cited.

Bc. Oleksii Zadorozhnii

I would like to thank the RG 1-14 Nanomagnetism group for the moral and practical support during the making of this thesis. I would like to thank my supervisor, Ing. Vojtěch Uhlíř, Ph.D for hand-on-the-pulse approach to supervision, as well as Ing. Michal Horký, M.Sc. Jon Ander Arregi Uribeetxebarria, Ph.D, Bc. Jan Hajduček, Ing. Michal Staňo, Ph.D, doc. Ing. Jan Čechal, Ph.D and Ing. Tomaš Krajňák for both practical as well as advisory help with the work presented in this thesis. Last but not least I would like to thank my parents which made all of this possible in the first place.
CzechNanoLab project LM2018110 funded by MEYS CR is gratefully acknowledged for the financial support of the measurements/sample fabrication at CEITEC Nano Research Infrastructure.

Bc. Oleksii Zadorozhnii

# Contents

# 1. Introduction

Exchange bias has been one of the cornerstones of modern HDD technology since the 1990's. Despite the widespread applicability and usefulness of this phenomenon, many questions as to the precise nature of the exchange bias remain and have remained unanswered for the past 50 years, attributable to the complexity of this phenomenon.

Exchange bias in its simplest interpretation is an effect which takes place when a Ferromagnet (FM) and an Antiferromagnet (AF) share a common interface. This arrangement, after cooling in an external magnetic field, results in pinning of the FM layer to the AF layer [1]. This means that as the external field is cycled and the hysteresis loop is measured, the loop shifts horizontally from the centre. This shift is utilized in readback heads to make sure that the head magnetisation remains the same even as the stray field produced by magnetic bits changes sign, or to pin one of two FM layers in a spin-valve device.

Despite its practical applications, the precise nature of this phenomenon is still under debate [2]. The consensus reached thus far is that the uncompensated atomic moments of the AF lattice exist due to local imperfections and defects surrounding them. They couple via exchange interactions with the neighbouring FM lattice. At the same time, these AF moments are pinned to the larger AF domain. This means that as we cycle external magnetic, AF remains unaffected, but the entire FM layer gains unidirectional anisotropy due to this exchange coupling, preferring one direction of magnetisation over any other. In turn, we observe shift of the entire hysteresis loop. Even from this rather simple description, one can appreciate the complexity of the process.

The description above serves the purpose of a qualitative explanation, but on a deeper level the topic of exchange bias is plagued by nuance: interfacial roughness [3], [4], [5]; chemical disordering [6], [7],[8],[9]; AF anisotropy [10],[11]; training effect [12], [13], [14]; asymmetric reversal [15], [16], [17]; higher-order anisotropies [18]; to name a few. All those factors influence exchange bias to a certain degree.A number of theories have been developed [19], [20], [21], but they do not fit well for all systems. Things become even more disagreeable on the scale of nanostructures [22].

Useful and not-yet-fully-understood nature of exchange bias makes it a fertile ground for study. We aim to contribute additional experimental information on its behaviour, primarily focusing on Fe/FeRh bilayers, but also on Fe/FeRh microstructures. The reasoning behind microstructures is a possible control of the local magnetic configurations (predictable magnetic domain structures). Exchange bias effects are analyzed through the precise character of magnetisaton reversal measured using a Magneto-Optical Kerr Effect microscope (MOKE). Moreover, the material system used within this thesis, i.e. Fe/FeRh bilayers, has very scarce presence in literature, and provides convenient tunability of the exchange bias close to room temperature as the FeRh layer features a phase transition from AF to FM at 360K.

In this thesis Chapter 2 is dedicated to the introduction of magnetism, including topics relevant for understanding of exchange anisotropy. Chapter 3 provides a wide overview on exchange bias in bilayer systems, including both experimental evidence as well as theoretical models developed. Chapter 4 will briefly mention the techniques used for sample preparation and characterisation, and Chapter 5 will encompass the experiments conducted as set in the goals of this Diploma Thesis. Chapter 6 provides the summary.

# 2. Magnetism

This chapter introduces different electron exchange interactions responsible for magnetic self-ordering in materials, as well as relevant magnetic phenomena in thin films and heterostructures which may influence exchange anisotropy. This will also be useful when describing specific AF exchange coupling. Although no connection has been made between exchange bias and particular mechanism of AF ordering yet, it is worth considering. Moreover, given the nature of exchange anisotropy and its dependence on temperature-varying behaviour of both FM and AF layers, we will also describe Curie and Néel temperatures which are the critical temperatures for Ferromagnetic and Antiferromagnetic ordering of the material, respectively.

## 2.1. Exchange interactions

The long-range ordering of some FM and AF materials can be well described by the theory of electron exchange interactions, independently discovered by Werner Heisenberg and Paul Dirac. This section will provide a brief overview of known exchange interactions, as well as examples of the materials which can be accurately described by them.

Exchange interactions may also play a role in exchange anisotropy, given how much the mechanism of long-range order varies material by material (for example, AF oxides vs. AF metals).

### 2.1.1. Direct exchange

As a first described and most basic exchange interaction, direct exchange occurs between nearest neighbour magnetic atoms, without an intermediary atom [23]. It happens due to an overlap of the electron orbitals and can be either bonding or antibonding in nature (fig. 2.1), depending on the electronic structure of the atom and the lowest energy configuration.

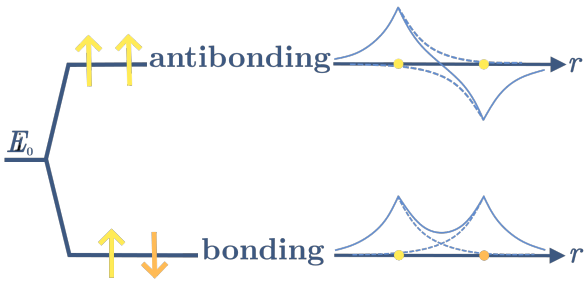


**Figure 2.1:** Molecular electron orbitals for a diatomic molecule. Bonding orbital corresponds to the sum of two atomic orbitals. Antiboding orbital corresponds to the difference of the two atomic oribtals. Taken from [23] and modified.

Direct exchange provides a good description of the interactions between the localized electrons of the same atom. As the direct exchange interaction depends directly on the overlap of the electron orbitals, it cannot explain ferromagnetism in rare earth FMs (Gd) by a direct exchange between the *4f* orbitals. In rare earths, *4f* orbitals are strongly localized, and possess very limited overlap when considering two separate atoms in a

lattice. Even when transition metal FMs are considered (Fe, Co, Ni) which have *3d* orbitals that extend much further, it is very difficult to quantitatively explain the magnetic properties by using the direct exchange interaction model only [23].

### 2.1.2. Indirect exchange

The indirect exchange interaction via a non-magnetic atom (Superexchange) was proposed as one of the possible mechanisms responsible for long-range magnetic order in some materials.

Indirect exchange in ionic solids, such as FeO, NiO, MnO, $FeF_2$, $MnF_2$, is mediated by a non-magnetic ion which is positioned in-between the magnetic atoms. It arises because there is a kinetic energy advantage for an antiferromagnetic arrangement (fig. 2.2). In some very specific cases, ferromagnetic arrangement is preferable [24], but in vast majority of cases the resulting coupling is antiferromagnetic.

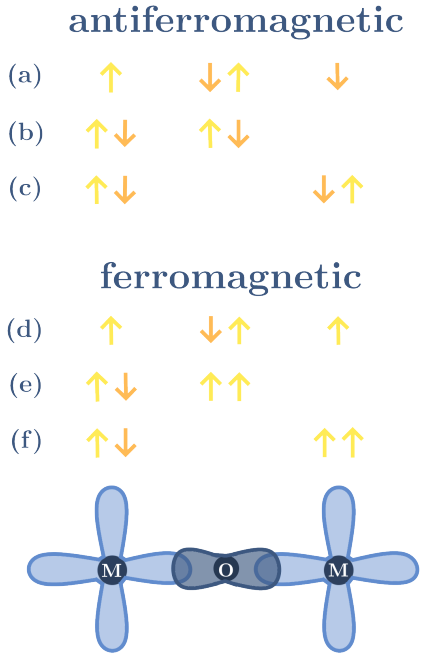


**Figure 2.2:** Superexchange in a magnetic oxide. For antiferromagnetic coupling of the moments (a,b,c), the ground state (a) can mix with excited configurations (b) and (c). For ferromagnetic coupling of the moments (d,e,f), the ground state is (d) and due to the Fermi exclusion principle it cannot mix with configurations (e) and (f). Taken from [23] and modified.

### 2.1.3. RKKY exchange

Another form of indirect exchange was specifically proposed to explain the ferromagnetism of metals. This kind of indirect exchange interaction could explain long-range ordering without the need for direct or mediatory orbital overlap, proposing conduction electrons as the messengers instead.

Indirect exchange in metals occurs by the spin-polarized conduction electrons [23]. Localized magnetic moment can spin-polarize the delocalized conduction electron, and this

spin-polarized electron can then interact with a neighbouring localized magnetic moment at some distance. This interaction is also known as RKKY interaction (Ruderman, Kittel, Kasuya and Yosida), or alternatively as the itinerant exchange.

This interaction is long range and has an oscillatory dependence on the distance between the magnetic moments within the lattice. Depending on the separation between the atoms, it may either be ferromagnetic or antiferromagnetic in nature. This model works particularly well in systems where both localized and delocalized electrons contribute to the overall self-ordering behaviour (for example, rare-earth ferromagnets).

### 2.1.4. Double exchange

For some oxides, ferromagnetic exchange interaction can occur due to magnetic ion having mixed valency, existing in more than one oxidation state [23]. Examples of this include compounds with $Mn^{3+}$ and $Mn^{4+}$ ions, as well as $Fe^{2+}$ and $Fe^{3+}$ (in $Fe_3O_4$).

This interaction provides ferromagnetic coupling between these mixed valency ions, and favours electron transfer only if the neighbouring ions are ferromagnetically aligned (fig. 2.3).

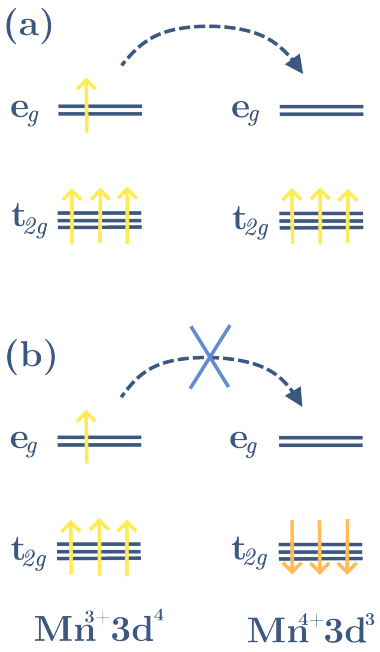


**Figure 2.3:** Double exchange mechanism for a system containing $Mn_{3+}$ and $Mn_{4+}$ ions. The electron hopping is favourable if the neighbouring atoms are ferromagnetically aligned (a) and not favoured for antiferromagnetically aligned (b). Taken from [23] and modified.

### 2.1.5. Anisotropic exchange

Anisotropic exchange interaction can also play a similar role to that of the oxygen atom in the super exchange interaction [23]. The excited state in this case is not connected to oxygen but is produced by the spin-orbit interaction in one of the magnetic ions. Exchange interaction is then established between the excited state of one ion and the ground state of the other ion. It is known as the anisotropic exchange interaction, or alternatively as the Dzyaloshinskij-Moriya interaction.

This effect occurs commonly in antiferromagnets, and then results in a small ferromagnetic component of the moments produced perpendicular to the spin-axis of the antiferromagnet, which is known as weak ferromagnetism. This kind of exchange interaction could play a role in exchange-biased bilayer systems, given how the FM is directly coupled to the AF spins, this weak ferromagnetism could potentially provide an additional mechanism by which FM and AF materials may couple to one another.

### 2.1.6. Stoner model

The Stoner model provides a good explanation for self-ordering behaviour in materials where magnetic long-range ordering is mediated primarily via delocalized electrons (for example Fe, Co, Ni ferromagnets).

In an applied field, density of states shifts depending on applied field orientation in what is described as Pauli paramagnetism (fig. 2.4a). The susceptibility increases with the density of states at the Fermi level [25] and when the susceptibility is high enough, it becomes energetically favourable for the bands to spontaneously split (fig. 2.4b), leading to an imbalance of spin-up and spin-down electrons, thus resulting in ferromagnetism.

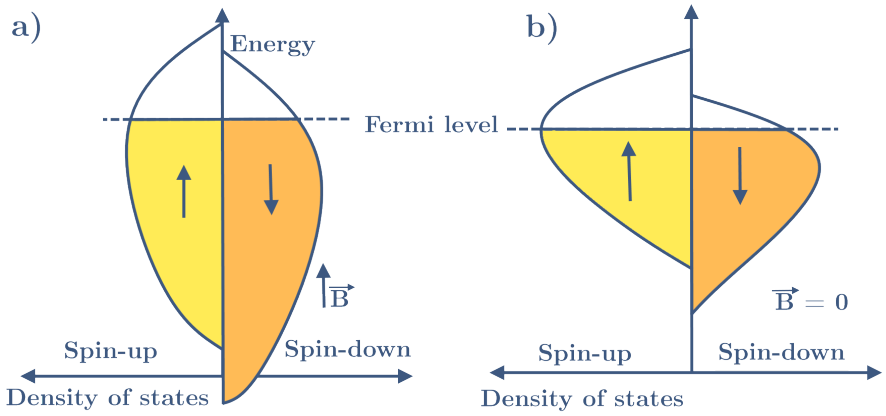


**Figure 2.4:** a) Density of states for a paramagnet in an applied magnetic field; b) density of states for a ferromagnet in an applied magnetic field. Inspired by [25].

Following this principle, Edmund Clifton Stoner derived a model based on Weiss mean field theory, which he applied to the free electron gas within the metal. He derived an expression for susceptibility assuming that the internal magnetic field varied linearly with a coefficient $n_S$:

$$\chi = M/H = \chi_{\mathrm{P}}/(1 - n_{\mathrm{S}}\chi_{\mathrm{P}}); \tag{2.1}$$

This susceptibility is enhanced when $n_{\mathrm{S}}\chi_{\mathrm{P}} < 1$, and diverges as $n_{\mathrm{S}}\chi_{\mathrm{P}}$ approaches 1. Stoner described this condition in terms of the local density of states at the Fermi level [25], from which he derived that the material becomes spontaneously ferromagnetic when the susceptibility diverges. This is known as the Stoner criterion:

$$IN_{\uparrow\downarrow}(\epsilon_{\mathrm{F}}) > 1, \tag{2.2}$$

where $N$ is the density of states per atom for each spin state, and $I$ is the so-called Stoner exchange parameter, being roughly 1 eV for $3d$ ferromagnets and $n_S$ being greater

than $10^3$ for spontaneous band splitting. For ferromagnetism to occur, the exchange parameter must be of comparable magnitude to the bandwidth. Ferromagnetic materials, in general have narrow bands, with a peak of density of states at or near the Fermi energy.

This theory, while not explicitly describing exchange interactions between localized electrons, provides a robust theoretical picture of delocalized (itinerant) ferromagnetism.

## 2.2. Temperature dependence

In this section temperature dependence of both FM and AF materials will be described, as both possess a critical temperature beyond which the self-ordering is suppressed, and this temperature plays a pivotal role in exchange anisotropy: once the system is heated above the ordering temperature of the AF, the exchange anisotropy is destroyed.

### 2.2.1. Curie temperature

Ferromagnetic order can be described by the Weiss model of a ferromagnet [23]. From the point of view of this model, FM is merely a paramagnet which has some intrinsic molecular field present within, which is responsible for the self-ordering within the material. At low temperatures, this molecular field can arrange the magnetic moments even if there is no external field present, and this alignment gives rise to the molecular field in the first place, "chicken-and-egg" style.

As the temperature is gradually raised, the previously self-sustaining magnetic order is gradually disturbed by thermal fluctuations, and at a critical temperature, this self-ordering is destroyed, the system now being paramagnetic (fig. 2.5). This critical temperature is known as the Curie temperature $T_C$.

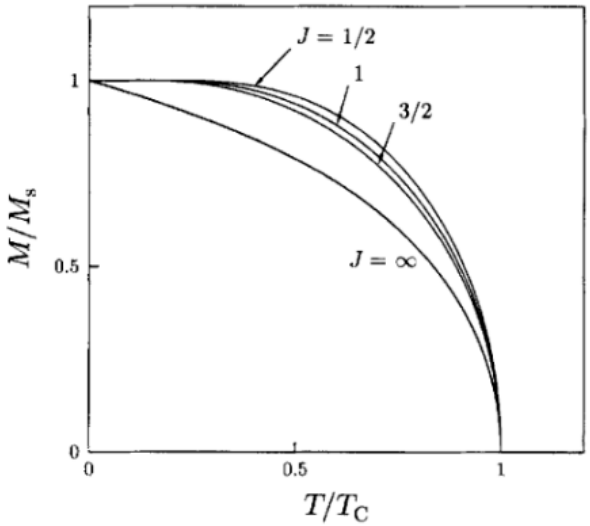


**Figure 2.5:** Mean-field magnetization as a function of temperature, for different values of the exchange constant $J$. Taken from [23].

### 2.2.2. Néel temperature

Antiferromagnetic order can be described by the Weiss model of an antiferromagnet [23], however in this case the molecular field, due to the exchange constant $J$ being less than zero, prefers to orient neighbouring atomic moments antiparallel. This antiparallel arrangement can be conceptually separated into 2 sublattices with 2 opposite magnetic moment configurations. Then, molecular field of each sublattice follows the same form as shown in fig. 2.5, and will disappear for temperatures above a transition temperature, which is known as the Néel temperature $T_{\mathrm{N}}$. If the coupling between sublattices varies with temperature at different rates for each sublattice, then the material is called a ferrimagnet. Despite having antiferromagnetic ordering, it presents a net magnetic moment.

## 2.3. Magnetism of thin films

Magnetic properties of FM-AF thin film bilayers, specifically the exchange anisotropy in those bilayers, is critically linked to the parameters and structural characteristics of the FM and AF films, including the growth conditions. The following section will specifically adress their impact on anisotropic behaviour of thin films.

### 2.3.1. Magnetic energies

The processes which govern the behaviour within a magnetic medium can be well described by continuous vector field approximation. The behaviour within the magnetic medium can be accurately described based on the sum of four basic energies [26]:

$$E_Z = -\mu_0 \mathbf{M} \cdot \mathbf{H}; \tag{2.3}$$

$$E_{ex} = A(\nabla \mathbf{m})^2; \tag{2.4}$$

$$E_a = K f(\theta, \phi); \tag{2.5}$$

$$E_d = -\frac{1}{2}\mu_0 \mathbf{M} \cdot \mathbf{H_d}. \tag{2.6}$$

$E_Z$ is known as the Zeeman Energy, which describes the energy relation between the sample's magnetization and applied field.

$E_{ex}$ is the exchange energy, with $A$ being the exchange stiffness, responsible for the alignment of neighbouring magnetic moments in the same direction.

$E_a$ is the anisotropic energy, with $K$ being the anisotropic constant and $f(\theta, \phi)$ describing the function of angle between the magnetisation and the easy axis (see section 2.3.2. For a uniaxial anisotropy, for example, this function would be equal to $\sin^2(\theta)$.

$E_d$ is the dipolar energy (also known as magnetostatic energy), which describes the energy relation between the magnetization and the stray field.

These energies provide a framework using which micromagnetic textures, such as domain walls as well as domains themselves can be described.

### 2.3.2. Magnetic anisotropies

Magnetic anisotropy (Magnetocrystalline anisotropy) is associated with a tendency of the sample's magnetization to lie along certain crystallographic axes (fig. 2.6), dubbed "easy axes" [25]. On the other hand, there also exist axes along which the material's magnetization does not want to orient, known as "hard axes". This property is rooted in the crystal-field interaction, as well as the spin-orbit coupling. For a simple case of uniaxially anisotropic ferromagnet, this kind of behaviour can be described by the anisotropic energy (eq. 2.5), with $f(\theta, \phi)$ behaving as a $sin^2(\theta)$ function. It is an intrinsic property of the material.

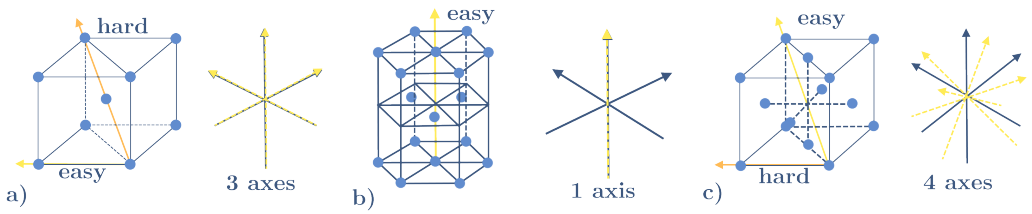


**Figure 2.6:** Examples of a) triaxial b) uniaxial and c) quadaxial magnetocrystalline anisotropies.

Shape anisotropy is related to the stray field dependence on the shape of the ferromagnet [25]. Long, 1D-like structures will gain an easy axis along the structure length (fig. 2.7c), as this orientation of magnetization results in the least amount of stray field. Containing the magnetic flux within the sample, as opposed to projecting it out in the form of a stray field, is, generally a less energetically taxing configuration. Likewise, for 2D-like thin films, with the exception of ultra thin films, the anisotropic easy axes (both shape and magnetic) tend to lie in-plane (fig. 2.7b). It is an extrinsic property.

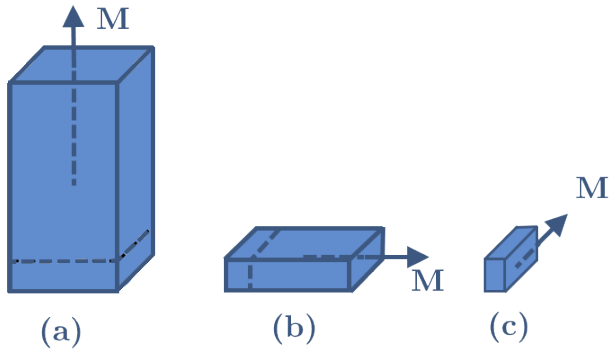


**Figure 2.7:** Examples of a) cubic element shape b) thin film shape and c) needle shape anisotropies.

Induced anisotropy occurs when anisotropic axes (easy and hard) are created by stressing the system. It can be done by magnetic thin film deposition in an applied field, annealing of disordered magnetic alloys, or epitaxial growth of strained or stressed magnetic thin films [25]. This kind of anisotropy depending on stability of such a material can be considered either intrinsic or extrinsic.

Typical anisotropic effects in thin films when compared to their bulk counterparts can differ significantly, and most often the factor that plays the main role is the strain and

epitaxy induced by the substrate [25]. As an example, in 3*d* metal thin films, separation between each surface-parallel plane tends to be slightly greater than in the bulk [25]. Additionally, surface atoms, lacking nearest neighbours, can also obtain perpendicular anisotropy even if the deeper part of the film is oriented in-plane [25].

### 2.3.3. Magnetic domains

The magnetization of most ferromagnets tends to break-up into magnetic domains (fig. 2.8). Magnetic domains are the areas of homogeneous magnetization within a larger sample [25]. These domains are formed with the sole purpose of minimizing the magnetostatic energy (eq. 2.3), and as a consequence, the stray field of the sample. In this process, a domain wall has to be formed (fig. 2.9), which costs both volume and energy.

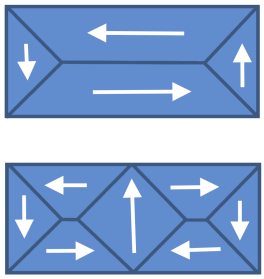

**Figure 2.8:** Examples of Landau magnetic domain patterns.

This energy (exchange energy, eq. 2.4) dictates how thick a domain wall has to be to accommodate the change of magnetization direction between two domains. For a system with high exchange energy, it means that magnetization direction change between two domains has to be more gradual, as the coupling between neighbouring magnetic moments is quite strong, resulting in a thick domain wall [27].

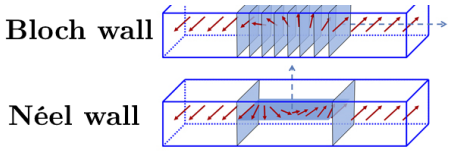


**Figure 2.9:** Examples of domain walls.

Domain formation is a complex process, involving exchange, magnetostatic and anisotropic energies. Generally, magnetic anisotropy decreases the domain wall thickness, as the magnetization is changing between two easy magnetocrystalline directions [27].

## 2.4. Magnetism of heterosystems

Beyond simple model geometries, specific surface, interface, and epitaxial effects in layered magnetic systems influences magnetic coupling in bilayers, including the exchange anisotropy. In this section, we cover a variety of ways how two magnetic films may couple to one another.

### 2.4.1. Magnetostatic coupling

The simplest form of interlayer coupling, magnetostatic coupling, is the interaction between layers which is transferred via the stray magnetic field [28]. This kind of coupling was extensively studied back when the preparation of atomically clean interfaces was not possible. The coupling can be either parallel or antiparallel depending on how the magnetisations of each film align with respect to one another (fig. 2.10).

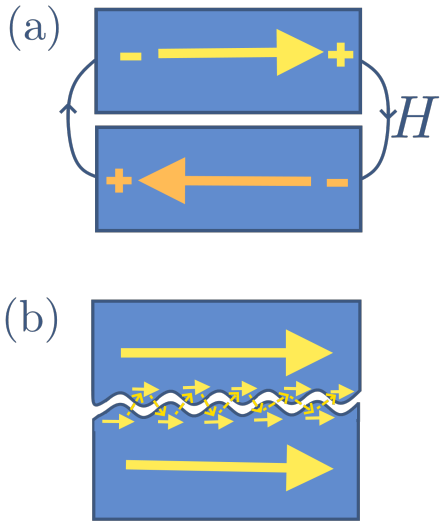


**Figure 2.10:** a) antiparallel and b) parallel magnetostatic coupling. Taken from [28] and modified.

Antiparallel coupling is due to stray fields at the edges of the film (fig. 2.10). It is especially significant in single domain films. Parallel coupling is induced by surface roughness as shown on fig. 2.10b. It is referred to as the Néel or orange peel coupling. It is caused by stray fields occuring at the rough interface [28]. This kind of coupling in nanoscale thin film systems is difficult to discern from quantum-mechanical exchange coupling which could occur due "pinholes" in the interface layer caused by a direct contact between the magnetic materials [28].

With the advent of atomic characterization and clean crystalline surfaces, it became possible to define the system more precisely. This spurred a new field of research related to atomically near-perfect magnetic multilayers. These magnetic layers in direct contact with one another exhibit direct coupling via exchange interactions.

### 2.4.2. Direct coupling

The simplest case of a directly coupled system is the surface layer of a bulk ferromagnet. Due to the changing boundary conditions, as we approach the surface of a bulk magnet, its values of magnetisation and magnetic anisotropy change (fig. 2.11). Moreover, saturation magnetisation also has a different temperature dependence. The surface effects can change magnetic interaction and anisotropy values strongly, leading to, for example, a different ordering (Néel or Curie) temperature at the surface compared to the bulk, or maybe antiferromagnetic order at the surface as opposed to bulk ferromagnetic order [28]. Surface effects can play a significant role in the magnetism of the material.

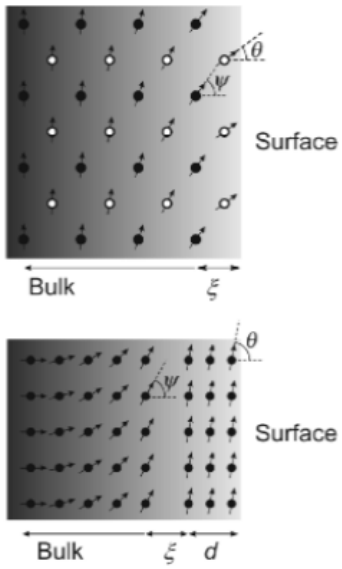


**Figure 2.11:** The upper picture represents an Fe(100) surface. The lower picture applies to $3d$-$4f$ alloys, such as FeTb, with surface level being mostly Fe due to the oxidation of Tb. Taken from [28]

Exchange coupling weakens in a perpendicular direction to the surface, as the lattice parameter expands in that direction near the surface [28]. Thus, surface magnetic anisotropy constant can be very different from the bulk anisotropy constant, being much stronger than bulk anisotropy and usually promoting a different easy-axis direction (fig. 2.11). The reason for this is related to the orbital moment not being quenched (angular momentum of an electron remains with the value of one of the electron spin instead of cancelling out; due to not having enough nearest neighbours) at the surface.

### 2.4.3. Indirect coupling

Another form of interlayer coupling is mediated through a non-magnetic spacer between two ferromagnetic layers, and is oscillatory in nature, varying between parallel and antiparallel as a function of the non-magnetic spacer thickness [28]. This indirect coupling is mediated via the RKKY exchange interaction. The periodicity of this coupling is correlated with standing electron waves, referred to as quantum well states in the non-magnetic interlayer (fig. 2.12).

An analogy can be drawn between a standing electromagnetic wave confined by two reflecting surfaces, commonly known as a Fabry-Perot interferometer, and an electron

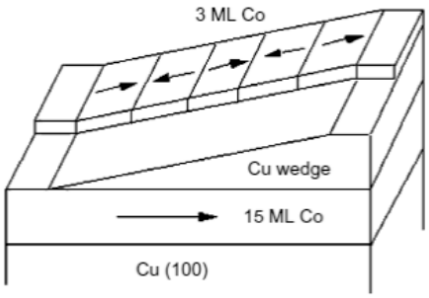


**Figure 2.12:** Indirect, thickness-dependent oscillatory interlayer coupling mediated by standing electron waves. Taken from [28]

captured in a square potential well which is the non-magnetic spacer [28]. Spin-dependent band gaps at the boundaries of this non-magnetic layer (due to ferromagnetic layers) generate a potential well that confines only one specific spin state of the electrons.

In contrast to optical Fabry-Perot interferometer, electrons are strongly absorbed by the medium and the reflection is not as perfect as for an optical system [28]. However, it was experimentally confirmed that standing waves do exist for one spin state, using spin-polarized electron spectroscopy. Based on this principle, one can create a system analogous to an optical interferometer by placing a non-magnetic metallic spacer between the two ferromagnetic layers. Since it is an interferometer-like device (due to spin-dependent band gaps at the interfaces), the coupling can be either parallel or antiparallel depending on the spacer thickness [28].

The Giant Magnetoresistance (GMR) effect is also based on such a system with intermediary non-magnetic spacer layer, where this spin-polarizing effect of both ferromagnetic layers is used to vary the electrical resistance of the structure. The system is in a low resistance state for the parallel magnetization in both layers, and in a high resistance state for the opposite magnetization of both layers.

# 3. Exchange bias

This section is dedicated to exchange anisotropy, and includes an extensive literature search on the topic. First, experimental characteristics will be covered in detail, both providing insight into how we can observe exchange anisotropy as well as to what happens in an exchange biased system. Next, we cover the models proposed for exchange anisotropy, progressively from the least to most descriptive and accurate.

## 3.1. Experimental evidence

This section is dedicated to experimental evidence and registered behaviours of exchange biased systems. It begins with the main characteristic features, namely the unidirectional and rotational anisotropies, and covers all the significant features of an exchange biased AF-FM bilayer system. This section should help to both identify a system subject to unidirectional anisotropy as well as to show how this unidirectional anisotropy is generally influenced by varying parameters such as surface roughness, spin configuration and crystallinity, to name a few.

### 3.1.1. Unidirectional & rotational anisotropies

The first and foremost property of an exchange biased system is the unidirectional anisotropy, which is also accompanied by rotational anisotropy. In this part, I covered a selection of experiments studying this property in different systems.

First experimental evidence of exchange bias as an induced anisotropic effect came from the article written by W.H. Meiklejohn and C.P. Bean [1], in which they studied a system of ferromagnetic Co nanoparticles coated by antiferromagnetic CoO shells. They measured unidirectional anisotropy after cooling the particles in an applied magnetic field from above the Néel temperature of CoO down to a cryogenic temperature before measuring an exchange biased hysteresis loop (fig. 3.1).

From the measurement of the magnetization vs applied field, they concluded that the anisotropy of this system was proportional to $\sin(\theta)$ instead of $\sin(2\theta)$, thus displaying the unidirectionality. They also carried out a measurement of the energy of rotation of oxide-covered Co nanoparticles, and obtained the energy values as a function of applied field angle (fig. 3.2).

Two years later in 1958, in a follow-up experiment [29] W.H. Meiklejohn and C.P. Bean also measured Fe/FeO nanoparticles, in which Fe was the ferromagnetic core and FeO was the antiferromagnetic shell. They showed another property of an exchange biased system, namely the rotational hysteresis.

Normally, in systems not subject to exchange anisotropy this rotational hysteresis is only present for intermediate fields (fig. 3.3a), disappearing at very low applied fields (because then the magnetization becomes reversible) and at very high fields (applied field overpowers the magnetic anisotropy). However, for an exchange biased system, with an application of strong magnetic field the value of rotational hysteresis does not vanish and remains constant (fig. 3.3b).

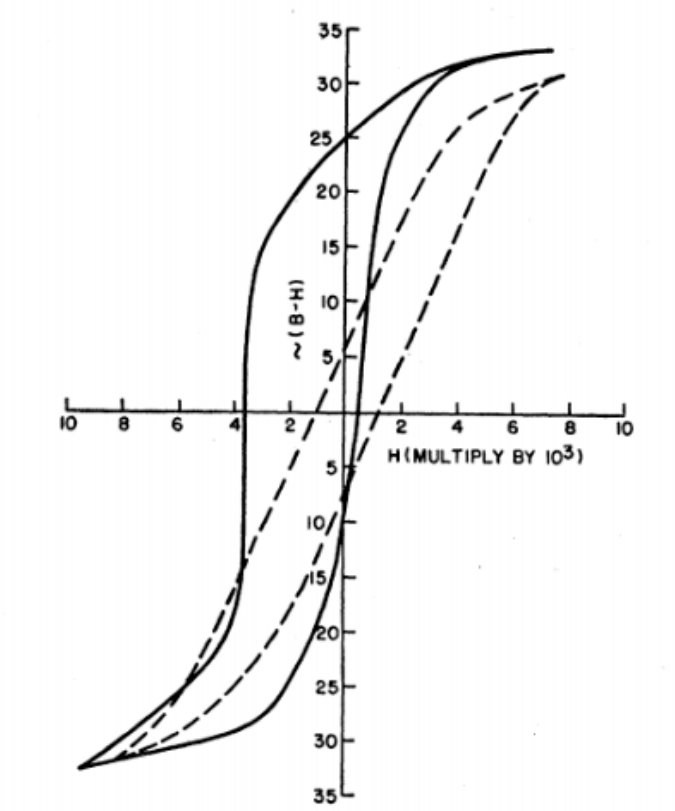


**Figure 3.1:** Hysteresis loop of oxide-covered Co nanoparticles. Dashed line represents nanoparticles which were cooled below the Né without an applied field, solid line represents the hysteresis loop for a material cooled in an applied magnetic field. Taken from [1].

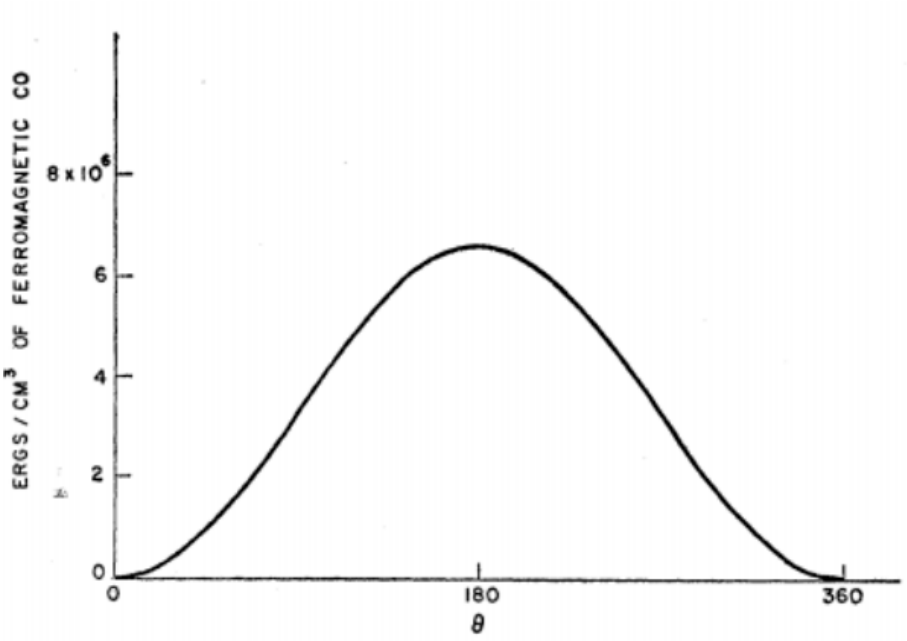


**Figure 3.2:** Energy of rotation of Co/CoO nanoparticles in a saturating magnetic field. Taken from [1].

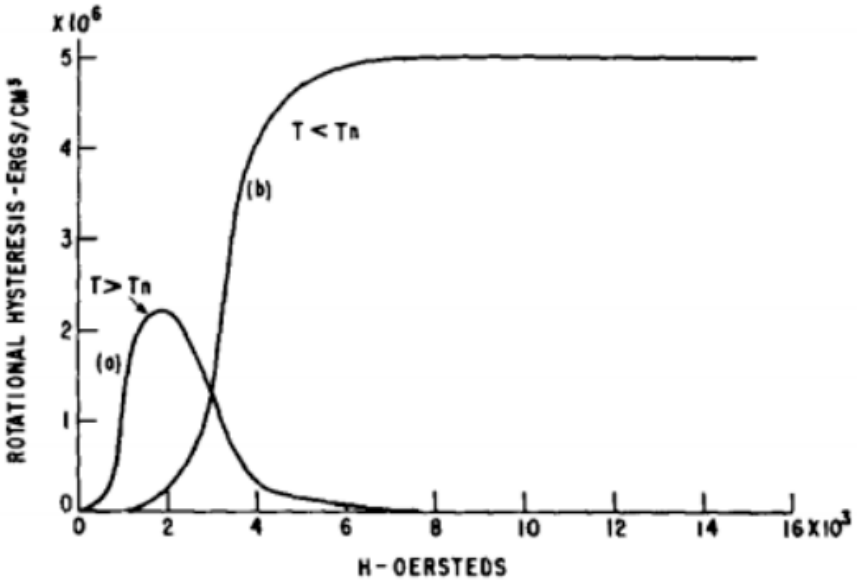


**Figure 3.3:** Rotational hysteresis of 20 nm Co particles with a CoO shell. Curve a) was taken at 300K and curve b) was taken at 77K. Taken from [1].

The data measured for Fe/FeO nanoparticles exhibited similar behaviour (fig. 3.4).

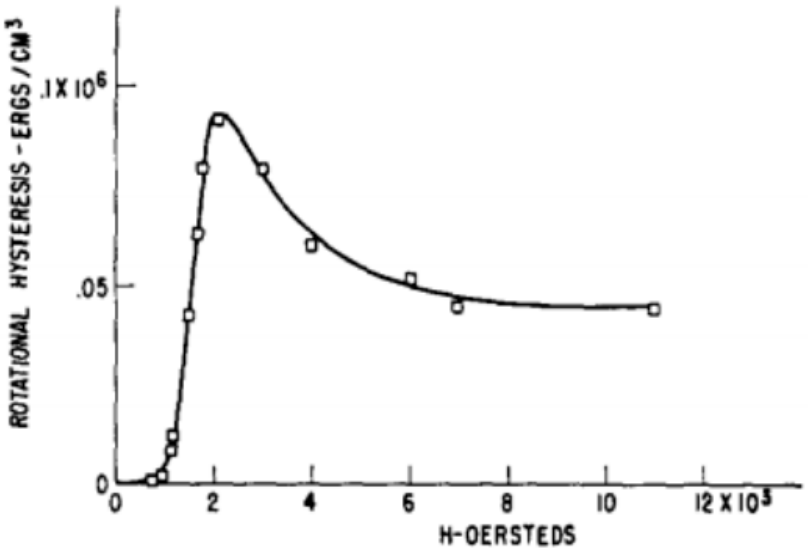


**Figure 3.4:** Rotational hysteresis of 20 nm Fe particles with an FeO shell. The curve was taken at 77K. Taken from [29].

In another measurement they wanted to verify how rotational anisotropy varied with increasing temperature. As expected, the rotational hysteresis vanished at Néel temperatures of both Co/CoO and Fe/FeO nanoparticle systems (FM-AF coupling ceases once the AF is heated above its ordering temperature) (fig. 3.5).

Following the discovery of exchange anisotropy in FM/AF nanoparticles, an entire wave of research into exchange bias was launched, which strangely enough took the turn for disordered metallic alloys. The reason for it was that in these disordered alloys ferro-

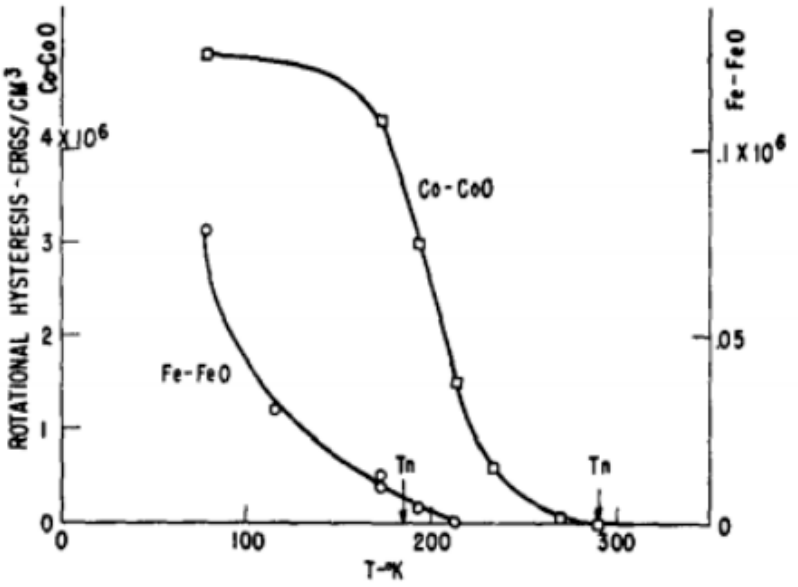


**Figure 3.5:** Rotational hysteresis versus temperature of Fe particles with an FeO shell. Taken from [29].

magnetic and antiferromagnetic phases could coexist at certain temperatures and chemical compositions, resulting in a measurable exchange biasing of the ferromagnetic parts of the alloys. Besides, ordered variants of these alloys had already been under active investigation at the time as potential strong ferromagnets.

To begin with, in 1959 J.S. Kouvel and C.D. Graham, Jr. [30] studied the $Ni_{0.7}Mn_{0.3}$ disordered polycrystalline alloy. They confirmed the qualitative description of unidirectional anisotropy from the measurements in the same direction in which field cooling was performed. In the same vein, research done on CoMn [31] and FeAl [32] as well as CuMn and AgMn [33] disordered alloys showed a near-identical mechanism.

After a brief period of study of disordered alloys, the focus finally shifted to thin films, in many respects thanks to the developments in surface-sensitive characterization and fabrication techniques. Among the first such experiments measuring exchange bias in thin film bilayers was a paper presented in 1979 by a Japanese crew [34] in which they prepared by evaporation the Co(FM)-CoO(AF) thin film bilayers.

In their systematic study, they discovered that before oxidation, only uniaxial anisotropy was present, the behaviour of which varied as a $\sin(2\theta)$ with the amplitude increasing as the temperature decreased. Unidirectional anisotropy was not present. After oxidation, uniaxial anisotropy varying as $\sin(2\theta)$ behaved in the same manner, but additionally there now was a unidirectional anisotropy present, varying as $\sin(\theta)$. It appeared only after the temperature had gone below the so called blocking temperature, and the magnitude of the loop shift increased with decreasing temperature [34].

This nearly identical behaviour had also been observed in oxidized NiFe [35] thin films. The only difference present is that in some systems the exchange bias increased more rapidly with decreasing temperature, whereas in others it did so less rapidly. In all cases a peak of coercivity near the temperature at which loop shift vanishes was observed.

As mentioned, thanks to the development of thin film technology, the next logical step was the study of properly layered systems. NiO/NiFe grown on MgO by R.P. Michel

and A. Chaiken et al. [36] showed the anisotropic behaviour like that of surface oxidized Cobalt and Nickel films, namely that besides the unidirectional anisotropy, the uniaxial anisotropy is also present. Next, J. Nogués, D. Lederman, T.J. Moran and Ivan K. Schuller did work on $FeF_2$/Fe bilayers grown on MgO [37]. The behaviour was like previously mentioned systems, with the most major difference being that the blocking temperature of $FeF_2$ thin film was remarkably close to the Néel temperature.

During the 1990's, a demand for new spintronic devices spurred a new direction for research related to exchange bias, namely bilayers with antiferromagnetic conductors, as opposed to insulating oxides. Full conductivity of multilayer stacks is an important quality for functional spin-valves [38]. In a paper studying NiFe/IrMn exchange bias coupling [39], the conclusions regarding unidirectionality and uniaxiality were identical to [34]. Same conclusions were drawn by the article investigating NiFe/NiMn and NiFe/IrMn systems [40]. In the article on epitaxial Fe/MnPd system [41] additionally to unidirectional and uniaxial anisotropies, strong cubic anisotropy was present as well.

Main properties of exchange bias (namely unidirectional anisotropy) are nearly universal across all kinds of exchange coupled FM-AF systems, be it nanoparticles, disordered FM-AF alloys, oxidized films or epitaxial bilayers. There is, however, some evidence that in some systems [41] higher order anisotropies can occur as well.

### 3.1.2. Magnetization reversal asymmetry

Another important feature of an exchange biased system is the asymmetric magnetization reversal. Under normal circumstances, as the hysteresis loop of a ferromagnet is measured, the magnetization switches symmetrically by either domain nucleation or by coherent rotation. When it is exchange biased, however, in the opposition to the cooling field direction it is preferential to nucleate a ferromagnetic domain and then expand it, rather than force the magnetization to rotate against the unidirectional anisotropy.

In the article [42] on magnetisation reversal asymmetry in Co/CoO bilayers, they saw purely rotational behaviour in an exchange unbiased state, where the magnetization direction was changed via rotation (in an applied field). In exchange biased state, this mechanism was predominantly driven by domain wall motion in one direction, and by rotation in the opposite direction. This behaviour is expected of a unidirectionally anisotropic system.

In the article studying asymmetric magnetisation reversal [43], they proved that this magnetization reversal asymmetry is only visible for a range of angles between the easy axis of the ferromagnet and the magnetization of the sample. As the magnetization of the ferromagnet approaches the easy axis direction, it, then, finishes with rotation, not domain wall propagation. This is the reason why if the hysteresis loop is only measured in the direction parallel to the applied magnetic field, this asymmetry is almost invisible. Generally, with thicker ferromagnetic layers, this asymmetry is less visible as this "critical angle" at which magnetization propagation mechanism changes from domain formation back to rotation is larger.

Another study of asymmetric magnetization reversal was performed by J. Nogués, Ivan K. Schuller et al. [44]. For this system they showed that biaxial anisotropy was responsible for enhanced coercivity, and threefold anisotropy component was responsible for asymmetric reversal (fig. 3.6). This, however, could be something specific to the system they had been studying, and not a general effect.

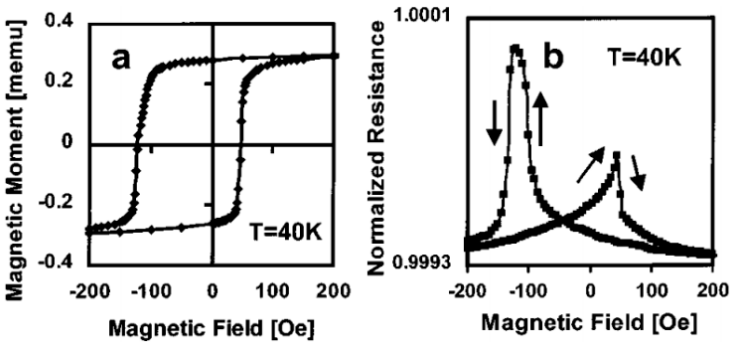


**Figure 3.6:** Magnetization and magnetoresistance hysteresis loops for $Fe/MnF_2$ measured along the [001] crystallographic direction of the MgO substrate at 40K for the cooling field magnitude of 100 mT. Asymmetry is evident from the magnetoresistance plot. Taken from [44].

This property of an exchange biased system was also confirmed by the magnetoresistance measurements [45], further supporting the domain formation vs. rotation picture hypothesized about earlier. Experiments done using Magneto-Optical Kerr Effect (MOKE) microscopy also confirmed these views [46].

Hence, magnetisation reversal asymmetry is another characteristic feature present due to unidirectional anisotropy. When the magnetization switches in the same direction in which the loop is shifted, due to coupling to the AF layer rotation does not happen, as it is more energetically favourable to create a new domain facing in the opposite direction to the preferential one, and expand it.

In the end, however, once a massive part of the material is magnetized in that opposing direction, mechanism can revert to rotation as mentioned in [43], which makes it exceedingly difficult to measure when only taking hysteresis loops with magnetization parallel or antiparallel to the applied field. It is also worth noting that with thicker ferromagnetic layers the reversal goes back from domain formation to rotation sooner.

The exact nature and behaviour of an asymmetric reversal can be influenced by higher order anisotropies due to material properties, however there is good evidence suggesting that unidirectional anisotropy is a sufficient condition for this asymmetry to happen.

### 3.1.3. Blocking temperature

Exchange anisotropy, as expected, will disappear whenever the antiferromagnet is heated above the Néel temperature. Experimentally, however, this can happen at a lower temperature than the Néel temperature. This temperature is often referred to as the "blocking temperature", or $T_B$. It is, in general, system-specific, with some systems exhibiting nearly identical blocking and Néel temperatures, and other systems having blocking temperature significantly lower than the Néel temperature. Responsible for this behaviour are the finite size effects, such as grain size and layer thickness [47]. If the grain size and/or layer thickness go below the system-dependent critical AF dimension, the Néel temperature of the AF is reduced. This is supported by evidence in the form of bulk and thick film AF layers in which blocking and Néel temperatures coincide [48], [49], [50]. The systems with very thin AF films have blocking temperature below the Néel temperature [51], [52].

Other finite size effects are related to the fact that the anisotropy of the AF layer depends on its dimensionality. If we assume that the AF anisotropy decreases as the thickness is reduced, a reduction in blocking temperature would be expected. Comparatively, smaller anisotropy means that the magnitude of exchange bias is smaller as well, and the blocking temperature is lower too.

Blocking temperature for thin films is generally below the Néel temperature. The main reason for this are the size effects. Very thin films, or very granular films have blocking temperature significantly lower than the Néel temperature of the bulk material. Additionally, there usually exists a distribution of blocking temperatures instead of a universal constant when the films are not homogeneous [53],[54],[55],[56]. Furthermore, the presence of multiple phases [53] and stoichiometry [57] can also influence the blocking temperature.

### 3.1.4. Coercivity enhancement

Another characteristic of an exchange biased system is the coercivity enhancement. Generally,coercivity is enhanced when the FM/AF bilayer system goes below the blocking temperature $T_B$, which is a requirement for exchange anisotropy to occur.

In systems with comparable FM and AF layer thicknesses, and similar AF materials (FeF2 – MnF2, NiO – CoO), those systems which have smaller AF anisotropy tend to have a larger increase in coercivity [58], [59].

This increase in coercivity below the blocking temperature can be interpreted in the following way: for an AF layer with small anisotropy, when the FM layer reorients due to an applied field it 'drags' the AF spins irreversibly with it, thus increasing the FM layer coercivity. For a large AF layer anisotropy, FM layer decouples as it cannot 'drag' the AF spins. Therefore, the measured coercivity is reduced for systems with high anisotropy AF films.

One of the consequences of this view is the peak of coercivity close to the blocking temperature [60],[53],[61],[62],[35] shown in fig. 3.7. The peak is related directly to the decrease of AF anisotropy close to the blocking temperature. As this anisotropy decreases, the FM layer can drag more AF layer's spins, thus increasing the coercivity. Above the blocking temperature, the FM layer becomes decoupled from the AF layer. The width of the peak in fig. 3.7 is related to factors disturbing the sample's homogeneity (spread of grain sizes, interface couplings, stress), which in turn causes a distribution of AF anisotropies. This distribution of anisotropies reflects itself in the coercivity vs. temperature curve width, thus containing information on the degree of the sample's inhomogeneity.

Similar behaviour close to the blocking temperature was also seen in the rotational hysteresis of some systems [64], which suggests that coercivity enhancement and the rotational hysteresis are different manifestations of the same effect, namely the losses during the rotation of the FM layer due to AF layer's spin drag [65].

The coercivity enhancement can also be viewed in the context of the AF layer thickness, where with decreasing thickness the AF anisotropy decreases as well (fig. 3.10). Finally, it is also worth bearing in mind that perhaps other pinning mechanisms, such as inhomogeneities in the FM/AF coupling or thermal fluctuations [35] could be the source of this behaviour.

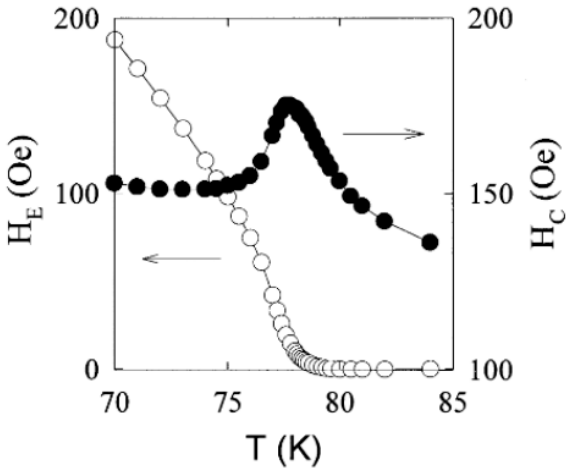


**Figure 3.7:** Exchange bias $H_E$ and coercivity $H_C$ versus temperature for a $FeF_2$/Fe bilayer after field cooling as a function of temperature. Taken from [63].

### 3.1.5. Training effect

Training effect is a property of an exchange biased system, which results in a diminishing and/or vanishing of exchange anisotropy over the course of several magnetization hysteresis loops by applied field (fig. 3.8) [66],[67],[68],[69]. In practice what this means is that each subsequent measurement of a Magnetization vs. Field hysteresis loop will result in a smaller and smaller shift as well as less and less pronounced magnetization reversal asymmetry.

Training effect is chiefly present in systems with polycrystalline antiferromagnets, and is exceedingly small or non-existent in single crystal antiferromagnets [37],[70]. Experimentally, this gradual decrease of loop shift is proportional to $1/\sqrt{n}$, where n is the number of consecutive loops measured.

The diminishing exchange anisotropy is related to partial reorientation of AF domains with each FM magnetization reversal. Proposed causes for this include growth induced metastable spin configuration [71] and thermal fluctuations when $K_{AF}t_{AF} < kBT$ [64]. The general view is that AF spins try to find energetically favourable configurations after each cycle.

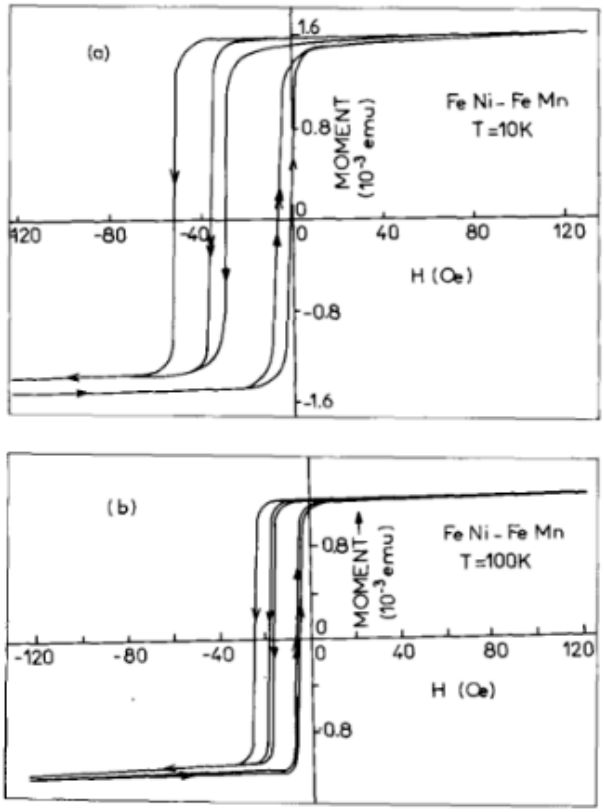


**Figure 3.8:** Successive hysteresis loops recorded between + 500 Oe and – 500 Oe at low temperature along the easy axis after cooing from 300K in a field of +500 Oe along the same direction. a) T = 10K; b) T = 100K. Film thicknesses: FeNi 50 nm; FeMn 20 nm. Each subsequent loop displays reduced coercivity and approaches closer to the centre. Taken from [69]

### 3.1.6. FM layer thickness dependence

The ferromagnetic layer's thickness is one of the important parameters affecting the exchange bias. It has been observed that for all systems, exchange bias is roughly inversely proportional to the thickness of the FM layer (fig. 3.9).

This shows that the exchange bias is an interfacial effect to some degree, and this relation holds for FM layers with thicknesses up to hundreds of nanometres [60],[37],[73],[74],[75], as long as the thickness is smaller than the FM domain wall size. However, if the FM layer is too thin, this relationship does not hold, most likely due to holes within the FM layer. This critical thickness, usually a few nm, varies from system to system and depends on the structure and growth of the FM layer.

### 3.1.7. AF layer thickness dependence

For the case of varying AF layer thickness, it was proven that for AF layers above 20 nm in thickness, exchange bias field $H_E$ is independent of the AF layer's thickness. As the AF layer thickness is reduced, however, $H_E$ decreases abruptly, and for thin enough AF layers (usually a few nm) $H_E$ becomes zero, as shown in fig. 3.10.

The exact thickness at which distinct stages of this diminishing effect take place depends on the specific system, its microstructure and temperature (fig. 3.11) [77],[78],[79],[80].

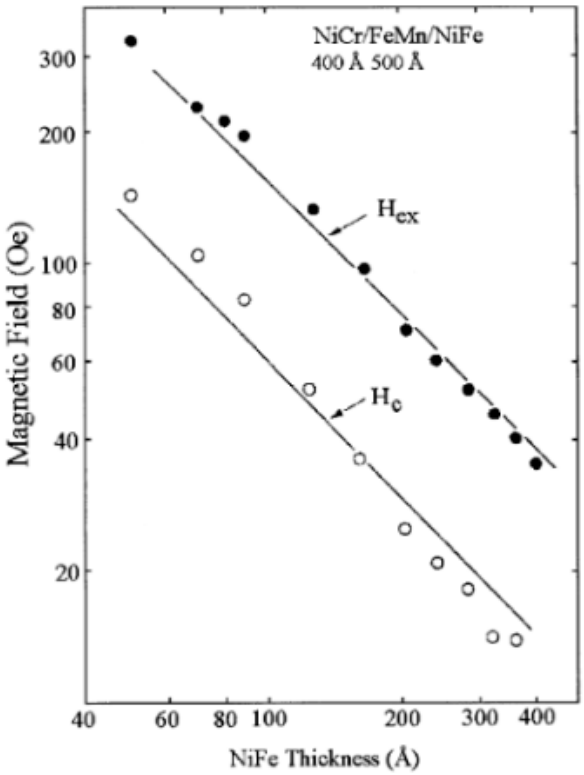


**Figure 3.9:** Dependence of exchange bias $H_{\mathrm{E}}$ (square symbols) and coercivity $H_{\mathrm{C}}$ (triangular symbols) on the FM layer thickness for $Fe_{80}Ni_{20}$/FeMn at a fixed $t_{\mathrm{AF}} = 50$nm. Taken from [72].

This is related to the anisotropy of the AF layer and how it decreases with decreasing thickness. Moreover, decreasing thickness of the layer influences the Néel temperature, and consequently the blocking temperature as well. Additionally, the AF's domain structure may also affect the coercive field if the thickness becomes comparable to the AF domain wall size. Finally, decreasing the thickness of the AF layer can influence the AF grain size, which in turn can influence the critical thickness at which exchange bias field vanishes.

There are two discrepancies for the picture described above. First, in some cases $H_{\mathrm{E}}$ decreases for large thicknesses after $H_{\mathrm{E}}$ reached some constant value [77],[81]. This can be connected to microstructural changes in the AF layer with thickness, for example one kind of phase becoming no longer stable above certain thickness of the AF layer. Second, in some systems as the thickness of the AF layer is reduced, there is a peak in $H_{\mathrm{E}}$ before the main decrease [82]. From theory, this behaviour was predicted for changing AF domain structure with decreasing thickness [77].

Generally, there exists an optimal AF layer thickness for which exchange bias is maximized. For decreasing thickness, exchange bias will gradually diminish until a critical thickness under which no exchange bias occurs due to changes in anisotropy of the AF layer, as well as changes in the grain sizes. Above the optimal thickness, a decrease in exchange bias magnitude can be measured as well, related to different structural phases existing at varying thicknesses.

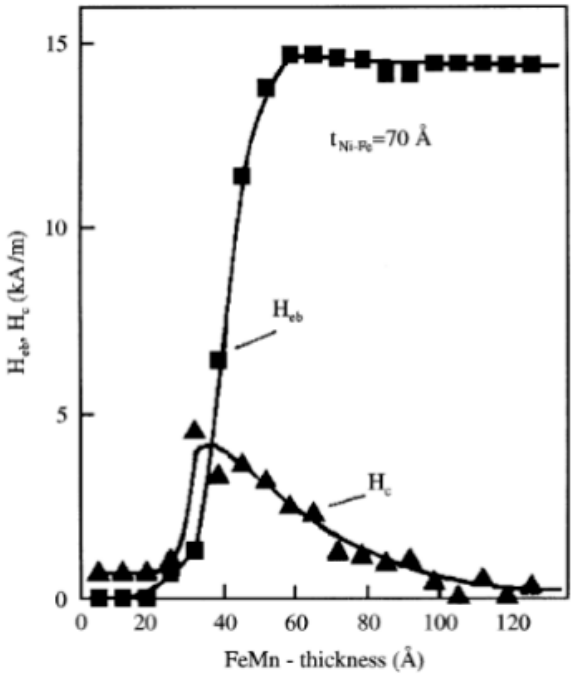


**Figure 3.10:** Dependence of exchange bias $H_E$ (square symbols) and coercivity $H_C$ (triangular symbols) as a function of the AF layer thickness for $Fe_{80}Ni_{20}$/FeMn at a fixed $t_{FM} = 7\,nm$. Taken from [76].

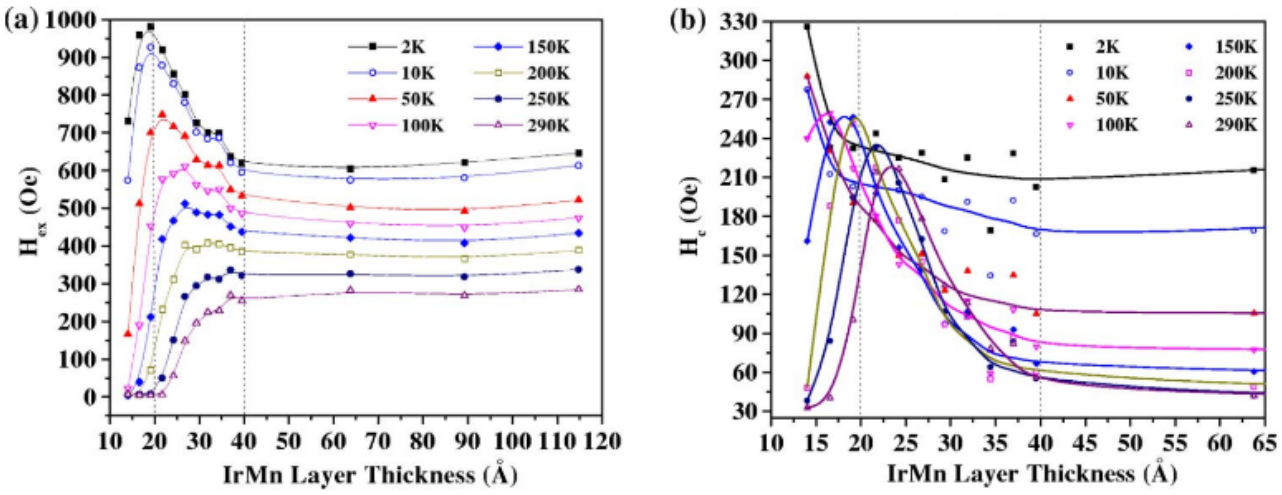


**Figure 3.11:** IrMn thickness dependence of the a) exchange bias field and b) coercivity for a number of temperatures. Lines between points are guide-to-the-eye. Taken from [77].

### 3.1.8. AF spin orientation at the interface

Given how exchange bias is an interfacial effect binding FM and AF layers, naturally the properties of the interface are of great interest for our understanding of the effect. A big number of studies have been carried out, focusing primarily on differences between spin compensated vs. uncompensated AF interfaces, and in-plane vs. out-of-plane interfacial AF spins.

### Compensated vs. uncompensated interface

In a compensated system, AF spins at the interface between FM and AF films are fully compensated by their neighbouring spin arrangement. An uncompensated system is such that the AF spins at the interface are not compensated and have an excess of spin-up or spin-down arrangements.

The experimentalists who first discovered and then expanded upon exchange anisotropy first assumed that compensated interfaces could not cause exchange bias, therefore the AF-FM interface, according to them, had to be somehow uncompensated, either due to roughness at the interface, or something else. Since these first experiments, with the advent of atomic layer-resolved techniques a flood of evidence to the contrary (CoO [49],[83],[84]; NiO [85],[86],[87]; $FeF_2$ [37],[88],[89]; FeMn [76],[90],[91] as some examples) came in, comfortably proving that fully compensated systems are just as capable of supporting exchange anisotropy as the uncompensated ones.

### Out-of-the-plane interfacial spins

Most theories assume that the AF spin orientation at the interface lies in-plane. For certain materials, if bulk spin structure is preserved, the spins may lay out-of-plane relative to the interface ($FeF_2$ (101), $FeF_2$ (001) [92]; FeMn (110), FeMn (001), FeMn (111) [76],[90]). In-plane exchange bias for AF interfacial spins pointing out-of-plane of the interface is zero, while for the in-plane orientation it reaches a maximum, this effect was studied in a $FeF_2$ based system [92]. For an intermediate angle between in-plane and out-of-plane, the loop shift is roughly half of the one obtained for the in-plane case [63]. This trend is repeated in a FeMn-based system [76],[90], but the analysis is made difficult due to the complex spin structure.

Compensation at the interface, while capable of affecting the magnitude of exchange anisotropy, is not a deciding factor of its presence. Counter-intuitively, even systems with fully compensated, monocrystalline AF layers could bias the FM layer. Furthermore, some systems with AF layers with fully compensated spins at the interface exhibit loop shifts larger than those with uncompensated interfaces.

Despite the general assumption by models of in-plane AF spin configuration at the AF-FM interface, experimentally it was studied and proven that for a perpendicular, out-of-plane orientation of the antiferromagnetic easy axis the in-plane exchange bias approaches zero, while for the in-plane orientation of the AF spins it is maximized. This trend was supported by crystal orientations which had an intermediate orientation between in-plane and out-of-plane, for which exchange bias was half of the value for in-plane orientation.

Finally, there exist systems which have both FM magnetisation and AF spin axis oriented out-of-plane, for which out-of-plane field cooling results in the out-of-plane exchange bias. As an example, this effect is documented for CoO/Permalloy multilayers [93], FeMn/FeNi multilayers [94], Pt/Co/NiO multilayers [95], and for the case of CoFe/IrMn bilayers, [96], which is a relatively new development. From the practical standpoint, such systems with perpendicular exchange bias may be useful for spin-valves or magnetic tunnel junctions where perpendicular magnetic anisotropy is needed.

### 3.1.9. Disorder at the interface

In the previous section we have touched upon the importance of spin-ordering at the interface for exchange anisotropy. Ideally, this section should cover the studies which focused on varying a certain parameter, for example roughness, while keeping others (crystallinity, grain size, impurities) the same. In practice, however, attempting to change roughness inevitably leads to changes in crystallinity and grain size. This problem is alleviated for single crystal antiferromagnets, where roughness can be independently influenced without affecting crystallinity or grain size.

#### Roughness

In most studies on roughness in the exchange biased FM-AF systems it was concluded that the magnitude of the loop shift decreases with increasing roughness (fig. 3.12) [3],[37],[89],[85],[90],[97],[55] with some systems being insensitive to it [98],[86], and in some with exchange bias increasing [88]. This general behaviour appears to be independent of the interfacial spin structure, whether it is with compensated, uncompensated, with in-plane or out-of-plane AF spins. An important exception, for which exchange anisotropy increases with increasing interfacial roughness, are the FM coated AF single crystals (with both compensated and uncompensated surface spins at the interface [48]), which suggests that the microstructure plays a significant role. The samples with polycrystalline AF layers appear to be less influenced by roughness [99],[81],[100].

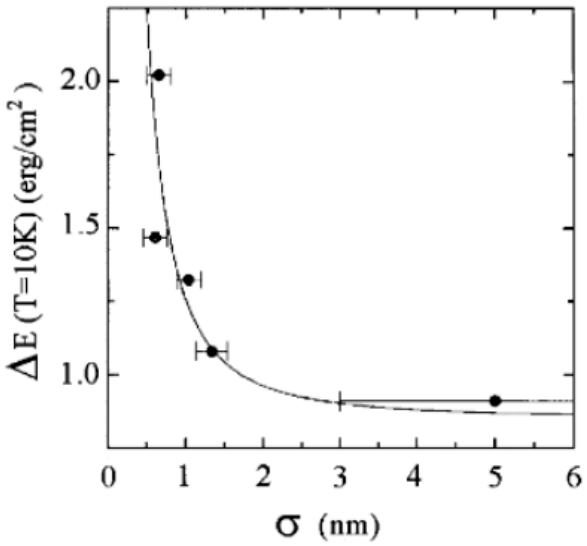


**Figure 3.12:** Dependence of the interface energy $\delta E$ at 10K on interfacial roughness $\sigma$ for $FeF_2$ (110)-Fe bilayers. Taken from [89].

### Crystallinity

For thin film bilayers, AF thin films are textured by the substrate below. The degree of texturing decides the crystallinity of the AF thin film, which can affect exchange anisotropy. If the texturing occurs in a single orientation, the loop shift increases with increasing texturing [101],[102],[4],[103],[50],[104],[105],[106],[107], with some exceptions [108],[62],[109]. As the growth conditions are changed, new emergent crystalline orientations can change exchange anisotropy drastically without following any trend [110],[90].

This varied behaviour can be explained in part by spin arrangement at the FM-AF interface, discussed in the previous section. For a larger spread of grain orientations, exchange biasing is reduced due to that. Another effect, valid for less crystalline samples, is that the long-range AF behaviour such as anisotropy or domain formation can change, thus influencing the exchange anisotropy as well.

### Grain size

For variations in grain size of the AF layer, no clear trend has been established, and the information obtained remains very system specific. In some systems, exchange anisotropy increases with grain size [53],[73],[81],[111],[112] while in others, exchange anisotropy decreases with increasing grain size [113],[114],[100],[115].

### Impurities

Presence of impurities at the interface, be it oxidation, amorphization or absorption of the AF layer, tend to decrease the magnitude of exchange anisotropy [116],[117],[118]. In a systematic study, a metal layer of increasing thickness was deposited between the AF and FM layers [119],[120]. Exchange anisotropy decreased with the presence of this metal impurity layer; however, it did not go to zero after a few monolayers as one would expect if exchange bias was indeed an interface phenomenon only. Several nanometres of the non-magnetic metallic layer were needed to suppress exchange biasing [119],[120].

## 3.1.10. Perpendicular exchange coupling

While the general assumption is that the coupling between FM and AF layers is parallel in nature, there also exist perpendicularly coupled systems, which have AF and FM spins coupled perpendicularly (FeMn/$Fe_{20}Ni_{80}$ [91], CoO/$Fe_3O_4$ [84], CoO/$Fe_{20}Ni_{80}$ [121], $FeF_2$/Fe [122]). Both compensated [91],[84] and uncompensated [121],[122] AF surfaces were found to be capable of perpendicular coupling. From a theoretical standpoint, this effect had been predicted for a case where FM anisotropy is low [123].

In a $FeF_2$/Fe system, as it is cooled from room temperature down to 10 K, the FM easy axis rotates 90 degrees, with the rotation starting around the $FeF_2$ Néel temperature [122]. Contrary to this behaviour, in a CoO/$Fe_3O_4$ system it is the AF spins which arrange themselves perpendicular to the ferrimagnetic lattice [84].

## 3.2. Theoretical models

There exists a long list of theoretical models attempting to explain exchange bias. As is natural in the world of physics, after the first experimental discoveries were made, some simple models were proposed. At first, the discrepancy between the theoretical models and the experiments was merely quantitative, but with further, more detailed experiments, serious qualitative discrepancies started to show, and due to very complicated nature of exchange bias, theoretical models have been playing catch-up ever since. In this section, I shall cover the most well-known models from least to most descriptive. At the end of each subsection, I included a brief critique of each model and described what it cannot account for or explain.

### 3.2.1. Early models

First attempt at developing a theory of exchange anisotropy was undertaken by W.H. Meiklejohn [124], the very same person who discovered it. In his model, he assumed a coherent rotation of both FM and AF magnetization, which he then wrote down as a following expression (eq.3.1):

$$\epsilon = -H\, M_{\mathrm{F}}\, t_{\mathrm{F}} \cos(\theta - \beta) + K_{\mathrm{F}}\, t_{\mathrm{F}} \sin^2(\beta) + K_{\mathrm{AF}}\, t_{\mathrm{AF}} \sin^2(\alpha) - J_{\mathrm{F/AF}} \cos(\beta - \alpha), \quad (3.1)$$

where $H$ is the applied magnetic field, $M_{\mathrm{F}}$ is the FM layer's saturation magnetization and $t_{\mathrm{F}}(t_{\mathrm{AF}})$ the thickness of the FM (AF) slab, $K_{\mathrm{F}}(K_{\mathrm{AF}})$ the bulk anisotropy of the FM (AF) and $J_{\mathrm{F/AF}}$ is the interfacial exchange constant. The alpha angle is between $M_{\mathrm{AF}}$ and the AF anisotropy axis, beta is the angle formed by $M_{\mathrm{F}}$ and the FM anisotropy axis and theta is the angle between H and the FM anisotropy axis. From this general equation W.H. Meiklejohn [124] obtained the following formula describing hysteresis loop shift:

$$H_{\mathrm{E}} = \frac{J_{\mathrm{F/AF}}}{a^2 M_{\mathrm{F}} t_{\mathrm{F}}}, \quad (3.2)$$

where $a$ is the lattice parameter. The order of magnitude of the exchange bias depends entirely on the parameter $J_{\mathrm{F/AF}}$, a common feature of all theoretical exchange anisotropy models developed. For the assumption $J_{\mathrm{F}} \geq J_{\mathrm{F/AF}} \geq J_{\mathrm{AF}}$, the resulting value of loop shift is orders of magnitude larger than the experimentally observed one [124].

If one were to look at this model as an intuitive guide for exchange anisotropy, the expectations would include exclusively negative exchange bias systems, uncompensated interfaces displaying the largest magnitude of loop shift, as well as the roughness of a compensated interface increasing the loop shift. It is fair to say, when compared against the experimental behaviour, these qualitative expectations are not validated.

### 3.2.2. Néel's model

The next person to step up to the task of describing exchange anisotropy was the legendary Louis Néel [125](chapter XV). Ten years after the contribution by Meiklejohn, he created a model applicable to a system which consists of an uncompensated, weakly anisotropic, interfacial AF layer (fig. 3.13) ferromagnetically coupled (fig. 3.13a) through the interface to an FM slab.

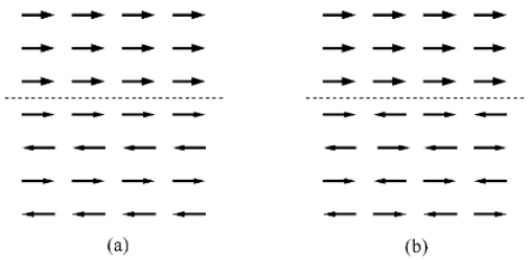


**Figure 3.13:** Parallel magnetic ordering at the interface. a) Ferromagnetic interfacial coupling ($J_{F/AF} > 0$) and b) antiferromagnetic interfacial coupling ($J_{F/AF} < 0$)

He also assumed that the magnetization $m_i$ of layer $i$, both in the FM and AF is uniform within the layer and parallel to the interface. He, then, adopted lattice parameter as equal to 1 as the unit of length, the condition for $m_i$ to be in equilibrium is (eq. 3.3):

$$JS^2[\sin\frac{1}{2}(\theta_{i+1} - \theta_i)\sin\frac{1}{2}(\theta_{i-1} - \theta_i)] - 2K\sin(\theta_i) = 0, \tag{3.3}$$

where $\frac{1}{2}\theta_i$ is the angle between $m_i$ and the easy magnetization axis, and J and K were defined by (eq. 3.1). If we apply a continuum approximation, this set of difference equations can be rewritten as a following differential equation (eq. 3.4):

$$JS^2\frac{d^2\theta}{di^2} - 4K\sin(\theta) = 0. \tag{3.4}$$

If we solve this equation for specific values of $J$ and $K$, assuming uniaxial anisotropy, we can derive the magnetization profile, and that is exactly what Louis Néel did.

Domains develop in both FM and AF if the conditions are correct, however, continuum approximation requires a minimum width of the FM and AF slabs to be valid. As an example, for Néel's theory to remain valid, an FM Fe slab thicker than 100 nm is required. Most systems which have been studied have FM layers soundly below the 100 nm minimum limit needed for this theory to be applicable.

### 3.2.3. Early random interface models

Another interesting model was proposed by Malozemoff [126], twenty years after Louis Néel's work. He proposed a model of exchange anisotropy based on the assumption of rough FM-AF compensated and uncompensated interfaces (fig.3.14).

The main idea behind this theory was that the interfacial roughness gave rise to random magnetic field acting on the interface spins, yielding unidirectional anisotropy, which then causes the hysteresis loop shift. Thinking about exchange bias in these terms reduced the overestimating discrepancy between experimental data and theory by two orders of magnitude when using eq. 3.2. The expression for the loop shift given in [126] is (eq. 3.5):

$$H_E = \frac{2}{M_F t_F}\sqrt{\frac{J_{AF}K_{AF}}{a}}. \tag{3.5}$$

This estimate differs from the originally proposed one in eq. 3.2 by $2a/\sqrt{J_{AF}/aK_{AF}}$, which is the ratio of twice the lattice parameter divided by the FM domain wall width

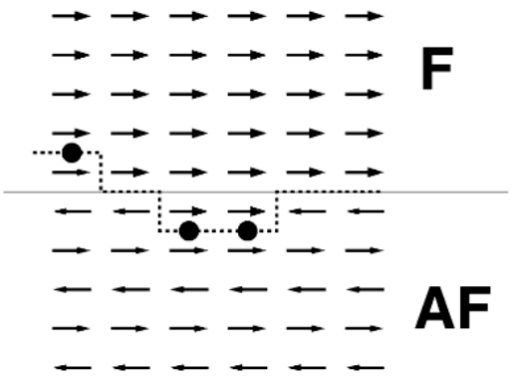


**Figure 3.14:** AF rough interface with frustrated bonds marked by full dots. Dashed line marks the boundary between the FM and AF layers. Taken from [126]

$d_w = \sqrt{J/aK}$. The role played by the ratio $a/d_w$ shows that the characteristic length scale of this problem is on the order of a domain wall width. Further refinements performed within the same paper reduced the ratio (eq. 3.2) even more, by allowing the formation of the AF domain walls near the interface.

This model managed to obtain a reasonable estimate for the value of loop shift, however, it assumes the disorder at the interface, which is not consistent with experiments (exchange bias occurring in bilayers with atomically resolved interfaces).

### 3.2.4. AF domain wall models

Shortly after the publication by Malozemoff, an alternative model was proposed by Mauri et al. [127]. The assumptions made included a) parallel interface coupling across a perfectly flat interface, b) FM and AF magnetization axes parallel in an absence of an applied field, c) FM slab thickness much thinner than the FM domain wall width, d) domain wall which develops inside the AF imposes an upper limit on the exchange coupling energy, in such a manner that it reaches much lower values than those resulting from eq. 3.2.

Assumptions a),b) and c) are disputable. First, antiparallel interface coupling is not only possible but probable. Nogués et al. [128] have confirmed experimentally that the antiparallel interface coupling is necessary for positive exchange bias. This model also does not explain how compensated interfaces can provide values of loop shift as large as, or even larger than, the uncompensated ones (more in section 3.1.8). Moreover, in the magnetic ground state configuration, the FM magnetic moments are orthogonal to the bulk AF easy axis [123],[122],[84]. To conclude, for a domain wall to develop in the AF layer, the anisotropy constant of this AF layer must be small; otherwise, it is energetically favourable for the DW to form in the FM layer [129],[15],[130],[131],[132]. As detailed in section 3.1.5, for AF layers with small anisotropies, only coercivity enhancement takes place.

### 3.2.5. Perpendicular coupling model

The next person to provide another insight into exchange bias mechanisms was N.C. Koon [123]. He tried to explain the problem of fully compensated FM-AF interfaces by the means of a micromagnetic calculation. He established, based on a Heisenberg model, that the ground state configuration of such a system corresponds to perpendicular orientation of FM moments relative to the AF's easy axis direction (fig. 3.15).

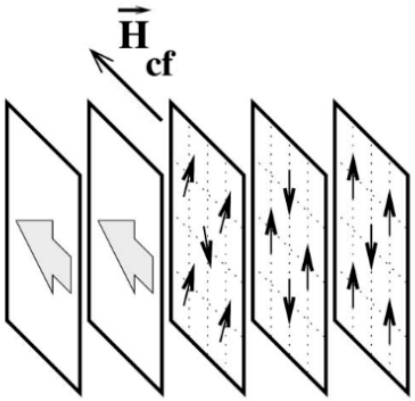


**Figure 3.15:** Illustration of the perpendicular FM and AF magnetic interface configuration with spin canting in the first AF layer. Taken from [123]

N.C. Koon also demonstrated that the magnetic moments at the AF interface exhibited canting. The minimum energy of the system is realized when the AF spins adopt a small canting angle, less than 10 degrees, relative to the AF bulk easy axis, with a component opposite to the cooling field direction.

As pointed out by Schulthess and Butler [133], while this work is relevant to the FM-AF interface, it fails to yield exchange anisotropy. The canted structure itself is not sufficient to produce a unidirectional anisotropy.

### 3.2.6. Random interface field models

Schulthess and Butler [133], [134] demonstrated that both Malozemoff's and Koon's models can be combined to provide a more descriptive model for exchange bias. Within their model, besides the usual exchange, they also added Zeeman and anisotropy energies, the dipolar interaction term $E_D$ (eq. 3.6):

$$E_{\mathrm{D}} = \sum_{i \neq j} \frac{[\vec{\mu_i} \cdot \vec{\mu_j} - 3(\vec{\mu_i} \cdot \hat{n_{ij}})(\vec{\mu_j} \cdot \hat{n_{ij}})}{\mid \vec{R_i} - \vec{R_j} \mid^3}, \tag{3.6}$$

where $u_i$ is the magnetic moment configuration, $\hat{n_{ij}}$ is a unit vector parallel to $\vec{R_i} - \vec{R_j}$. Magnetic properties were found using micromagnetic simulations, solving LLG-K equations to obtain stable or metastable equilibrium.

When this model is applied to Koon's orthogonal interface coupling, for flat interfaces there is no unidirectional anisotropy; however, there is irreversible magnetization curves with finite coercivity. This irreversibility is a result of a bifurcation in the solution of the equation. Additional elements are needed to generate unidirectional anisotropy.

Now, following the general idea behind Malozemoff's model [126], surface defects were introduced. First, an assumption of 4x4 2D interface cell was made, with one interfacial FM site occupied by an AF magnetic moment. This precise arrangement provided good agreement for the values of loop shift and coercivity for the CoO/FM system (FM: Co and Permalloy) [114], if exchange and anisotropy parameters are of reasonable magnitude, and a canting angle of 10 degrees are adopted.

It is important to emphasize the fact that the relation between surface roughness and exchange anisotropy is quite complex experimentally. As mentioned in the experiments section, depending on the system, interfacial disorder can either increase or decrease the magnitude of hysteresis loop shift.

Zhang et al. [135] theoretically investigated how random fields at the FM-AF interface influence the coercivity of an exchange biased system. They included domain walls on the FM side of the interface, and derived temperature dependence of the coercivity $T^{-3/2}$, within the correct order of magnitude.

Another random field model was investigated by Dimitrov et al. [136], with an assumption that the interface exchange interaction between FM and AF magnetic moments is given by (eq. 3.7):

$$\epsilon = J_1 \vec{\mathbf{m}}_{\mathrm{F}} \cdot \vec{\mathbf{m}}_{\mathrm{AF}} + J_2 (\vec{\mathbf{m}}_{\mathrm{F}} \cdot \vec{\mathbf{m}}_{\mathrm{AF}})^2, \tag{3.7}$$

where $J_1$ and $J_2$ are the normal and biquadratic [137] exchange constants. For $J_1$, either parallel or antiparallel alignment is preferential. For $J_2$, orthogonal (spin-flop like) FM/AF coupling is preferential. Summation over all the interactions leads to the following form for the total energy (eq. 3.8):

$$E = C_1 + C_2\, J_1 \cos(\theta) + C_3\, J_2 \sin^2(\theta), \tag{3.8}$$

where $\theta$ is the angle formed by the easy axes of the FM and AF; $C_{\mathrm{k}}$ are the coefficients which can be calculated when detailed interface information is known. With a generous application of an educated guess, qualitatively correct conclusions were obtained from this model.

The models in this subsection all hinge on Malozemoff's assumptions of rough interface, and quantitative results depend heavily on the nature and concentration of the interface defects.

### 3.2.7. Frozen interface model

Kiwi et al. [20],[138],[139] proposed a model for exchange anisotropy which applies to a large variety of systems which have significant AF layer anisotropy, for which the energy cost of a domain wall inside of the AF layer is high. Thus, $Fe/FeF_2$ and $Fe/MnF_2$ systems were adopted as prototypes thanks to high AF layer anisotropy as well as extensive experimental information. Attention was focused on the (110) compensated AF crystal face, which exhibits the largest exchange anisotropy. The zero applied field AF spin configuration at the interface is like that in fig. 3.15. This spin configuration is a consequence of a large difference between AF and FM domain wall widths [140]. While the domain wall width of iron approaches 100 nm, domain wall width of $FeF_2$ or $MnF_2$ is on the order of monolayers [141].

This model a priori assumes that the AF interface layer freezes into the canted spin configuration it obtains close to the Néel temperature. Since the FM slab is much thinner than the FM domain wall width, discrete treatment is an accurate one (eq. 3.9):

$$\mathcal{H} = \mathcal{H}_{\mathrm{AF}} + \mathcal{H}_{\mathrm{F/AF}} + \mathcal{H}_{\mathrm{F}}, \tag{3.9}$$

where $\mathcal{H}_{\mathrm{AF}}$,$\mathcal{H}_{\mathrm{F/AF}}$ and $\mathcal{H}_{\mathrm{F}}$ describe the AF substrate, interface coupling and the FM slab, respectively.

One can obtain a set of equations for a single magnetic cell [20] from eq. 3.9. This set of equations can be solved using Camley's method [142],[143]. The resulting value of the loop shift, with a single adjustable parameter (the interface coupling constant $J_{\mathrm{F/AF}}$) agrees with the experiment [20]. What's more, the calculations also show the behaviour of exchange bias inversely proportional to the thickness of the FM layer, as long as the thickness of this FM layer is below the domain wall width. The energy is reversibly stored in an incomplete domain wall in the FM layer. This domain wall has a twist smaller than 20 degrees, and is qualitatively compatible with neutron scattering performed by Ball et al. [129]. Nolting et al. [144] established that the alignment of spins in individual FM domains close to the interface is determined, domain by domain, by the spin direction in the underlying AF layer. Another set of evidence supporting this view was provided by Matsuyama et al. [145]. They observed Fe domains deposited on the fully compensated face (001) of NiO, and observed that the Fe spin polarization of each domain is roughly perpendicular to an easy axis of the NiO. They also suggest that the NiO interfacial spins are canted against the Fe spins.

What is more, the model set forth by Kiwi et al. provides a simple explanation of positive exchange bias [139], which was a major point of failure in previous models.

As is customary with exchange anisotropy models, an assumption is made as to the interfacial structure, in this case having spin-flop-like coupling. The condition of the AF thin film having very high AF layer anisotropy is a restrictive condition, and as has been shown experimentally, exchange bias can occur even in systems with weak AF layer anisotropy, accompanied by th training effect. For this group of models, however, experimental support has proven to be significant.

### 3.2.8. AF grain coupling model

In the work done by Stiles and McMichael [140] they approached the problem from a different angle. Instead of considering individual magnetic moments and their interactions, they opted for polycrystalline interface AF grains with stable magnetic order as their "units which couple". They assumed that the interfacial AF grains in the absence of the FM layer can order in many different equally energetically favourable arrangements, but when the FM layer is present, a particular stable energy configuration is chosen due to contact with the FM layer. Due to the weakness of Zeeman energy, this FM-AF configuration remains stable and retains a memory of the original FM magnetization direction, meaning the FM magnetization direction when the AF order first sets in. They also suggest that due to the polycrystalline nature of the system, even for uncompensated AF interfaces, there is a substantial compensation of the magnetic moments due to the fluctuating easy axis direction of each individual grain. Thus, in this model [140] a fraction of uncompensated spins at the AF-FM interface drives the exchange bias.

Calculations begin with a single domain AF grain. The energy of each such grain coupled to the FM layer above is given by (eq. 3.10):

$$\frac{E}{Na^2} = \frac{-J_{net}}{a^2}[\widehat{\mathbf{M}}_{\mathrm{FM}} \cdot \widehat{\mathbf{m}}(\mathbf{0})] + \frac{J_{\mathrm{sf}}}{a^2}[\widehat{\mathbf{M}}_{\mathrm{FM}} \cdot \widehat{\mathbf{m}}(0)]^2 + \frac{1}{2}a[1 - \widehat{\mathbf{m}}(0) \cdot (\pm\widehat{\mathbf{u}})], \tag{3.10}$$

where $a$ is the lattice constant, $M_{\mathrm{FM}}$ is the FM magnetization, $\widehat{\mathbf{m}}(0)$ is the net sublattice magnetization, and $\pm\widehat{\mathbf{u}}$ are the two easy uniaxial anisotropy directions. $J_{\mathrm{net}}$ is the average coupling energy to the net moment of the AF grain. $J_{\mathrm{sf}}$ is the spin-flop energy, and sigma is the energy of a 180 degree domain wall in the AF. From this, we conclude that there is a competition between parallel alignment by $J_{\mathrm{net}}$ and a perpendicular alignment due to $J_{\mathrm{sf}}$. The similarity between eq. 3.10 and eq.3.7 is quite telling, but with an important distinction: the former deals with entire grains, the latter deals only with atomic moments. Additionally, possibility of a domain wall forming in the AF is described by the term proportional to $\sigma$.

Based on the description above, they calculated the relevant physical properties of the system (the magnitude of loop shift, coercivity enhancement, rotational torque and FMR behaviours). They performed these calculations for a host of different parameter values, both including and excluding spin-flop-like coupling.

This model requires additional assumptions; to lock the interface spin configuration, partial domain walls are required to wind up in the AF layer. Furthermore, it is stated that for some AF grains a critical winding angle exists, and if it is exceeded, can lead to instability of the AF ordering. This way, the AF grains can either support a particular AF order, or they may switch between two possible states, meaning, if the critical angle is not exceeded, we get a reversible behaviour (winding and unwinding of the "exchange spring"), and if it is exceeded, we get a hysteretic behaviour (coercivity enhancement).

### 3.2.9. Domain state model

As the final step in the evolution of exchange bias models so far, U. Nowak et al. [146] developed a model which related AF domains to the concentration of nonmagnetic sites in the AF layer. As the dilution increases, it leads to an increase in the number of domains having uncompensated magnetic moments. These uncompensated magnetic moments are then responsible for the coupling between the AF and FM layers. Such a domain state, with pinned, uncompensated magnetic moments (PUMs) is metastable, evolves and finally becomes frozen over the course of field cooling. Thus, it requires no further assumptions about the interface, structure or size of the AF domains being formed. In [146] they also demonstrated that both Ising and Heisenberg approaches to modelling a system give a strong dependence of the exchange anisotropy loop shift on dilution. Their model is based heavily on diluted Ising antiferromagnets in an external field model (DAFF model).

The origin of the AF magnetic domain formation was originally investigated by Imry and Ma [147], where they concluded, that the reason for the domain formation is rooted in a statistical imbalance between the number of spins of two sublattices of the AF layer due to impurities and defects (this is now known as the Imry-Ma argument). This leads to a net magnetization within that region which can couple to the external field. Therefore, a formation of a domain within that region can lower the energy of the system. The energy needed to form a domain wall can be minimized if this domain wall passes preferentially through non-magnetic defects (fig. 3.16).

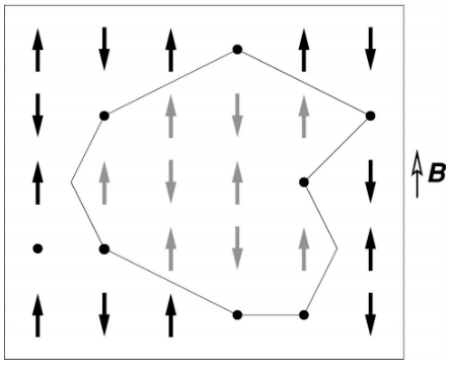


**Figure 3.16:** Schematic illustration of the Imry-Ma argument. Dots denote non-magnetic defects, grey arrows denote an AF domain area.

The AF layer is modelled as a magnetically diluted Ising system, with an easy axis parallel to that of the FM layer. Energy contributions in the Hamiltonian can be separated into the FM layer energy, diluted AF layer energy, and the exchange coupling between the FM and AF layers, assuming that the Ising spins in the top atomic layer of the AF film interact with the z-component of the Heisenberg spins of the FM. Another assumption is made as to the values of FM and AF magnetic moments being identical. They then derived the following equation to describe the magnitude of the exchange bias field (eq. 3.11):

$$I\,\mu\,B_{\mathrm{EB}} = J_{\mathrm{INT}}\,m_{\mathrm{INT}}, \tag{3.11}$$

where $I$ is the number of FM layers (in simulations done by [146] it was always $I = 1$) and $m_{\mathrm{INT}}$ is the interface magnetization of the AF per spin. For an ideal, uncompensated interface one would expect $m_{\mathrm{INT}} = 1$ which leads to a much too high bias field, while for an ideal compensated interface, one would expect $m_{\mathrm{INT}} = 0$, which then leads to no biasing field whatever. Experimentally, however, there is no big difference between compensated and uncompensated interfaces. It is also found that $B_{\mathrm{EB}}$ is much smaller than $J_{\mathrm{INT}}/I\mu$. The solution to this is the fact that $m_{\mathrm{INT}}$ does not remain constant through the reversal, nor is it a simply known quantity [146].

The authors of [146] further performed Monte-Carlo simulations to figure out the temperature dependence of the exchange bias field. An example is provided for a fixed dilution of $= 0.5$ (fig. 3.17). The magnitude of the exchange bias field was almost linearly decreasing to zero as the system approached the blocking temperature.

This result corresponds nicely to the well-known experimental behaviour of exchange bias gradually diminishing as one approaches the blocking temperature.

Next, they [146] performed a simulation to explain the training effect (exchange bias disappearing over the course of multiple hysteresis loop measurements). For the domain state model, based on the dynamics of DAFF, it is known that the remanent magnetization of the Domain State (DS) relaxes non-exponentially on extremely long timescales after the field is switched off [148],[149],[150]. They relate these dynamics of the DAFF to the decrease of exchange bias due to slow relaxation of the AF domain state.

Experiments to support this model [151] showed a remarkably close correspondence to what they have modelled, giving further credibility to exchange anisotropy being a phenomenon fully based around AF domains and atomic magnetic defects which give

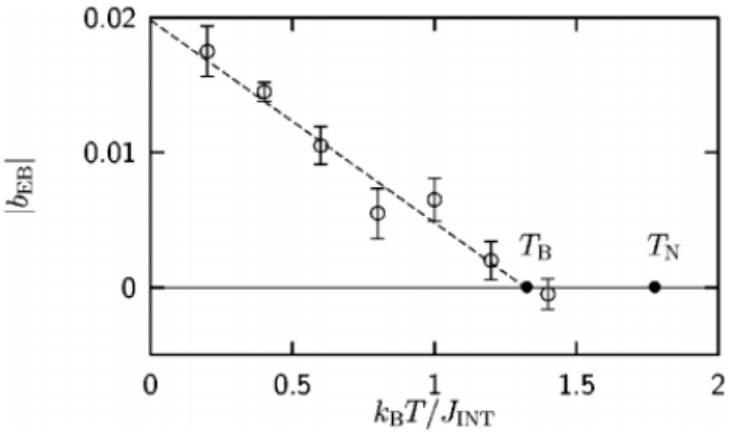


**Figure 3.17:** Temperature dependence of the EB field for 50% diluted AF. Taken from [146]

rise to these domains. Additionally, applying defects to the interface in the DS model, contrary to Malozemoff's random field model, results in vanishing number of domains within the AF layer, thus decreasing exchange bias.

For this model type, domain formation is critical for the existence of exchange anisotropy. Without domain formation, there would be no EB for compensated interfaces, and very high EB for uncompensated ones. They have successfully modelled the dilution dependence of EB, temperature dependence, training effect, positive EB as well as the dependence of EB on AF thickness.

The DS model considered in this work, however, is designed for systems with strong uniaxial AF anisotropy, for the Ising approximation to hold valid. For systems with weaker anisotropies, Heisenberg model would be more appropriate. The authors also claim that the basic feature of the DS model, namely the formation of AF domains within the bulk is not restricted to an AF layer with strong anisotropy.

## 3.3. Summary

This section presents a summary of both experimental and theoretical parts of this chapter in a concentrated form.

### 3.3.1. Experimental evidence summary

Unidirectional anisotropy remains the most basic and universal feature of an exchange biased system, being present across all the systems.

When considering the magnetization reversal dynamics, an exchange biased system has an asymmetry related to unidirectional anisotropy induced by exchange coupling. Due to preferential pinning direction, whenever the magnetization must reverse in the opposite direction from the pinning one, the unidirectional anisotropy component causes a reversal via nucleation of a new domain additionally to the rotation (fig. 3.18(6-10)). In contrast, for normal, un-biased FM films reversal happens symmetrically regardless of the applied field direction(fig. 3.18(1-5)).

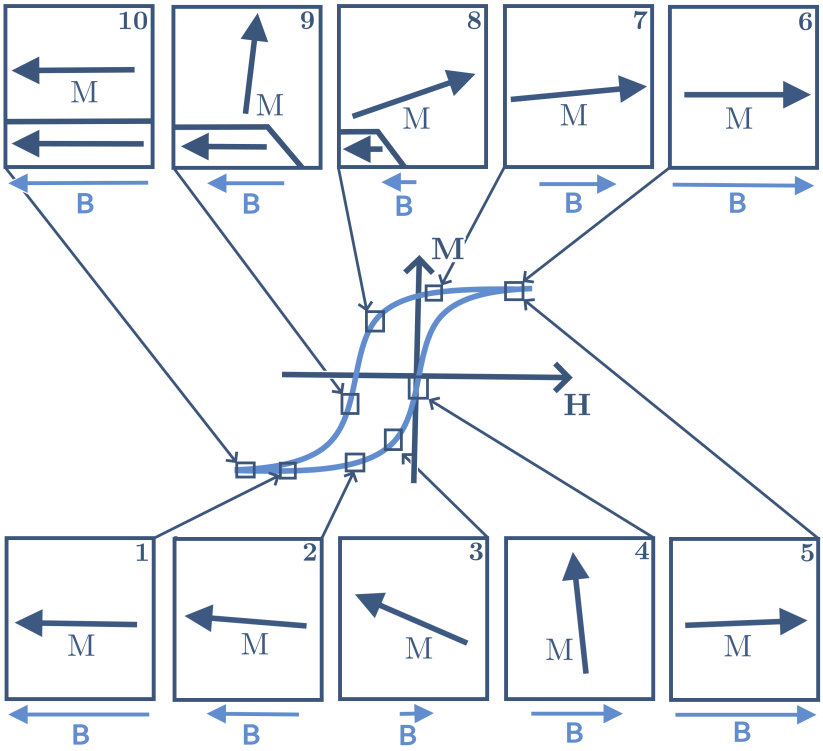


**Figure 3.18:** (1-5) coherent rotation in the exchange bias direction. (6-10) rotation and nucleation opposite to exchange bias direction.

When considering the magnetocrystalline anisotropy and its effect on the exchange bias, then it is clear from the experiments that with increasing AF layer anisotropy, the magnitude of exchange bias increases as well. In contrast, coupling to a low anisotropy AF layer results only in an increase of coercivity, as the FM layer would then cause the AF atomic moments to irreversibly rotate along with the applied field (fig. 3.19).

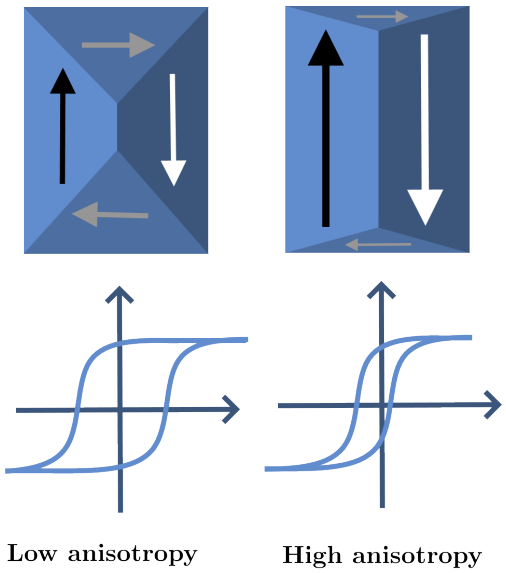


**Figure 3.19:** Effects of low and high anisotropy AF on exchange bias and coercivity.

When taking into account the polycrystalline AF systems, during the field cycling of exchange biased AF-FM bilayer, diminishing of exchange bias occurs due to irreversible rearrangements of AF grains under the influence of coupled FM layer above (fig. 3.20), known as training effect. Systems with single-crystal AF films are either not subject to this behaviour, or negligibly so.

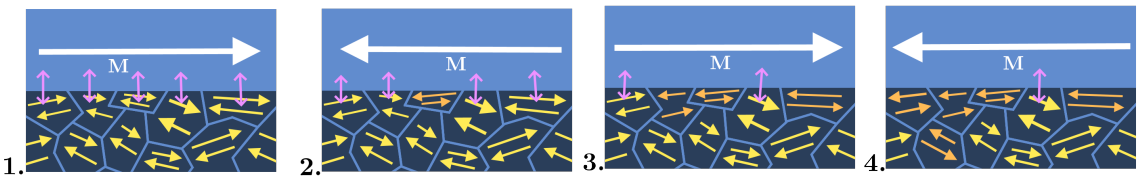


**Figure 3.20:** AF grain rearrangement under the influence of the FM layer exchange coupled to individual AF grains. Sequence (1-4) represents the training effect and gradual decrease in number of the coupled AF grains. Pink double arrows represent the coupling.

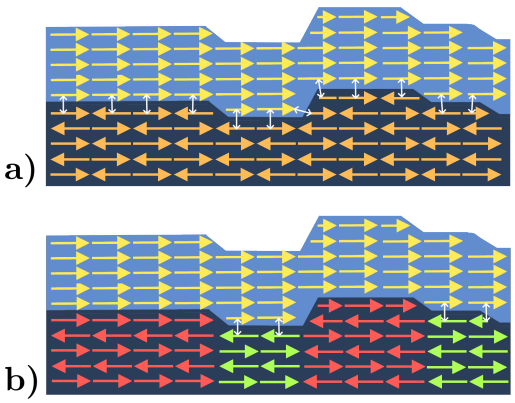


**Figure 3.21:** (a) Compensated AF-FM interface, insensitive to roughness; (b) Uncompensated AF-FM interface. AF tends to separate into domains, thus weakening the exchange bias.

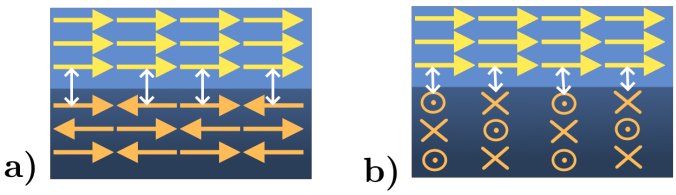


**Figure 3.22:** (a) Parallel FM-AF exchange coupling; (b) Perpendicular FM-AF exchange coupling. Double arrows indicate the coupling.

Better AF crystallinity generally improves exchange bias (grains having less of a statistical spread of orientations). Interestingly, grain size has not shown any trends in influencing exchange bias, being very system-specific. This is likely due to being a result of other factors such as crystallinity or film thickness.

At the interface, AF can either have its spins arranged in a fully compensated, or uncompensated manner (fig. 3.21). Experimentally it was proven that exchange bias is, counter-intuitively, stronger for fully compensated interfaces. Those statements only hold true if the interfacial AF spins are oriented in-plane, as it has also been shown that interfacial AF spins oriented out-of-plane do not produce any exchange anisotropy for in-plane magnetization, and systems with AF spins oriented in an intermediate direction between 0 and 90 degrees in-plane and out-of-plane show exchange anisotropy proportional to the in-plane component.

The interfacial roughness generally decreases the magnitude of exchange bias in most systems (by creating areas of uncompensated moments oriented in random directions, fig. 3.21). In the case of single-crystal, fully compensated films, the exchange bias either stays the same or mildly increases (such interfaces typically remain compensated regardless of roughness, fig. 3.21a), due to the increased surface area of the AF-FM interface.

Exchange bias is inversely proportional to the FM thickness. In case of AF, there exists an optimal thickness below which exchange bias gradually diminishes, and above which it can also decrease. The decrease above the critical thickness is related to new phases forming in thicker AF layers, being less ideal for exchange anisotropy.

Impurities at the interface decrease exchange anisotropy. Having multiple monolayers of a non-magnetic spacer at the AF-FM interface still allows for some exchange anisotropy to happen, even though the decrease is exponential with the thickness of the non-magnetic spacer.

Perpendicular coupling (fig. 3.22b) occurs in some systems as a favourable arrangement which takes place during field cooling. Both cases of an AF layer arranging itself perpendicular to FM layer as well as FM layer arranging itself perpendicular to the AF layer have been found.

For an optimal exchange biased system, one must strive for an FM/AF system in which the AF has large anisotropy, is single-crystalline, has fully compensated as well as in-plane oriented interfacial spins. Both FM and AF thicknesses need to be optimized.

### 3.3.2. Theoretical model summary

Early models (Meiklejohn, Néel) attempted to describe coupling between the FM and AF layers from a macroscopic perspective. Meiklejohn focused on the general description of an FM layer coupling to an uncompensated AF layer (fig. 3.23a), and Néel proposed a partial domain wall wound up within an FM layer acting as an "exchange spring" (fig. 3.23b). While robust and simple, their theories suffered from the lack of accuracy both qualitative and quantitative. They also made some rather restrictive assumptions which are not justified experimentally (a minimum FM layer thickness, for example).

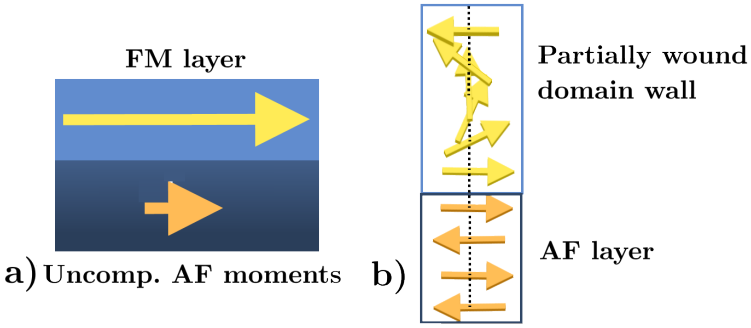


**Figure 3.23:** (a) Meiklejohn model, (b) Néel model.

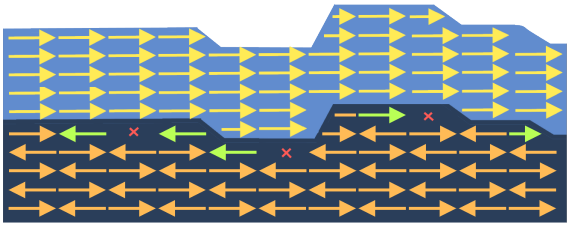

**Figure 3.24:** Schematic illustration of Malozemoff's model. Red crosses denote non-magnetic defects, green arrows denote uncompensated AF moments.

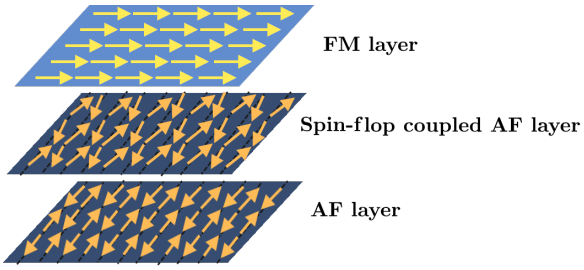


**Figure 3.25:** A schematic illustration of the frozen interface model.

Random interface field models provided a much better quantitative and qualitative relation to the experiment. It assumes that the interfacial roughness is chiefly responsible for exchange bias by creating locally uncompensated AF moments which are then capable of coupling to the FM layer (fig. 3.24). While these models provide quantitatively good results, having a rough interface is not a necessary condition for exchange bias to occur.

The frozen interface model was devised for atomically flat interfaces, it however assumed that the interfacial spins were frozen in a spin-flop-like coupling (fig. 3.25). This

theory showed similar accuracy to random interface field models and also explains perpendicular coupling, yet restrictive assumptions regarding both interfacial spin structure as well as strong AF layer anisotropy were made, neither of which is strictly necessary for exchange bias.

The local pinning field variation model is based on the idea of entire AF grains coupling to the FM layer. While quantitatively sound, monocrystalline AF films also show exchange bias, rendering the assumption of polycrystallinity as overly restrictive.

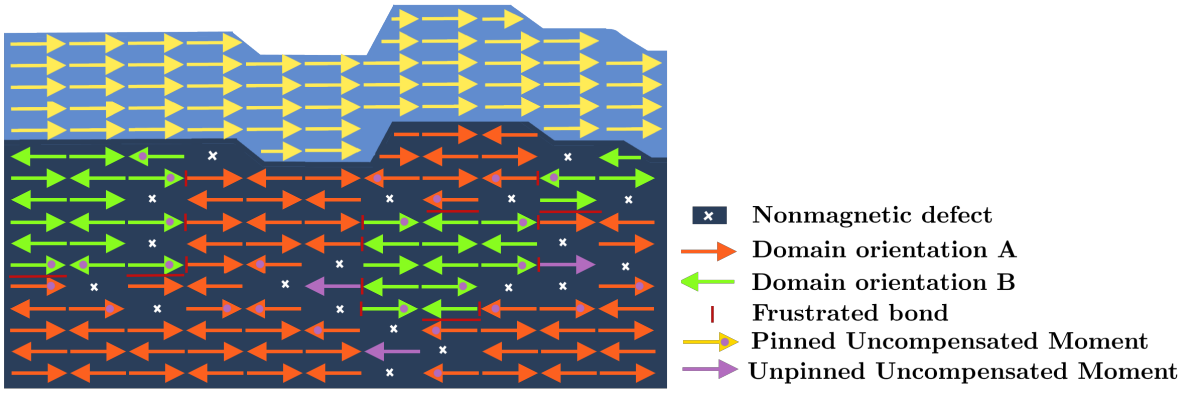


**Figure 3.26:** Schematic illustration of the domain state model.

The Domain State Model is the most accurate model to date. It builds upon the Imry-Ma argument that any finitely sized AF will have a spin imbalance between the two AF sublattices. This notion is then extended by modeling the AF domain formation alongside the defects that are naturally present (fig. 3.26). The AF domains, due to the presence of these defects, then possess uncompensated magnetic moments near the boundary (still coupled to the AF domain), which are free to couple to the FM layer above. This model makes no assumptions about the interfacial structure whatever and is in an excellent agreement with the experiment for systems with strong uniaxial AF anisotropy. The main limitation, however, is that the Ising model (up and down atomic magnetic moments) is only valid for AF layers with strong uniaxial anisotropy. For other systems with weak AF anisotropy, one must use the Heisenberg model, which, according to [146], worked just as well.

# 4. Experimental Methods and Techniques

This chapter will describe the techniques used for preparation of the sample as well as characterization and measurement, with the main part dedicated to Magneto-Optical Kerr Effect (MOKE) microscopy.

## 4.1. Magneto-Optical Kerr Effect

The magneto-optical Kerr effect (MOKE) was discovered by Reverend John Kerr in 1877. The phenomenon of magneto-optics can be described in the context of either macroscopic dielectric or microscopic quantum theory. From the macroscopic point of view, magneto-optic effects occur due to the antisymmetric off-diagonal elements in the dielectric tensor. Microscopically, the coupling between the electrical field of the light wave and the electron spin within a magnetic medium occurs through the spin-orbit interaction.

The classical approach assumes that the optical properties of a medium are determined by a dielectric tensor that is determined by the motion of the electrons in the medium. Thus, a microscopic description of the magneto-optic effect is related to different response of the electrons to different polarization of electromagnetic waves.

There exist three common configurations of measuring Magneto-Optic Kerr Effect in practice (fig. 4.1). Longitudinal and Polar MOKE modes cause the change of light polarization (rotation and ellipticity) as a function of the sample's magnetisation, whereas the Transverse MOKE is visible by the changing intensity of reflected light.

### 4.1.1. MOKE microscopy

The experimental setup consists of a ZEISS brand optical microscope, with a multiple LED white light source, connected to the microscope via optical fibers. The system includes a polariser as well as an analyser, both of which are necessary to register a change of polarization. The objective lens is cradled between two horizontally aligned, z-axis rotatable induction coils with split magnetic poles (used to induce in-plane magnetization). A bipolar current source is powering both coils, allowing for the field sweep in both positive and negative directions. Maximum safe magnetic field which can be achieved for a short period of time is 0.3 T, with maximum safe continuous field being equal to 0.1 T.

MOKE can be measured in three basic geometries, defined based on the orientaton of magnetisation with respect to the light plane of incidence (fig. 4.1a,b,c). For our experiments, all measurements were carried out in two different longitudinal MOKE configurations.

### 4.1.2. Longitudinal MOKE

In longitudinal MOKE (fig. 4.1a), linearly polarised light is incident on the sample at an angle interacts with the sample's magnetisation due to the Lorentz force acting on conduction electrons under acceleration from the EM wave. Upon reflection, a change

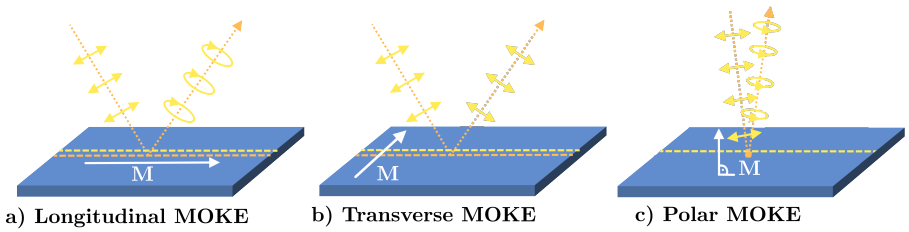


**Figure 4.1:** (a) Longitudinal (b) Transverse and (c) Polar MOKE geometries. Orange dashed line defines the plane of incidence, yellow dashed line defines the plane of incident light polarization, $M$ defines the magnetization component measured. In Longitudinal and Polar MOKE change of polarization in measured, whereas in Transverse MOKE change of light intensity is measured.

of polarisation (ellipticity and rotation) is measured. As the magnetisation direction is reversed, this ellipticity and rotation changes direction as well. In our case, all measurements were taken using Longitudinal MOKE mode in directions along the applied field and perpendicular to the applied field.

## 4.2. Thin film deposition and basic characterisation

Magnetron sputtering is a physical vapour deposition method of thin film deposition [152]. It is based on the collision process between the incident ions (typically Argon) and the target. In our case, once ionized, positive Argon ions then impact the sputter target, and transfer their energy to the target atoms effectively sputtering them off. This sputtered material then condenses on the surface opposite to the target, which is where the substrates are typically positioned.

Vibrating Sample Magnetometry (VSM) technique is used for the analysis of the whole sample after deposition. Its principle of operation is based on Faraday's law of induction. The sample is held vertically in between a set of two coils, one being the induction coil and the other being the reader coil. As the sample begins to vibrate, the signal received at the reader coil can be translated into the value of magnetizaion. This technique allows for the measurement of diamagnetic, paramagnetic as well as FM samples. With strong enough magnets, it is also possible to measure magnetic signal from AF materials after the spin-flop transition, or in our case, it is done by heating the sample above the AF-FM phase transition temperature.

X-Ray Diffraction (XRD) and X-Ray Reflectivity (XRR) techniques are based on X-rays diffracting/reflecting off the crystalline grid of the sample. Generally, XRD is used to determine the crystalline structure of the sample, and XRR is used to determine the sample thickness, and in the case of multilayers the individual thicknesses of each layer. However, the latter technique can be quite complicated, and requires curve fitting to work, as well as knowing some material parameters beforehand.

# 5. Exchange Bias Measurements

This chapter focuses on sample preparation and experiments performed with the goal of establishing exchange bias in Fe/$Fe_{50}Rh_{50}$ bilayers, Fe/$Fe_{50}Rh_{50}$ microstructures, ion irradiation-induced metastable FM $Fe_{50}Rh_{50}$ patterns as well as $Fe_{50}Rh_{50}$ nanowires at the AF-FM phase coexistence temperature.

## 5.1. Exchange bias in Fe-FeRh thin film bilayers

The bilayer system chosen for this project is based on the approach by Ippei Suzuki et al. [153]. In their article, they investigated exchange anisotropy in a Fe/$Fe_{50}Rh_{50}$ system grown on both MgO and $Al_2O_3$ substrates, with (001) and (111) film growth orientations, respectively. The reason why they selected these two particular configurations is that when $Fe_{50}Rh_{50}$ is prepared on the MgO(001) substrate, it is grown in the (001) orientation and has a G-type AF lattice (fig. 5.1a,c) which leads to a spin-compensated AF surface. In contrast, when it is grown on $Al_2O_3$ (0001) in the (111) orientation, it contains AF coupled spin-planes parallel to the substrate, with an uncompensated FM surface (fig. 5.1b,c).

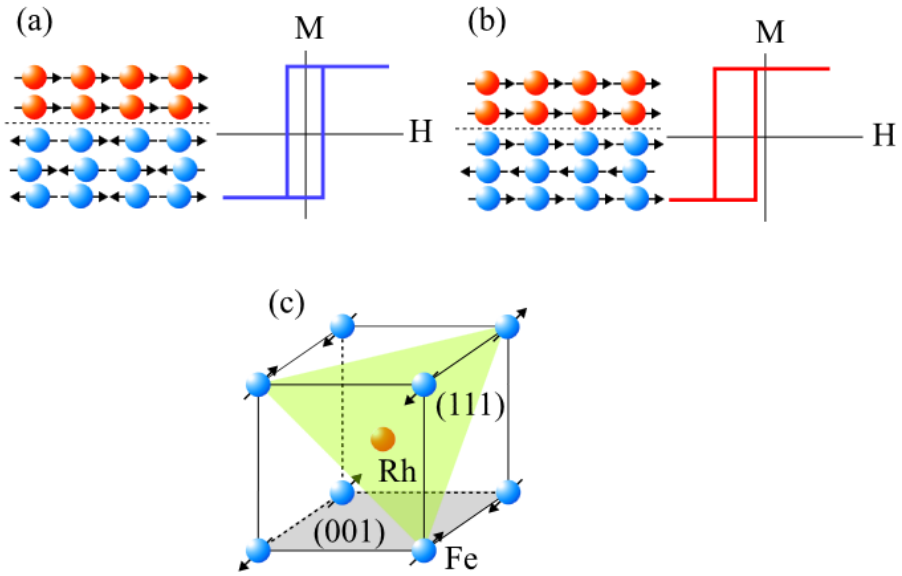


**Figure 5.1:** (a) Schematic illustrations of a FM/FeRh(001) interface and a hysteresis curve with no exchange bias and (b) a FM/FeRh(111) interface and a hysteresis curve with exchange bias. (c) Magnetic structure of AF FeRh with the compensated AF (001) planes and uncompensated FM (111) planes. Taken from [153]

.

$Fe_{50}Rh_{50}$ is an alloy featuring a metamagnetic (AF to FM) phase transition [154] at temperatures close to room temperature, at approximately 360 K in the bulk form. This enables easy-to-perform field cooling, which together with the FeRh high tunability, including high sensitivity of the phase transition to ion irradiation and subsequent thermal treatment (induction of a metastable FM phase [155],[156]) makes it an ideal candidate to investigate different aspects of exchange anisotropy in a single material. The lack

of understanding of the exchange coupling between the AF and FM phases as well as coupling to other materials provides a fertile ground for the study of exchange bias with the possibility of future applications.

### 5.1.1. Sample preparation

$Fe_{50}Rh_{50}$ thin films, 30 nm thick, were epitaxially grown on MgO (001) and $Al_2O_3$ (111) substrates using the BESTEC Magnetron sputtering system. After deposition, these films were annealed at 1070K for 45 minutes to restore the proper crystalline structure and chemical order, and thus the AF phase. Films were grown by Jon Ander Arregi Uribeetxebarria.

Due to BESTEC Magnetron system going out of service, the $Fe/Fe_{50}Rh_{50}/Al_2O_3$ sample was created by modifying an existing $Fe_{50}Rh_{50}/Al_2O_3$ sample in a UHV cluster system (fig. 5.2). Firstly, around 6 nm of $Fe_{50}Rh_{50}$ was sputtered off by Argon ion bombardment to make sure no impurities or oxides remained before the Fe deposition. Afterwards, the sample was annealed to restore the crystalline properties, and checked, within the same UHV cluster, using X-ray Photoelectron Spectroscopy (done by Ing. Tomáš Krajňák) for the presence of any unwanted contamination. Once the surface purity had been established, a 6 nm thick layer of Fe was deposited on the sample within the same UHV cluster using E-beam evaporation at room temperature (as to limit the diffusion of Fe into $Fe_{50}Rh_{50}$). This work was done by doc. Ing. Jan Čechal, Ph.D. and Ing. Tomáš Krajňák with the help of the author.

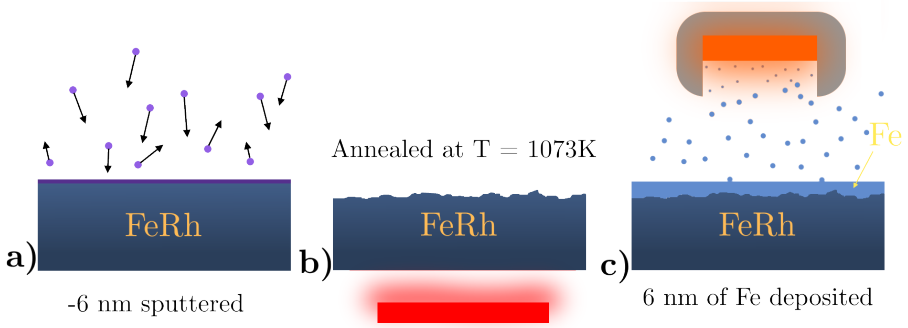


**Figure 5.2:** Fe/FeRh bilayer preparation procedure. a) Ar plasma etching to remove surface contamination. b) Annealing of FeRh to restore the AF phase, c) Deposition of the Fe layer.

### 5.1.2. Sample characterization

After sputtering, annealing, and deposition of Fe, Scanning Electron Microscope (SEM) and Atomic Force Microscopy (AFM) images were taken to gain insight into the character of the sample surface (fig. 5.3).

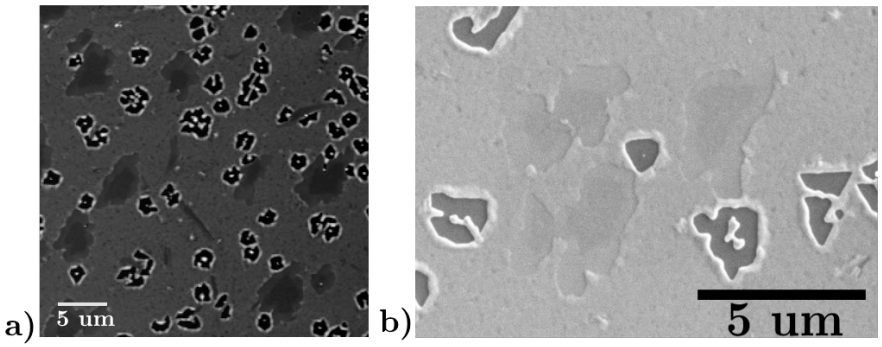


**Figure 5.3:** (a) AFM image of the Fe/FeRh/$Al_2O_3$ sample; (b) SEM image of the Fe/FeRh/$Al_2O_3$ sample.

The sample itself is covered in dewetted areas, valley terraces and has an otherwise relatively rough surface (fig. 5.3). Dewetted, deep hole areas are a characteristic side effect of FeRh thin film annealing process, and very likely existed before the Fe deposition was made. From the AFM data one can extract that the holes are as deep as the film, around 30 nm. The terraces, on the other hand, are interesting in that they are graduated in steps of 5 and 10 nm in depth. When measured using longitudinal MOKE, both terrace areas as well as the rough film showed ferromagnetic behaviour at room temperature, with terraces having lower coercivity and similar saturation magnetization signal. The terraces likely formed when the Fe film was deposited over some dewetted areas.

With the help of Jon Ander Arregi Uribeetxebarria, X-Ray Reflectivity (XRR) spectrum was measured to find the approximate layer thickness. Using curve fitting it was found that the thicknesses correspond to 6 nm of Fe and 22 nm of FeRh.

### 5.1.3. Field cooling

Field cooling (fig. 5.4) was performed in the sample chamber of the Quantum Design VERSALAB Vibrating Sample Magnetometer (VSM), with the exact conditions mentioned in the paper by Suzuki et al. [153], in order to best replicate the results they achieved. The field cooling sequence has the following steps:

- Heat the sample up to 400 K, above the metamagnetic AF-FM phase transition temperature.
- Apply magnetic field of 1.5 T.
- Apply magnetic field of 0.8 T.
- Cool the sample down to 250 K in an applied field of 0.8 T.
- At 250 K, stop the application of the magnetic field.
- Return to 300 K and remove the sample.

### 5.1.4. Interface coupling configuration of a Fe/FeRh system

The first exeriment addressed the question whether the exchange bias takes place perpendicular to the Field Cooling (FC) direction or parallel to it. In practice, this means that if the exchange bias is perpendicular to FC, then the AF film is coupled perpendicularly to the FM film (fig. 5.4). According to the article by Suzuki et al. [153], the unidirectional anisotropy for a $Fe/Fe_{50}Rh_{50}/Al_2O_3$ system can be seen when the applied field is perpendicular to the FC direction, which means that the AF moments couple parallel to the FM layer.

Using MOKE, the problem was approached using 4 different measurement configurations (fig. 5.5), in order to establish the presence and orientation of the exchange anisotropy with respect to the FC direction (fig. 5.4).

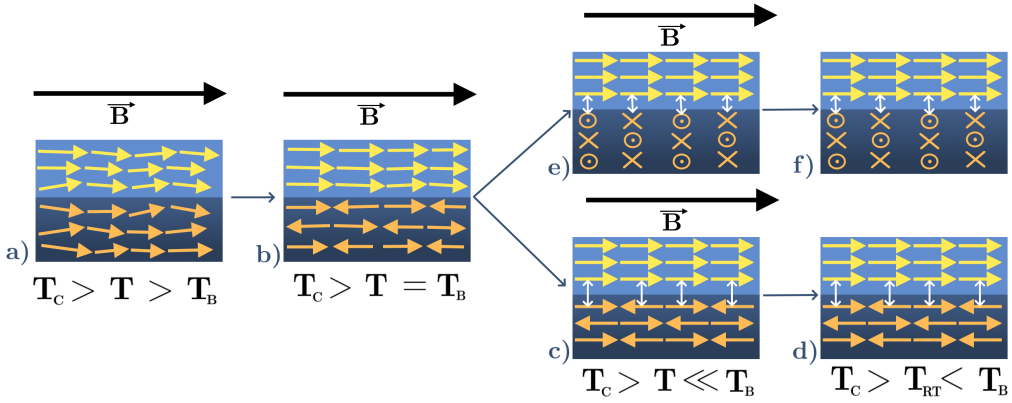


**Figure 5.4:** Field cooling process: a) Sample is heated above the blocking temperature, b) It is cooled down below the blocking temperature in an applied field, c)e) it is then cooled down significantly below the blocking temperature and the field is removed. d)f) Sample is at room temperature, c),d) represent parallel FM-AF coupling, while e),f) represent perpendicular FM-AF coupling.

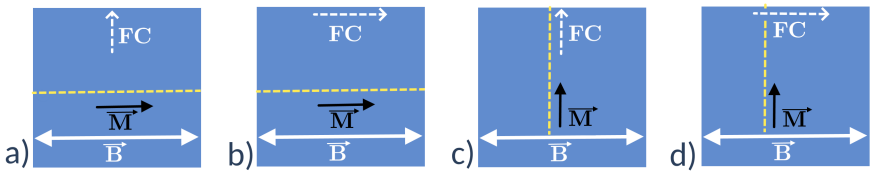


**Figure 5.5:** Possible MOKE arrangements for measuring the exchange biased magnetization components in the Fe film: a) Longitudinal MOKE with FC perpendicular to the applied field; b) Longitudinal MOKE with FC parallel to the applied field; c) Longitudinal MOKE of transverse magnetisation with FC perpendicular to the applied field; d) Longitudinal MOKE of transverse magnetization with FC parallel to the applied field. The dashed line indicates the plane of incidence.

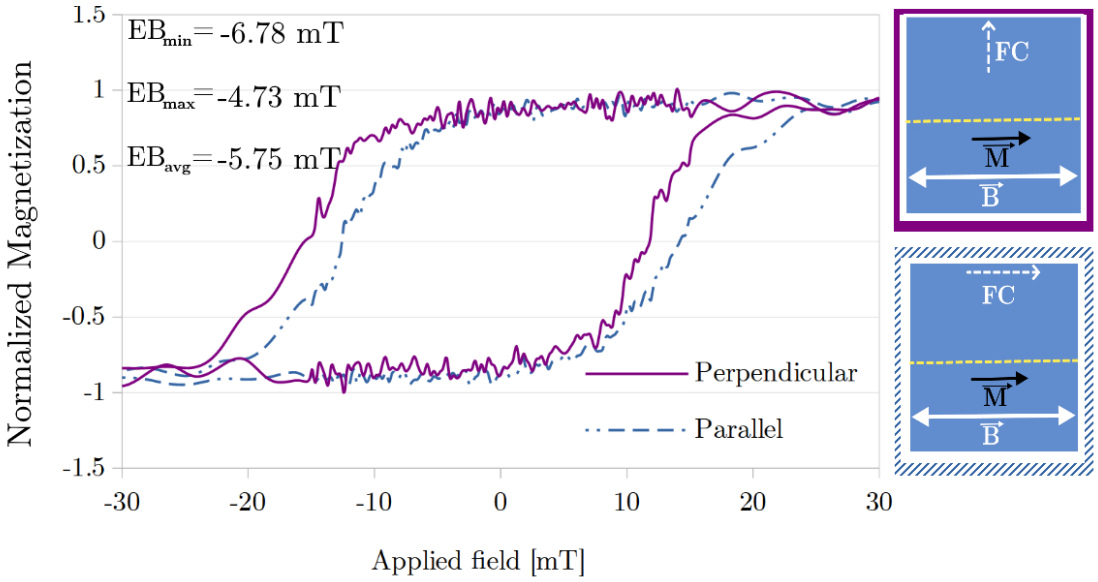


**Figure 5.6:** Comparison between the hysteresis loops measured parallel to FC direction and perpendicular to FC using longitudinal MOKE. $EB_{min}$, $EB_{max}$ and $EB_{avg}$ mark the maximum, minimum (95% confidence) and average value of the relative loop shift between the parallel and the perpendicular FC orientations.

The measurements of the longitudinal magnetisation reversal parallel and perpendicular to the FC direction (fig. 5.6) demonstrate that for the perpendicular FC direction, the loop is visibly shifted to negative values. The shift of the parallel direction loop to positive values is likely related to an error in the system zero field value. Nevertheless, calculating the difference between the centres of these two hysteresis loops provides a value of the loop shift of -5.8 mT (fig. 5.6), and it agrees reasonably well with the value obtained by Suzuki et al. [153], which is between -4.4 mT and -3.2 mT depending on the exact FC orientation relative to the sample crystallographic orientation.

Longitudinal MOKE measurements of the transverse magnetization component (perpendicular to the external field) in the parallel FC and perpendicular FC configurations contain information about the rotational asymmetry (fig. 5.7). In a normal, unbiased system, the magnetization under an applied field changes its direction primarily by rotation (fig. 5.8(1-5)), and this change is symmetric regardless of the magnetization reversal direction.

However, i the fig. 5.7 for the case of FC-perpendicular applied field, there is a significant peak asymmetry, which suggests that as the magnetization reverses in the direction opposite to the biasing field, unidirectional anisotropy pins the magnetization and makes it more energetically favourable to create a domain facing in the opposite direction, which is then expanded by the externally applied field (fig. 5.8(6-10)).

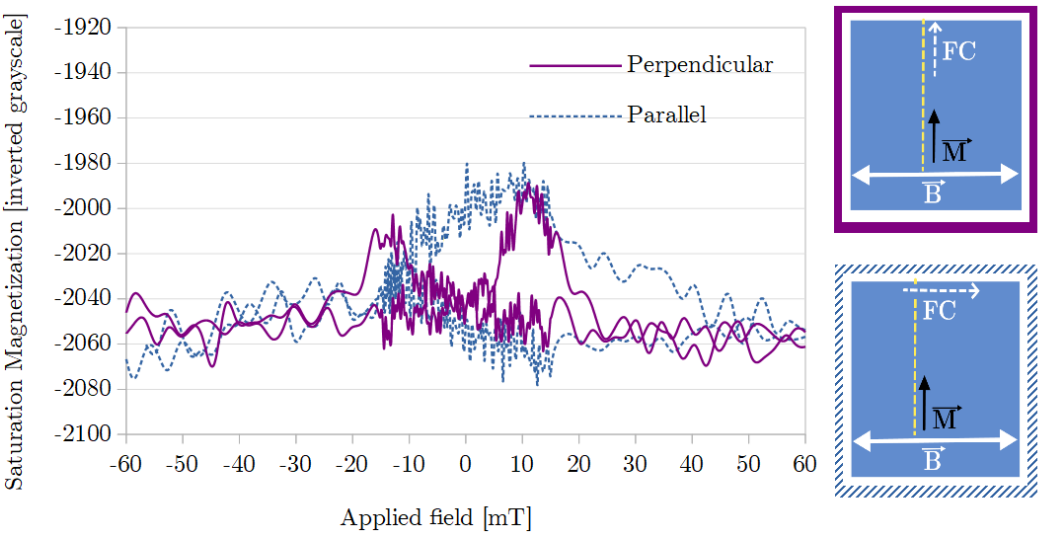


**Figure 5.7:** Comparison between the reversals of magnetisation component transverse to the applied field, measured in FC-parallel direction and FC-perpendicular direction.

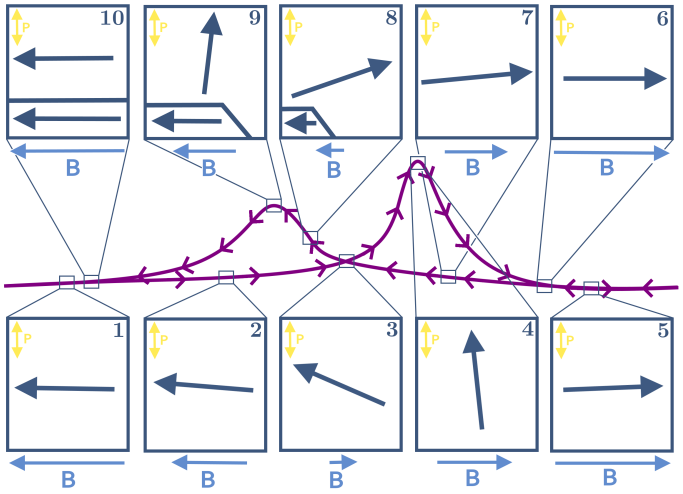


**Figure 5.8:** Scheme of magnetisation reversal asymmetry from an exchange biased thin film. For diagrams 1-5, magnetization reversal proceeds through coherent rotation. For diagrams 6-10, as the reversal takes place in the opposite direction to the exchange bias, it involves a combination of rotation and domain nucleation.

In the case of field applied parallel to FC direction (fig. 5.7), we can also find this peculiar rotational asymmetry, as well as significant peak broadening. The peak broadening can be explained by the fact that we have a unidirectional anisotropy perpendicular to the applied field. Given that the transverse magnetisation component coincides with the exchange bias direction, the magnetization of the sample appears to reverse much earlier and gets ”stuck” in that direction induced by exchange bias. Likewise once the negative field is applied, the peak keeps on broadening as the magnetic moments are stuck in the direction set by exchange bias.

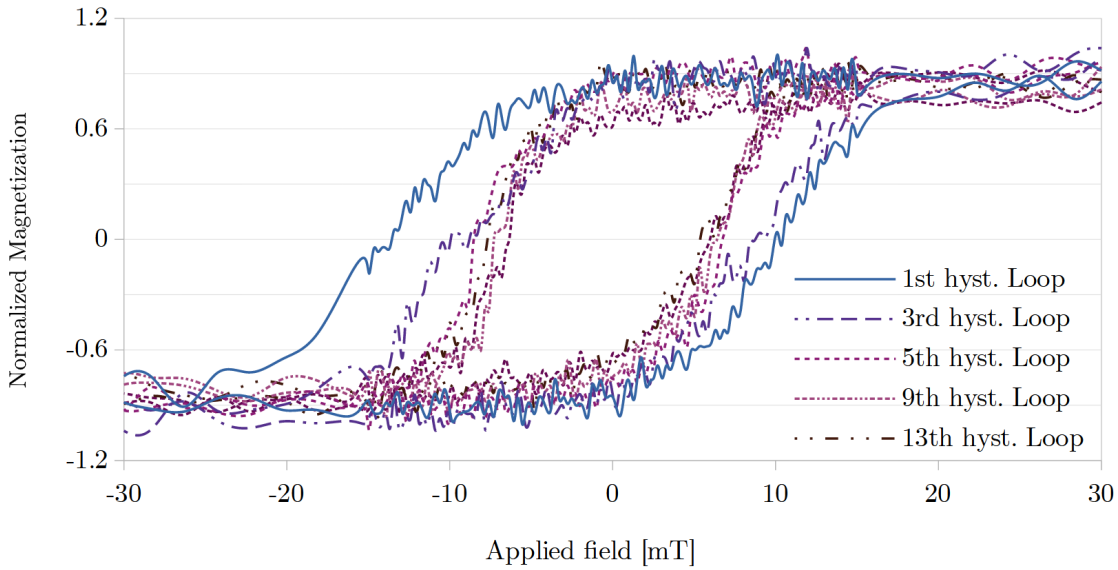


**Figure 5.9:** Subsequent hysteresis loop measurements of Fe/FeRh bilayer taken at room temperature, perpendicular to the FC direction; only odd measurements of the series are shown.

### 5.1.5. Training effect in the Fe/FeRh system

A series of longitudinal MOKE measurements of magnetisation reversal perpendicular to the FC direction (fig. 5.9) shows that within the first 3 hysteresis loops, both loop shift and coercivity dropped significantly (fig. 5.10). This is related to the AF grains reorienting themselves in a more stable configuration after a few cycles of complete FM layer reversal (read more in section 3.1.5). The training effect is a common feature of exchange biased systems with polycrystalline or weakly anisotropic AF films. This suggests that the epitaxial FeRh films feature AF anisotropy weak enough to present the training effect, i.e., the AF texture is suspectible to rearrangement by AF-FM exchange coupling.

The magnetisation component transverse to the applied field presents a similar trend in the evolution of rotational asymmetry, marking the gradual disappearance of exchange bias. The transverse magnetisation was analysed at even field cycles, yielding a significant peak asymmetry during the second field cycle. In contrast, the 16th field cycle showed two nearly symmetrical peaks (fig. 5.11). Plotting the peak asymmetry vs. the number of field cycles (fig. 5.12) yields a dependence that closely resembles the vanishing of the loop shift and the decrease of coercivity (fig. 5.10).

### 5.1.6. Discussion

The presented data agree both quantitatively and qualitatively with the results found in [153]. Firstly, exchange bias was present in the direction perpendicular to FC, but not parallel, in full accordance with [153]. Furthermore, the loop shift is quantitatively very close to the one reported. We have expanded upon the current understanding of the system by evaluating the training effect in the direction parallel and transverse to the applied field. The loop shift is accompanied by rotational asymmetry, and as described in the chapter on experimental evidence of exchange bias (section 3.1.1, it is a convincing signature of exchange anisotropy.

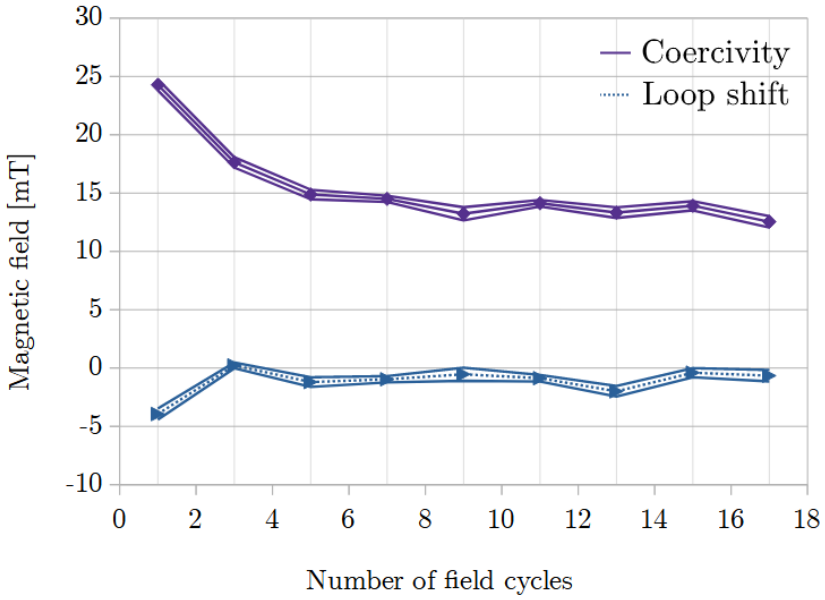


**Figure 5.10:** Coercivity and loop shift magnitude as a function of the number of field cycles.

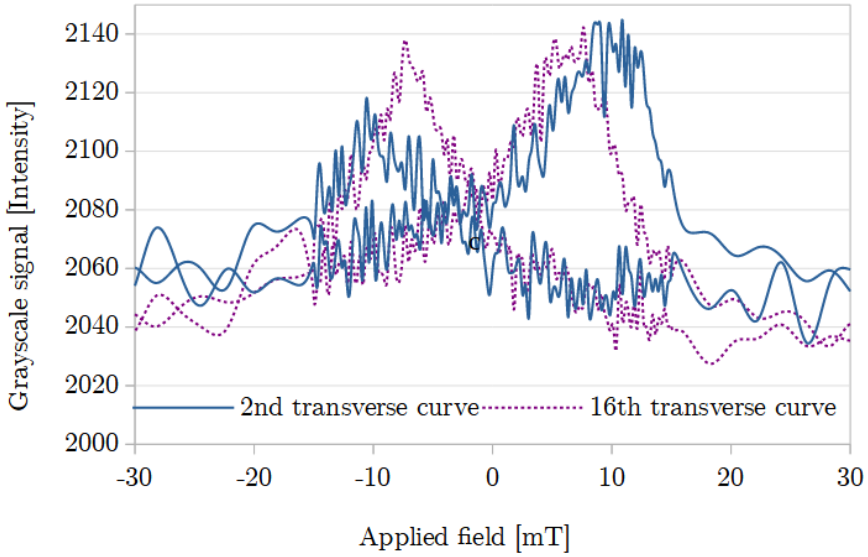


**Figure 5.11:** MOKE signal of the magnetization transverse to the applied field as a function of applied magnetic field. The field is applied perpendicular to the FC direction.

It is worth noting that the processes used for preparation of Fe/FeRh bilayers in our case were different to [153], which used Molecular Beam Epitaxy (MBE) for the entire deposition process, whereas we used magnetron sputtering for the preparation of FeRh and e-beam evaporation for Fe after ion irradiation and annealing of the FeRh thin film. This suggests that both the interface quality as well as the thin film quality in our case was inferior to the MBE prepared system. Interestingly despite having an uncompensated spin-plane at the interface, it appears that interface roughness does not play a significant role, as quantitatively we obtained very similar, even slightly larger, values of exchange bias.

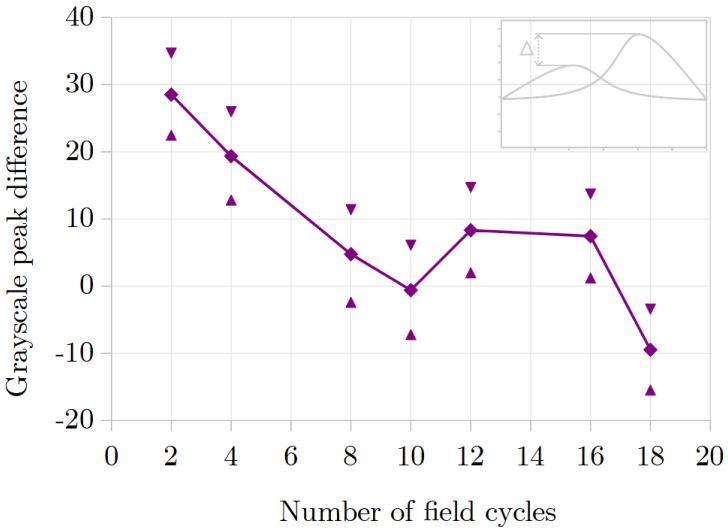


**Figure 5.12:** Transverse magnetization peak height difference as a function of the number of field cycles. Triangles mark the 95% confidence interval.

It can be concluded that exchange bias in $Fe/FeRh/Al_2O_3$ cannot be solely attributed to highly uncompensated interfacial structure, otherwise there would have been a significant discrepancy between our data and those obtained by Suzuki et al. [153] given the different process of sample preparation. This is also supported by further experimental evidence hinting at the fact that compensation at the interface is not the deciding factor of exchange bias presence (more in section 3.1.8).

## 5.2. Exchange bias in Fe-FeRh microstructures

The next goal was to investigate the exchange anisotropy behaviour in bilayered microstructures. The general expected behaviour of confined bilayers involves the decrease of blocking temperature and exchange bias, due to weakening of the magnetocrystalline aniostropy [157].

### 5.2.1. Microstructure preparation

Preparation of $Fe/Fe_{50}Rh_{50}/Al_2O_3$ microstructures was done using an XMU MIRA3 Scanning Electron Microscope/E-beam writer combined system following the procedure described in Appendix A.

The geometry of selected microstructures consisted of rectangles, oriented at 0, 90 and 45 degrees and with different aspect ratios, as well as arrays of microdiscs (fig. 5.13). These shapes were chosen to investigate the effects of shape anisotropy and confinement in varying directions relative to the field cooling direction and crystallography axes.

### 5.2.2. Exchange bias measurements

The measurement of the patterned microstructures proved to be difficult, as the MOKE signal was very weak. Nevertheless, we have measured a series of hysteresis loops on a 10x8 $\mu m^2$ structure and find the expected loop shift (5.14). The extracted

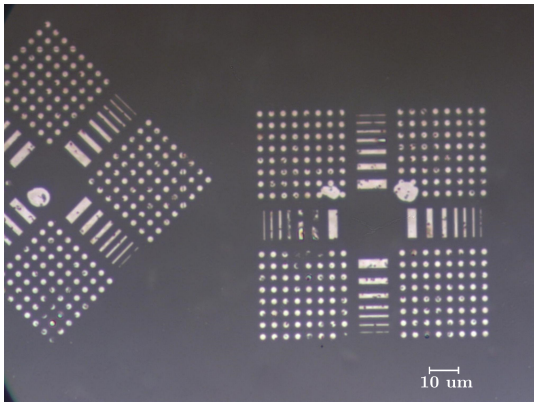


**Figure 5.13:** Optical microscope image of E-beam lithography prepared microstructures.

values of coercivity and loop shift are plotted in fig. 5.15 analogously to fig. 5.10. The measurements of even smaller structures lead to no ferromagnetic signal whatsoever, so they were, unfortunately, omitted.

The signal-to-noise ratio in this measurement is generally not enough to suggest any clear trend, either for the coercivity or loop shift. Following the results on the training effect in continuous films, one might expect the first hysteresis loop after field cooling to show the strongest exchange bias, but any loop shift can be discarded within the 95 % confidence interval.The oscillations in 7th and 9th measurements, are only attributable to poor signal-to-noise ratio, as it was very difficult to obtain reasonable linear regression lines for those measurements.

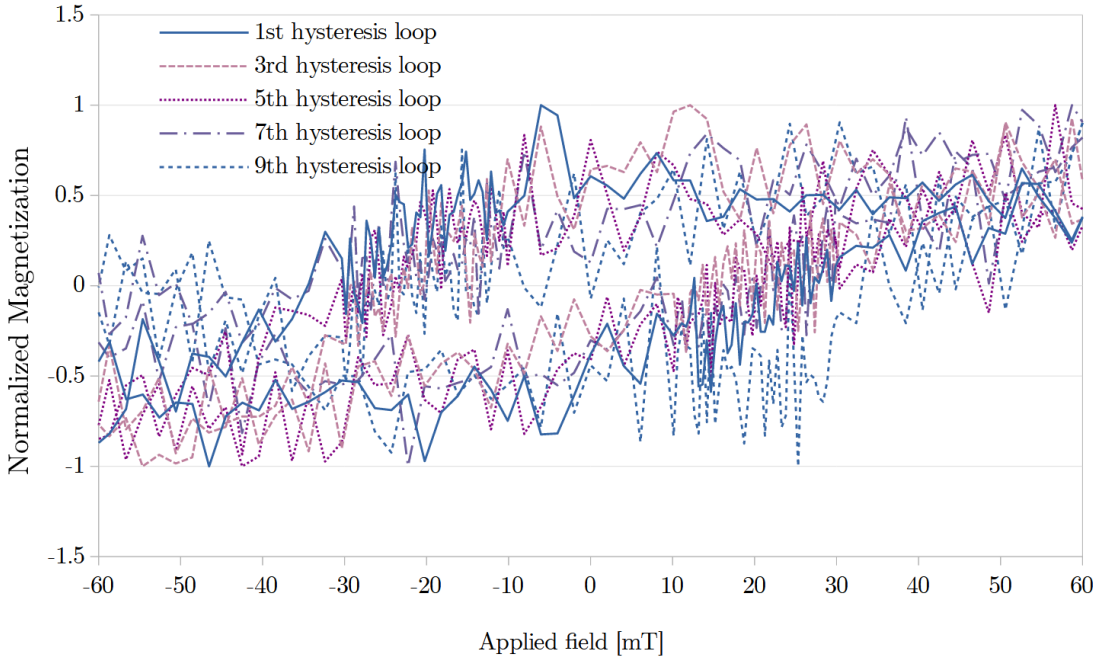


**Figure 5.14:** Subsequent hysteresis loops measured on Fe/FeRh microstructures using longitudinal MOKE.

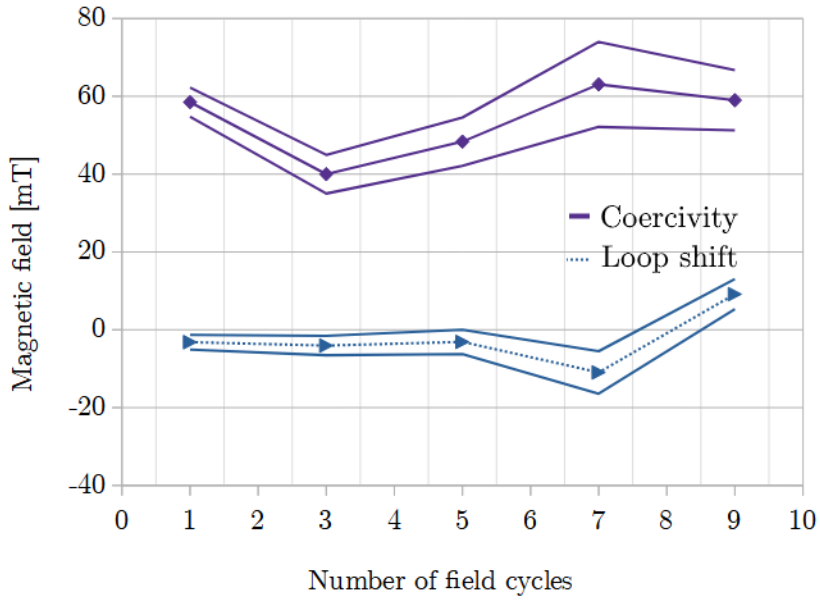


**Figure 5.15:** Coercivity and loop shift measured on a 10x8 $\mu m^2$ structure as a function of subsequent field cycles. Solid lines define the 95% confidence intervals.

### 5.2.3. Discussion

Measurements of exchange bias in Fe/FeRh microstructures were inconclusive due to exceedingly weak ferromagnetic signal from the Fe layer, which prevented measurement of the FM signal from the patterned microstructures. Exchange bias in such microstructures likely still occurs, but magnitude may be lower due to shape confinement effects [157]. The reason for the weak and unreliable signal could likely be traced back to the lithographic preparation process not being done correctly to completely remove the 60 nm $SiO_2$ layer, which could have reduced the signal considerably. In future, the lithography process will be further optimized.

## 5.3. Exchange bias in FeRh nanowires at FM-AF phase coexistence

This experiment was primarily motivated by the fact that exchange bias was found to spontaneously form in systems undergoing structural (and as a consequence, magnetic) phase transition [158], as well as within chemically heterogeneous systems with FM and AF phase coexistence [30],[31],[32],[33]. Spatial confinement to the wire geometry is intended to achieve well defined AF-FM phase boundaries.

### 5.3.1. Nanowire preparation

The nanowires were prepared using the same procedure listed in Appendix A. Wires of width of 1 $\mu$m, 0.5 $\mu$m and 0.25 $\mu$m were prepared (fig. 5.16). We selected the 0.5 $\mu$m wide wires for the measurements, as they represented a compromise between the stepwise FM-AF phase transition with large domains at the phase coexistence [159] and the diffraction limit of our visible light MOKE setup.

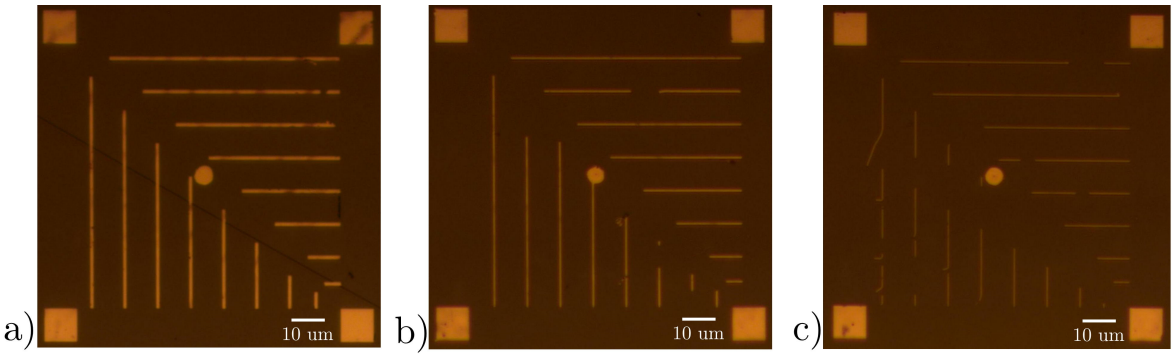


**Figure 5.16:** FeRh nanowires on the MgO substrate prepared using E-beam lithography; (a) 1 $\mu$m wires, (b) 0.5 $\mu$m wires, (c) 0.25 $\mu$m wires.

### 5.3.2. Exchange bias measurements

The first step was to establish the phase coexistence of both FM and AF domains. Unfortunately, due to weakness of the signal as well as the diffraction limit, direct observation of domains was not possible. The phase transition was followed by monitoring the integral MOKE signal with decreasing temperature which marked a decrease of the saturation magnetization (fig. 5.17). The aim was to obtain a state in which the majority of the wire transitioned to the AF phase, and minority of the wire remained in the FM phase. In practice this would mean a point at which the FM signal from the wire was nearly diminished, which is exactly what happens at $T = 95°\mathrm{C}$ (fig. 5.17).

Once this temperature was reached, the wire was measured in separate sections to evaluate the local FM content (fig. 5.18). The next step cconsisted in finding an area where both FM and AF phases coexisted. This was achieved by selecting a region of interest at the bondary of sections where some FM signal was recorded with that of no FM signal.

Area E (fig. 5.18) was selected as a candidate for possible exchange bias evaluation. Performing the measurement in the longitudinal MOKE with field applied along the wire

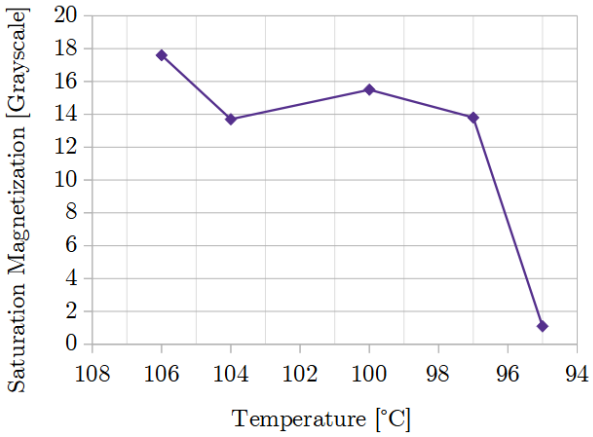


**Figure 5.17:** Relative saturation magnetization as a function of decreasing temperature.

results in recognizable hysteresis loops (fig. 5.19). From this data, we can plot the coercivity and loop shift (fig. 5.20). Additionally, longitudinal MOKE measurements with field applied perpendicular to the wire were performed, however the nature of such hysteresis loops (with ambiguous crossing of the M = 0 line) as well as a poor signal-to-noise ratio preclude any analysis of either the coercivity or loop shift of that configuration (fig. 5.21).

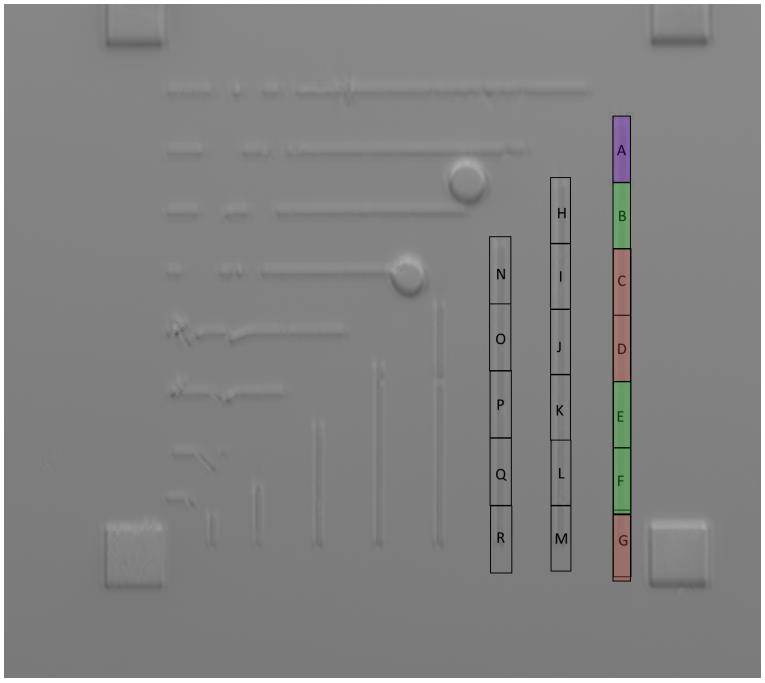


**Figure 5.18:** Map of wires as imaged by the Kerr microscope. Green areas have measurable FM signal, red areas do not show any FM signal, and purple areas show complex (superposition of two or more hysteresis loops) signal.

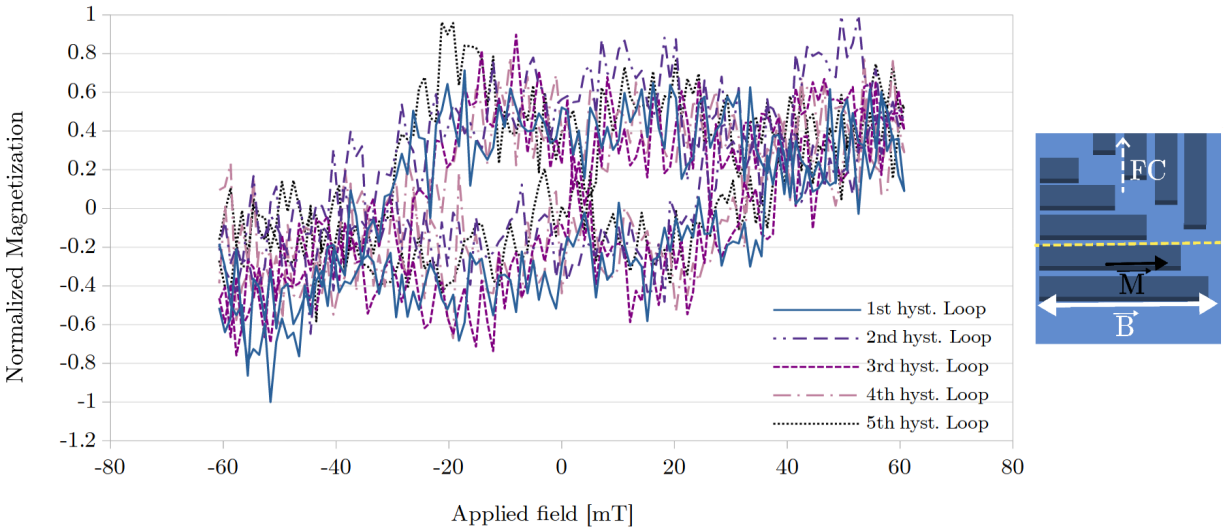


**Figure 5.19:** Subsequent longitudinal MOKE hysteresis loops measured from the E area of a 500 nm wide wire at 95°C.

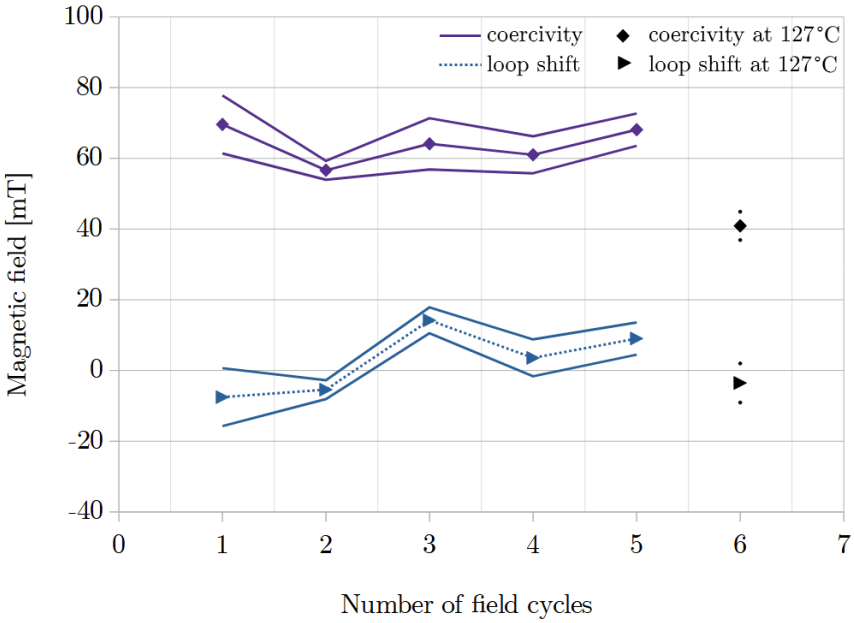


**Figure 5.20:** Coercivity and loop shift plotted for each subsequent hysteresis loop taken at 95°C. Solid lines above and below the measurement denote the 95% confidence interval of linear regression. Measurement 6 is from the entire wire taken at 127 °C.

### 5.3.3. Discussion

From the analysis of longitudinal MOKE measurements in suspected areas of FM and AF phase coexistence, we highlight the following findings. Firstly, as plotted in fig. 5.20, it is apparent that when compared to measurements of the same wire, the coercivity is significantly higher, which is an indicative sign of the AF-FM coupling. Secondly, from

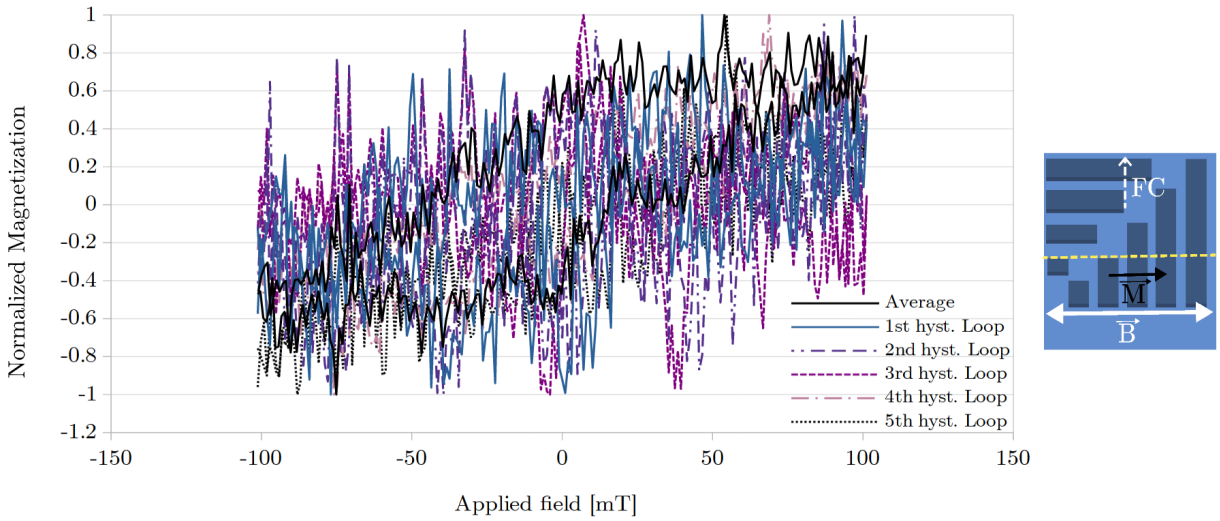


**Figure 5.21:** Hysteresis loops measured using longitudinal MOKE with field applied perpendicular to the 500 nm wire axis. Measured at 95°C.

fig. 5.20 it can be deduced that besides the first and the second measured loops, third, fourth, and fifth have the loop shifted comfortably to the positive values.

This shift appears to be positive likely because all the measurements in this section finished the scan with the wire left in the negative remanent magnetization state (fig. 5.22a), which could act as a pinning direction reference. In this case, instead of cooling in an applied field, cooling from an FM state at 127 °C with a well-defined remanent magnetisation vector may be sufficient for inducing unidirectional AF anisotropy (fig. 5.22b,c,d). This would set the AF uncompensated spins prior to the subsequent field cycling. The quantitative magnitude of the resulting loop shift can be disputed, but qualitatively it needs to be positive (see fig. 5.22e).

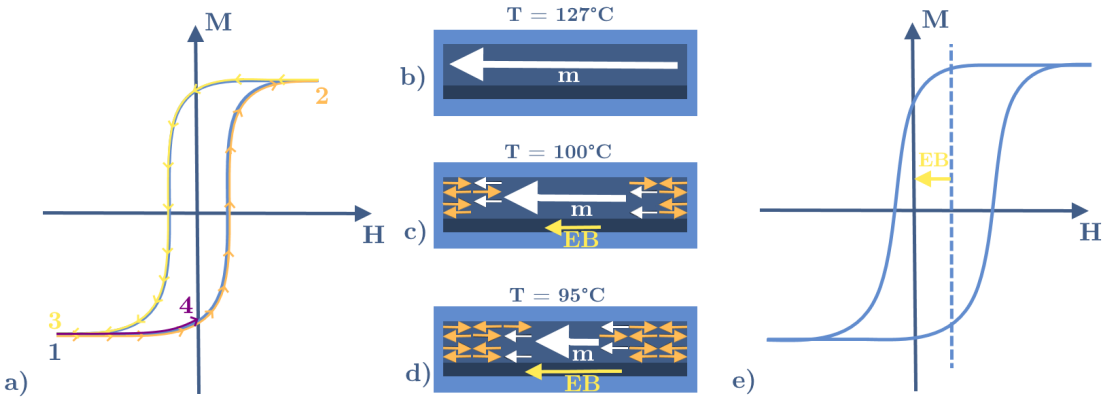


**Figure 5.22:** Explanation of the positive loop shift for FeRh/MgO nanowires. (a) Hysteresis loop measurement procedure: starting at the negative applied field, first hysteresis loop branch is measured going from negative to positive field (1-2); then the second branch is measured going from positive to negative field (2-3), and then the field is reduced to zero, leaving magnetization in the negative remanence state (3-4). (b-d) The sample is gradually cooled across the FM-AF phase transition. (e) Negative exchange bias due to negative remanence results in the hysteresis loop shifted to positive field values.

The exchange bias loop shift detected along the wire implies that the AF spin axis is also oriented along the wire axis. This seems surprising, as FC across the phase transition from the FM phase results in an AF spin axis perpendicular to the FC direction (see fig. 5.23a) [160]. In FeRh thin films, the symmetric compressive strain exerted by the substrate results in biaxial AF anisotropy (fig. 5.23b). However, in nanowires, there is significant strain relaxation due to the removed material [161] in the in-plane direction perpendicular to the wire axis (fig. 5.23c). This relaxation means that the atoms are spaced closer along the wire axis and further apart perpendicular to it (fig. 5.23d). Because of this, the AF axis orients along the direction of closer atom spacing [162], thus causing exchange bias in the respective direction. We suggest that this magneto-elastic effect is behind the exchange bias orientation at AF-FM coexistence in FeRh nanowires.

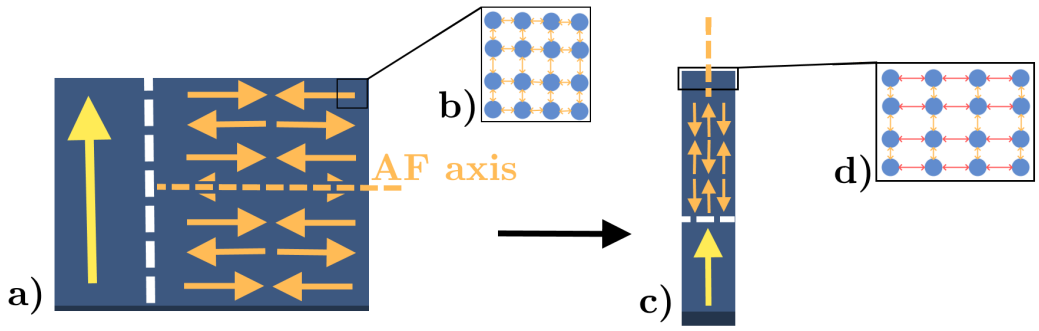


**Figure 5.23:** AF axis orientation in FeRh systems: a) FeRh thin film, AF axis orientation perpendicular to the FM magnetization after FC across the FM-AF transition; b) Laterally symmetric compressive strain exerted by the MgO substrate; c) FeRh nanowires, AF axis orientation is along the wire and parallel to the FM magnetization during the FM-AF transition; d) FeRh in the form of nanowire experiences strain relaxation in the direction perpendicular to the wire direction, which causes the AF axis to orient along the direction of nearest neighbor atoms.

## 5.4. Exchange bias in irradiated FeRh stripes

The final experiment aims to create AF-FM bondaries by inducing permanent FM phase within the FeRh thin film by ion irradiation [155]. This effect is mainly based on energetic ions creating defects and dislocations via collision cascades which result in the disturbance of stoichiometry, giving rise to FM behaviour. Such an irradiated area would be surrounded by the AF film, providing a condition for the exchange anisotropy to occur.

### 5.4.1. Pattern preparation

The stripe patterns (fig. 5.24) were inscribed using a TESCAN LYRA3 SEM/FIB dual beam microscope. Gallium ions accelerated to an energy of 30 keV were used, with an optimal area dose for inducing FM order set at $5 \cdot 10^{12}$ ions/cm$^2$ according to [155]. Different orientations were defined in order to verify both the possible influence of the magnetocrystalline anisotropy, as well as the field cooling direction. Patterns of different widths (500 nm, 1 $\mu$m, 1.5 $\mu$m and 2.0 $\mu$m) were prepared.

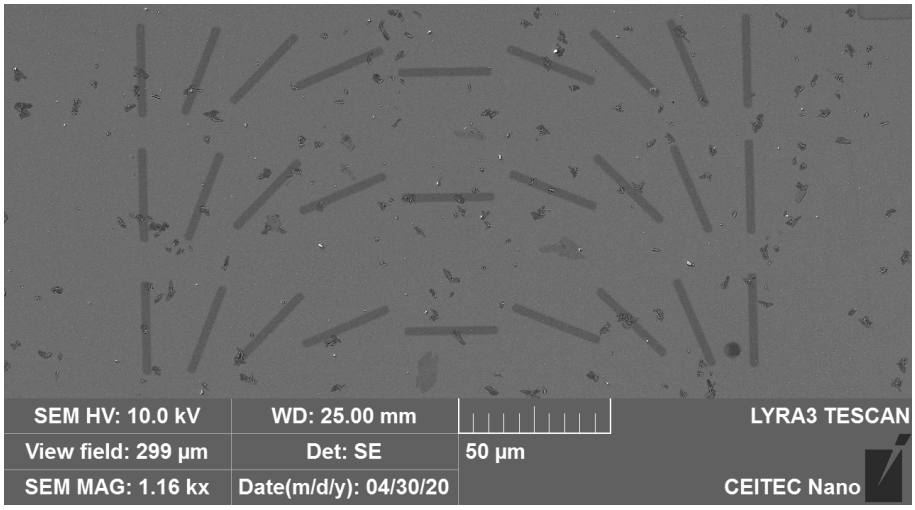


**Figure 5.24:** Irradiated stripes (2x30 $\mu$m$^2$) created by Gallium FIB as imaged in TESCAN LYRA3 SEM.

### 5.4.2. Field cooling

Field cooling (fig. 5.4) was performed in the sample chamber of Quantum Design VERSALAB Vibrating Sample Magnetometer (VSM), with the following steps and parameters:

- Heat the sample up to 400 K, above the metamagnetic AF-FM phase transition temperature.
- Apply magnetic field of 3 T.
- Cool the sample down to 55 K in an applied field of 3 T.
- At 55 K, remove the magnetic field.
- Return to 300 K and remove the sample.

### 5.4.3. Exchange bias measurements

Two primary stripe orientations relative to FC direction were investigated and measured. First, using longitudinal MOKE hysteresis loops of patterns of different widths were measured and analyzed for the presence of exchange anisotropy. Then the sample was rotated by 90 degrees to measure the stripes which were perpendicular to the FC direction.

For the case of FM stripes oriented both along the FC direction (fig. 5.25) as well as perpendicular to it (fig. 5.26), no discernible exchange bias was detected (fig. 5.27).

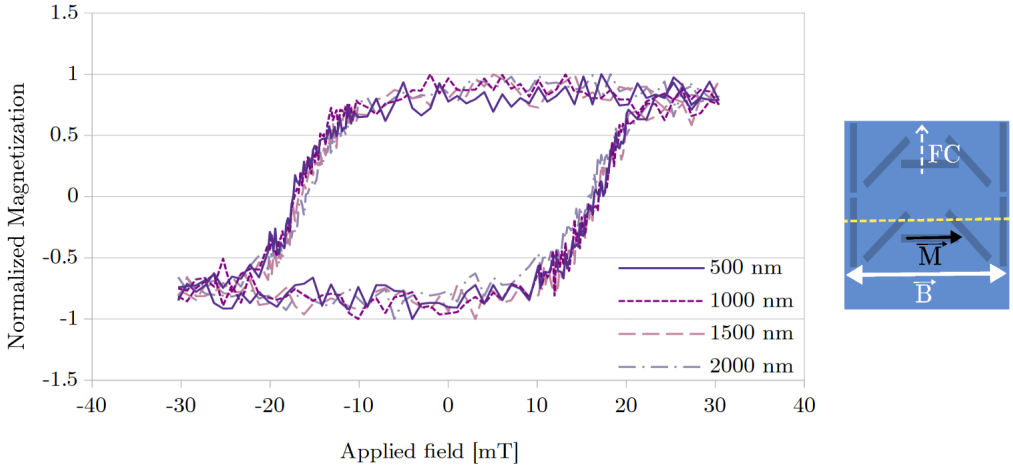


**Figure 5.25:** Longitudinal MOKE measurements taken for FIB-patterned FM stripes along the field cooling direction.

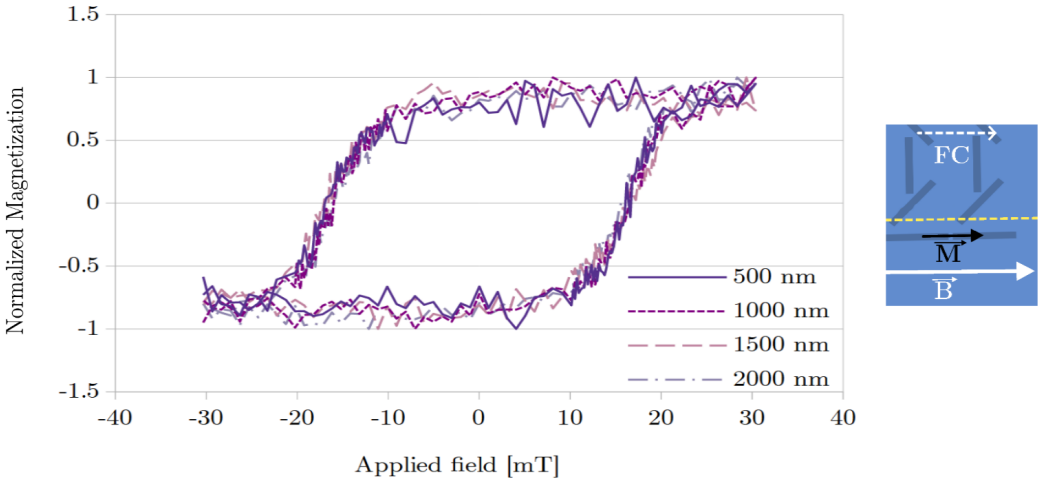


**Figure 5.26:** Longitudinal MOKE measurements taken for FIB-patterned FM stripes perpendicular to the field cooling direction.

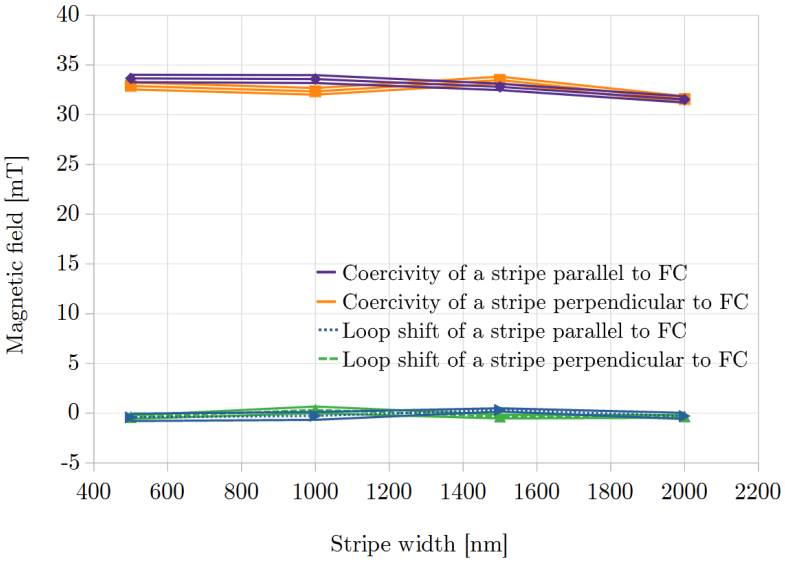


**Figure 5.27:** Coercivity and loop shift of FIB-induced FM stripe patterns in FeRh perpendicular and parallel to the FC direction.

### 5.4.4. Discussion

No exchange bias was detected in FIB-induced FM stripes in FeRh in any of the selected configurations. This is likely because the Ga ions upon entering the sample create a disordered interface between the irradiated, metastable FM phase (fig. 5.28b)and stable AF phase (fig. 5.28a). A study evaluating exchange bias between an FM and AF layer separated by a non-magnetic spacer [120] shows that exchange bias decreases exponentially with increasing thickness of the spacer, and is completely suppressed at a spacer thickness on the order of a few nm. If one considers the intermediate phase separating the transformed FM and well-ordered AF phase to be also non-magnetic, spanning on the order of the spot-size of the Ga FIB (around 30 nm), then it is reasonable to expect that the exchange bias in such a system may be completely suppressed (fig. 5.28c). The same FIB irradiation experiment was also performed for FeRh grown on $Al_2O_3$ with identical results, so likely the AF ordering orientation is not the explanation for the absence of exchange bias in this system.

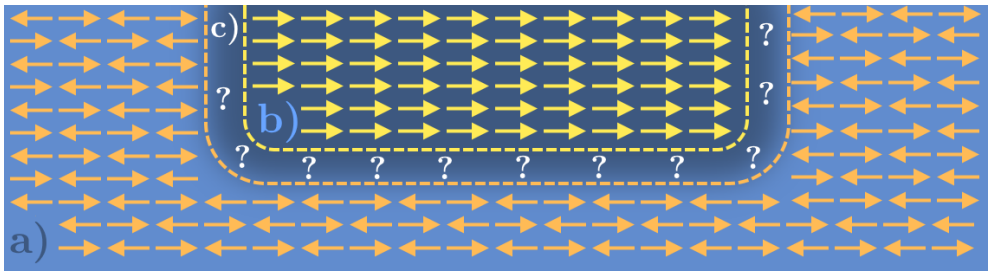


**Figure 5.28:** Schematic illustration of (a) AF FeRh thin film and (b) FIB-induced metastable FM FeRh area with an intermediate disordered phase at the interface induced by Ga ion irradiation.

# 6. Summary

The presented thesis covers multiple approaches of inducing exchange bias in different model systems along with a detailed literature review on the topic of exchange bias in bilayers, including detailed experimental evidence to the mechanism of the effect and the factors which influence it. From experimental evidence, it follows that exchange bias stems not simply from the interfacial character, but also from the disorder within the AF lattice, while the AF-FM interface also plays a role.

Chapter 3 also details the most well-known theoretical models, listing their assumptions as well as judging their qualitative and quantitative accuracy. According to the most recent and accurate model (both quantitatively and qualitatively) exchange bias is a phenomenon that stems from the innate imbalance between the two sublattices of the AF layer, related to its finite size, which results in the excess of spin-up or spin-down atomic moments.

In the experimental part, the Fe/FeRh/$Al_2O_3$ exchange-biased FM-AF bilayer system was first investigated. Following a pioneering paper on this system, presence of exchange bias was confirmed using measurements of magnetization reversal via longitudinal MOKE, providing the the relative loop shift as well as rotational asymmetry. Moreover, the training effect was found and analysed in this system for the first time. Furthermore, we showed that even multiple preparation steps using diffferent approaches likely resulting in an increased disorder at the Fe-FeRh interface, do not prohibit significant exchange bias in such a system, as the obtained exchange bias value was of comparable or superior value to a well-defined system prepared by MBE. This suggests that exchange bias in Fe/FeRh/$Al_2O_3$ bilayers is rather insensitive to interfacial ordering, so the main mechanism responsible for coupling simply cannot be solely the fully uncompensated surface of a (111) oriented FeRh film.

The investigation of Fe/FeRh/$Al_2O_3$ microstructures showed that while the lithography process was overall successful, still needs to be optimized to maximize the MOKE signal.

Significant exchange bias was found for the FM phase in 500-nm-wide FeRh nanowires prepared on an MgO(001) substrate at FM and AF phase coexistence. From the results it appears that remanent magnetization is sufficient to set the orientation of the exchange bias along the wire axis, while the AF axis is set along the wire because the compressive strain exerted by the MgO substrate relaxes in nanowires in the direction perpendicular to the wire.

Finally, FIB irradiation induced FM FeRh stripes surrounded by the AF phase in FeRh/MgO thin films was investigated for possible exchange bias. However, no exchange bias was found for different stripe widths and FC orientations, with likely explanation being a disordered layer between the metastable FM FeRh pattern and the stable AF FeRh film.

In conclusion, we point out potential future directions of this research. First of all, it would be useful to verify the dependence of exchange bias on field cooling parameters, as this information is simply absent for FM/FeRh systems. Also, inducing an exchange biased system by low dose Helium ion irradiation of FeRh thin films is a promising avenue.

Further opportunities are offered in FeRh nanowires with phase coexistence.

From the applications standpoint, the FM/FeRh systems have the potential to be applied as temperature-sensitive active parts of recording media, GMR logic gates, tem-

perature and magnetic field sensors, etc. This work brings forth an array of different leads to follow up in the research of metamagnetic nanostructures in particular and exchange biased systems in general.

# A. Lithography processes

Lithographic process used for the preparation of FeRh nanostructures was optimized by Ing. Michal Horký and Bc. Jan Hajduček, with the following steps:

- Deposition of FeRh.
- Deposition of a 3 nm thick layer of Ti to increase adhesion to FeRh; deposition of 60 nm of $SiO_2$ using E-beam evaporator.
- Application of AR-N 7520.07 resist, and consequent spin-coating for 60 s at 4000 RPM, with 1000 RPM/s acceleration in order to achieve a 120 nm thick layer.
- Soft-baking of the resist at 85°C for 1 minute.
- Application of AR-PC 5090.02 protective coating (Electra) in order to provide surface conductivity to an otherwise insulating layer; spin-coating for 60 s at 2500 RPM, with 1000 RPM/s acceleration.
- Soft-baking of the Electra at 90°C for 2 minutes.
- Exposition of the sample to the electron beam with 450 $\mu C/cm^2$ dose.
- Removal of the conductive Electra layer by submerging the sample in distilled water for 2 minutes.
- Development of the negative resist by submerging the sample into AR 300-47 solution for 90 s, with consequent neutralization using de-ionized water and drying by Nitrogen gas.
- Dry etching of the $SiO_2$ layer using Reactive Ion Etching, involving combination of $CHF_3 + O_2$ gasses. Parameters of etching are listed in Table A.1.
- Dry etching of FeRh using Ar ions. The material not covered by resist and $SiO_2$ is etched away. Parameters of Ar etching are listed in Table A.1
- Leftover resist and $SiO_2$ layer are removed by wet etching in Buffered Oxide Etch solution by submerging the sample for 960 s.

| Reactive Ion Etching parameters | | | | | |
|---|---|---|---|---|---|
| Mat. 1 (sccm) | Mat. 2 (sccm) | $t$ (min) | $p$ (mTorr) | $P$(W) | DC bias (V) |
| $CHF_3$(50) | $O_2$(5) | 2 | 55 | 150 | 430 |
| Ar (50) | - | 10 | 20 | 200 | 555 |

**Table A.1:** Parameters for $SiO_2$ and FeRh dry etching. All dry etching was done in Oxford Instruments Plasma Technology PlasmaPro 80. The gasses used are listed in the first two columns followed by their flows in sccm, $t$ is the etching time, $p$ is the pressure in the chamber, and $P$ is the power of plasma generator while DC bias sets the acceleration voltage to the electrode on which the sample is positioned.

# Bibliography


[1] W. H. Meiklejohn and C. P. Bean, "New magnetic anisotropy," *Physical Review*, vol. 105, no. 3, pp. 904–913, feb 1957. [Online]. Available: https://journals.aps.org/pr/abstract/10.1103/PhysRev.105.904

[2] M. Kiwi, "Exchange Bias Theory: a Review," *Journal of Alloys and Compounds*, vol. 234, no. May, p. 22, 2001. [Online]. Available: http://arxiv.org/abs/cond-mat/0107097

[3] C. Liu, C. Yu, H. Jiang, L. Shen, C. Alexander, and G. J. Mankey, "Effect of interface roughness on the exchange bias for NiFe/FeMn," *Journal of Applied Physics*, vol. 87, no. 9 III, pp. 6644–6646, may 2000. [Online]. Available: https://doi.org/10.1063/1.372797

[4] J. Wang, T. Sannomiya, J. Shi, and Y. Nakamura, "Influence of interface roughness on the exchange bias of Co/CoO multilayers," *Journal of Applied Physics*, vol. 113, no. 17, pp. 111–114, 2013.

[5] J. Moritz, P. Bacher, and B. Dieny, "Numerical study of the influence of interfacial roughness on the exchange bias properties of ferromagnetic/antiferromagnetic bilayers," *Physical Review B*, vol. 94, no. 10, pp. 1–11, 2016.

[6] V. Cantelli, J. Von Borany, J. Grenzer, J. Fassbender, R. Kaltofen, and J. Schumann, "Influence of He-ion irradiation on thin NiMn/FeNi exchange bias films," *Journal of Applied Physics*, vol. 99, no. 8, pp. 8–102, apr 2006. [Online]. Available: https://doi.org/10.1063/1.2159227

[7] D. Schafer, P. L. Grande, L. G. Pereira, and J. Geshev, "Ion irradiation effects on the exchange bias in IrMn/Co films," *Journal of Applied Physics*, vol. 109, no. 2, p. 23905, jan 2011. [Online]. Available: https://doi.org/10.1063/1.3532044

[8] T. Mewes, R. Lopusnik, J. Fassbender, M. Jung, D. Engel, A. Ehresmann, H. Schmoranzer, and B. Hillebrands, "Influence of ion irradiation on the exchange bias effect," in *Digests of the Intermag Conference*. IEEE, 2000.

[9] M. Fecioru-Morariu, S. R. Ali, C. Papusoi, M. Sperlich, and G. Güntherodt, "Effects of Cu dilution in IrMn on the exchange bias of CoFe/IrMn bilayers," *Physical Review Letters*, vol. 99, no. 9, aug 2007. [Online]. Available: https://pubmed.ncbi.nlm.nih.gov/17931034/

[10] M. Ślezak, T. Ślezak, P. Dróżdż, B. Matlak, K. Matlak, A. Kozioł-Rachwał, M. Zajac, and J. Korecki, "How a ferromagnet drives an antiferromagnet in exchange biased CoO/Fe(110) bilayers," *Scientific Reports*, vol. 9, no. 1, pp. 1–8, dec 2019. [Online]. Available: www.nature.com/scientificreports/

[11] S. H. Chung, A. Hoffmann, and M. Grimsditch, "Interplay between exchange bias and uniaxial anisotropy in a ferromagnetic/antiferromagnetic exchange-coupled system," *Physical Review B - Condensed Matter and Materials Physics*, vol. 71, no. 21, jun 2005.

[12] A. Hoffmann, "The origin for training effects in exchange bias systems: Frustration and multiple anisotropy axes at the interface," in *INTERMAG 2006 - IEEE International Magnetics Conference*, 2006, p. 582.

[13] A. G. Biternas, R. W. Chantrell, and U. Nowak, "Dependence of training effect on the antiferromagnetic structure of exchange-bias bilayers within the domain-state model," *Physical Review B - Condensed Matter and Materials Physics*, vol. 89, no. 18, may 2014.

[14] T. Hauet, J. Borchers, P. Mangin, Y. Henry, and S. Mangin, "Training Effect in an Exchange Bias System: The Role of Interfacial Domain Walls," *Physical Review Letters*, vol. 96, no. 6-17, 2006. [Online]. Available: https://hal.archives-ouvertes.fr/hal-01345166

[15] M. R. Fitzsimmons, P. Yashar, C. Leighton, I. K. Schuller, J. Nogués, C. F. Majkrzak, and J. A. Dura, "Asymmetric magnetization reversal in exchange-biased hysteresis loops," *Physical Review Letters*, vol. 84, no. 17, pp. 3986–3989, apr 2000. [Online]. Available: https://journals.aps.org/prl/abstract/10.1103/PhysRevLett.84.3986

[16] E. Girgis, R. D. Portugal, M. J. Van Bael, K. Temst, and C. Van Haesendonck, "Asymmetric magnetization reversal in exchange-biased NiFe/CoO submicron-sized structures," *Journal of Applied Physics*, vol. 97, no. 10, p. 103911, may 2005. [Online]. Available: https://doi.org/10.1063/1.1905794

[17] R. Wu, J. Z. Wei, X. L. Peng, J. B. Fu, S. Q. Liu, Y. Zhang, Y. H. Xia, C. S. Wang, Y. C. Yang, and J. B. Yang, "The asymmetric magnetization reversal in exchange biased granular Co/CoO films," *Appl. Phys. Lett*, vol. 104, p. 182403, 2014. [Online]. Available: https://doi.org/10.1063/1.4875594

[18] S. Choi, S. K. Bac, X. Liu, S. Lee, S. Dong, M. Dobrowolska, and J. K. Furdyna, "Exchange bias in ferromagnetic bilayers with orthogonal anisotropies: the case of GaMnAsP/GaMnAs combination," *Scientific Reports*, vol. 9, no. 1, pp. 1–7, dec 2019. [Online]. Available: www.nature.com/scientificreports

[19] U. Nowak, K. D. Usadel, J. Keller, P. Miltényi, B. Beschoten, and G. Güntherodt, "Domain state model for exchange bias. I. Theory," *Physical Review B - Condensed Matter and Materials Physics*, vol. 66, no. 1, pp. 1–9, 2002.

[20] M. Kiwi, J. Mejía-López, R. D. Portugal, and R. Ramírez, "Exchange bias model for Fe/FeF2: Role of domains in the ferromagnet," *Europhysics Letters*, vol. 48, no. 5, pp. 573–579, dec 1999. [Online]. Available: https://iopscience.iop.org/article/10.1209/epl/i1999-00522-9https://iopscience.iop.org/article/10.1209/epl/i1999-00522-9/meta

[21] J. Keller, P. Miltényi, B. Beschoten, G. Güntherodt, U. Nowak, K. D. Usadel, J. Keller, P. Miltényi, B. Beschoten, and G. Güntherodt, "No Title," *Physical Review B - Condensed Matter and Materials Physics*, vol. 66, no. 1, jul 2002. [Online]. Available: https://journals.aps.org/prb/abstract/10.1103/PhysRevB.66.014431

[22] J. Nogués, J. Sort, V. Langlais, V. Skumryev, S. Suriñach, J. S. Muñoz, and M. D. Baró, "Exchange bias in nanostructures," *Physics Reports*, vol. 422, no. 3, pp. 65–117, 2005.

[23] S. Blundell and D. Thouless, " Magnetism in Condensed Matter ," *American Journal of Physics*, vol. 71, no. 1, pp. 94–95, jan 2003.

[24] A. A. Tsirlin, O. Janson, and H. Rosner, "Unusual ferromagnetic superexchange in CdVO 3 : The role of Cd," *PHYSICAL REVIEW B*, vol. 84, p. 144429, 2011.

[25] J. M. Coey, *Magnetism and magnetic materials*. Cambridge University Press, jan 2010, vol. 9780521816. [Online]. Available: https://www.cambridge.org/core/books/magnetism-and-magnetic-materials/AD3557E2D4538CAA8488A8C1057313BC

[26] M. Staňo and O. Fruchart, "Magnetic nanowires and nanotubes," CEITEC - Central European Institute of Technology, Brno University of Technology, Brno, Czech Republic, Tech. Rep., 2018.

[27] M. A. Howson, "Magnetism of thin films and multilayers," *Contemporary Physics*, vol. 35, no. 5, pp. 347–359, 1994. [Online]. Available: https://www.tandfonline.com/doi/abs/10.1080/00107519408222100

[28] J. Stöhr and H. C. Siegmann, *Magnetism: From fundamentals to nanoscale dynamics*. Springer Berlin Heidelberg, 2006, vol. 152.

[29] W. H. Meiklejohn, "Exchange anisotropy in the iron-iron oxide system," *Journal of Applied Physics*, vol. 29, no. 3, pp. 454–455, jun 1958. [Online]. Available: https://doi.org/10.1063/1.1723179

[30] J. S. Kouvel and C. D. Graham, "Exchange anisotropy in disordered nickel-manganese alloys," *Journal of Physics and Chemistry of Solids*, vol. 11, no. 3-4, pp. 220–225, oct 1959.

[31] J. S. Kouvel, "Exchange anisotropy in Cu-Mn and Ag-Mn alloys," *Journal of Applied Physics*, vol. 31, no. 5, p. 142, aug 1960. [Online]. Available: https://doi.org/10.1063/1.1984637

[32] ——, "Exchange Anisotropy in an Iron-Aluminum Alloy," *Journal of Applied Physics*, vol. 30, p. 313, 1959. [Online]. Available: https://doi.org/10.1063/1.2185950

[33] ——, "Exchange anisotropy in cobalt-manganese alloys," *Journal of Physics and Chemistry of Solids*, vol. 16, no. 1-2, pp. 107–114, nov 1960.

[34] M. Takahashi, A. Yanai, S. Taguchi, and T. Suzuki, "A study of exchange anisotropy in Co-CoO evaporated thin films," *Japanese Journal of Applied Physics*, vol. 19, no. 6, pp. 1093–1106, 1980.

[35] E. Fulcomer and S. H. Charap, "Thermal fluctuation aftereffect model for some systems with ferromagnetic-antiferromagnetic coupling," *Journal of Applied Physics*, vol. 43, no. 10, pp. 4190–4199, nov 1972. [Online]. Available: https://doi.org/10.1063/1.1660894

[36] R. P. Michel, A. Chaiken, C. T. Wang, and L. E. Johnson, "Exchange anisotropy in epitaxial and polycrystalline NiO/NiFe bilayers," Materials Science and Technology Division, Lawrence Livermore National Laboratory, Livermore, California 94551, Tech. Rep., 1998.

[37] J. Nogués, D. Lederman, T. J. Moran, I. K. Schuller, and K. V. Rao, "Large exchange bias and its connection to interface structure in FeF 2-Fe bilayers," *Applied Physics Letters*, vol. 68, no. 22, p. 3186, jun 1995. [Online]. Available: https://doi.org/10.1063/1.115819

[38] D. E. Heim, J. Tsang, V. S. Speriosu, B. A. Gurney, M. L. Williams, and R. E. Fontana, "Design and Operation of Spin Valve Sensors," *IEEE Transactions on Magnetics*, vol. 30, no. 2, pp. 316–321, 1994.

[39] M. Tsunoda, Y. Tsuchiya, T. Hashimoto, and M. Takahashi, "Magnetic anisotropy and rotational hysteresis loss in exchange coupled Ni–Fe/Mn–Ir films," *Journal of Applied Physics*, vol. 87, no. 9, pp. 4375–4388, may 2000. [Online]. Available: https://doi.org/10.1063/1.373081

[40] T. Pokhil, S. Mao, and A. Mack, "Study of exchange anisotropy in NiFe/NiMn and NiFe/IrMn exchange coupled films," *Journal of Applied Physics*, vol. 85, no. 8 II A, pp. 4916–4918, apr 1999. [Online]. Available: https://doi.org/10.1063/1.369141

[41] Y. J. Tang, X. Zhou, X. Chen, B. Q. Liang, and W. S. Zhan, "Exchange anisotropy of epitaxial Fe/MnPd bilayers," *Journal of Applied Physics*, vol. 88, no. 4, pp. 2054–2057, aug 2000. [Online]. Available: https://doi.org/10.1063/1.1305907

[42] M. Gierlings, M. J. Prandolini, H. Fritzsche, M. Gruyters, and D. Riegel, "Change and asymmetry of magnetization reversal for a Co/CoO exchange-bias system," *Physical Review B - Condensed Matter and Materials Physics*, vol. 65, no. 9, pp. 1–4, feb 2002. [Online]. Available: https://journals.aps.org/prb/abstract/10.1103/PhysRevB.65.092407

[43] J. Camarero, J. Sort, A. Hoffmann, J. M. García-Martín, B. Dieny, R. Miranda, and J. Nogués, "Origin of the asymmetric magnetization reversal behavior in exchange-biased systems: Competing anisotropies," *Physical Review Letters*, vol. 95, no. 5, p. 057204, jul 2005. [Online]. Available: https://journals.aps.org/prl/abstract/10.1103/PhysRevLett.95.057204

[44] I. N. Krivorotov, C. Leighton, J. Nogués, I. K. Schuller, and E. D. Dahlberg, "Relation between exchange anisotropy and magnetization reversal asymmetry in Fe/FeF2 bilayers," *Physical Review B - Condensed Matter and Materials Physics*, vol. 65, no. 10, pp. 1–4, feb 2002. [Online]. Available: https://journals.aps.org/prb/abstract/10.1103/PhysRevB.65.100402

[45] C. Leighton, M. Song, J. Nogués, M. C. Cyrille, and I. K. Schuller, "Using magnetoresistance to probe reversal asymmetry in exchange biased bilayers," *Journal of Applied Physics*, vol. 88, no. 1, pp. 344–347, jun 2000. [Online]. Available: https://doi.org/10.1063/1.373665

[46] J. McCord, R. Schäfer, R. Mattheis, and K. U. Barholz, "Kerr observations of asymmetric magnetization reversal processes in CoFe/IrMn bilayer systems," *Journal of Applied Physics*, vol. 93, no. 9, pp. 5491–5497, may 2003. [Online]. Available: https://doi.org/10.1063/1.1562732

[47] D. Lederman, C. A. Ramos, V. Jaccarino, and J. L. Cardy, "Finite-size scaling in FeF2/ZnF2 superlattices," *Physical Review B*, vol. 48, no. 11, pp. 8365–8375, sep 1993. [Online]. Available: https://journals.aps.org/prb/abstract/10.1103/PhysRevB.48.8365

[48] T. J. Moran, J. M. Gallego, and I. K. Schuller, "Increased exchange anisotropy due to disorder at permalloy/CoO interfaces," *Journal of Applied Physics*, vol. 78, no. 3, pp. 1887–1891, jun 1995. [Online]. Available: https://doi.org/10.1063/1.360225

[49] P. J. Van Der Zaag, A. R. Ball, L. F. Feiner, R. M. Wolf, and P. A. Van Der Heijden, "Exchange biasing in MBE grown Fe3O4/CoO bilayers: The antiferromagnetic layer thickness dependence," *Journal of Applied Physics*, vol. 79, no. 8 PART 2A, pp. 5103–5105, apr 1996. [Online]. Available: https://doi.org/10.1063/1.361315

[50] G. Choe and S. Gupta, "High exchange anisotropy and high blocking temperature in strongly textured NiFe(111)/FeMn(111) films," *Applied Physics Letters*, vol. 70, no. 13, pp. 1766–1768, mar 1997. [Online]. Available: https://doi.org/10.1063/1.118650

[51] M. G. Blamire, M. Ali, C. W. Leung, C. H. Marrows, and B. J. Hickey, "Exchange bias and blocking temperature in Co/FeMn/CuNi trilayers," *Physical Review Letters*, vol. 98, no. 21, p. 217202, may 2007. [Online]. Available: https://journals.aps.org/prl/abstract/10.1103/PhysRevLett.98.217202

[52] J. G. Hu, G. Jin, A. Hu, and Y. Q. Ma, "Temperature dependence of exchange bias and coercivity in ferromagnetic/antiferromagnetic bilayers," *European Physical Journal B*, vol. 40, no. 3, pp. 265–271, aug 2004. [Online]. Available: https://link.springer.com/article/10.1140/epjb/e2004-00272-0

[53] M. Tsunoda, M. Konoto, K. Uneyama, and M. Takahashi, "Effect of surface cleaning of substrate on the exchange coupling Field in Ni-Fe/25at%Ni-Mn films," *IEEE Transactions on Magnetics*, vol. 33, no. 5 PART 2, pp. 3688–3690, 1997.

[54] C. H. Lai, T. J. Regan, R. L. White, and T. C. Anthony, "Temperature dependence of magnetoresistance in spin valves with different thicknesses of NiO," *Journal of Applied Physics*, vol. 81, no. 8 PART 2A, pp. 3989–3991, apr 1997. [Online]. Available: https://doi.org/10.1063/1.364916

[55] S. Soeya, T. Imagawa, K. Mitsuoka, and S. Narishige, "Distribution of blocking temperature in bilayered Ni81Fe 19/NiO films," *Journal of Applied*

*Physics*, vol. 76, no. 9, pp. 5356–5360, jun 1994. [Online]. Available: https://aip.scitation.org/doi/abs/10.1063/1.358488

[56] V. S. Speriosu, D. A. Herman, I. L. Sanders, and T. Yogi, "Magnetic thin films in recording technology," *IBM Journal of Research and Development*, vol. 34, no. 6, pp. 884–902, 1990.

[57] Y. Tsuchiya, K. Kosuge, S. Yamaguchi, and N. Nakayama, "Exchange anisotropy of CrNx/FeNy/CrNx trilayer thin films prepared by reactive sputtering," *Materials Transactions, JIM*, vol. 38, no. 2, pp. 91–98, 1997.

[58] M. J. Carey and A. E. Berkowitz, "Exchange anisotropy in coupled films of Ni81Fe19 with NiO and CoxNi1-xO," *Applied Physics Letters*, vol. 60, no. 24, pp. 3060–3062, jun 1992. [Online]. Available: https://doi.org/10.1063/1.106756

[59] C.-H. Lai, H. Matsuyama, R. L. White, T. C. Anthony, and G. G. Bush, "Exploration of magnetization reversal and coercivity of epitaxial NiO {111}/NiFe films," *Journal of Applied Physics*, vol. 79, no. 8, p. 6389, aug 1996. [Online]. Available: https://doi.org/10.1063/1.362007

[60] F. B. Hagedorn, "Exchange anisotropy in oxidized permalloy thin films at low temperatures," *Journal of Applied Physics*, vol. 38, no. 9, pp. 3641–3645, jun 1967. [Online]. Available: https://doi.org/10.1063/1.1710185

[61] H. Kishi, Y. Shimizu, K. Nagasaka, A. Tanaka, and M. Oshiki, "Spin-Valve Films with PdPtMn Antiferromagnetic Layer," *Journal of the Magnetics Society of Japan*, vol. 21, no. 4_2, pp. 521–524, 1997.

[62] A. J. Devasahayam and M. H. Kryder, "A study of the NiFe/NiMn exchange couple," *IEEE Transactions on Magnetics*, vol. 32, no. 5 PART 2, pp. 4654–4656, 1996.

[63] J. Nogués and I. K. Schuller, "Exchange bias," *Journal of Magnetism and Magnetic Materials*, vol. 192, no. 2, pp. 203–232, feb 1999.

[64] C. Schlenker, "Couplage ferro-antiferromagnétique et traînage magnétique dans des couches minces multiples Co CoO et Ni NiO Par," *physica status solidi (b)*, vol. 28, no. 2, pp. 507–517, jan 1968. [Online]. Available: https://onlinelibrary.wiley.com/doi/full/10.1002/pssb.19680280207https://onlinelibrary.wiley.com/doi/abs/10.1002/pssb.19680280207https://onlinelibrary.wiley.com/doi/10.1002/pssb.19680280207

[65] D. Paccard, C. Schlenker, O. Massenet, R. Montmory, and A. Yelon, "A New Property of Ferromagnetic-Antiferromagnetic Coupling," *physica status solidi (b)*, vol. 16, no. 1, pp. 301–311, jan 1966. [Online]. Available: https://onlinelibrary.wiley.com/doi/full/10.1002/pssb.19660160131https://onlinelibrary.wiley.com/doi/abs/10.1002/pssb.19660160131https://onlinelibrary.wiley.com/doi/10.1002/pssb.19660160131

[66] C. Tsang and K. Lee, "Temperature dependence of unidirectional anisotropy effects in the Permalloy-FeMn systems," *Journal of Applied Physics*, vol. 53, no. 3, pp. 2605–2607, jun 1982. [Online]. Available: https://doi.org/10.1063/1.330967

[67] Y. Chen, D. K. Lottis, E. D. Dahlberg, J. N. Kuznia, A. M. Wowchak, and P. I. Cohen, "Exchange effects in molecular-beam-epitaxy grown iron films," *Journal of Applied Physics*, vol. 69, no. 8, pp. 4523–4525, aug 1991. [Online]. Available: https://doi.org/10.1063/1.348347

[68] C. Schlenker, S. S. Parkin, J. C. Scott, and K. Howard, "Magnetic disorder in the exchange bias bilayered FeNi-FeMn system," *Journal of Magnetism and Magnetic Materials*, vol. 54-57, no. PART 2, pp. 801–802, feb 1986.

[69] B. Kuhlow, M. Lambeck, H. Schroeder-Fürst, and J. Wortmann, "Critical curves of thin ferromagnetic films with antiferromagnetic exchange coupling," *Physics Letters A*, vol. 34, no. 4, pp. 223–224, mar 1971.

[70] B. Warot, E. Snoeck, P. Baulès, J. C. Ousset, M. J. Casanove, S. Dubourg, and J. F. Bobo, "Growth and stress relaxation of Co/NiO bilayers on MgO(001)," *Journal of Applied Physics*, vol. 89, no. 10, pp. 5414–5420, may 2001. [Online]. Available: https://doi.org/10.1063/1.1361240

[71] A. P. Malozemoff, "Random-field model of exchange anisotropy at rough ferromagnetic-antiferromagnetic interfaces," Tech. Rep.

[72] D. Mauri, E. Kay, D. Scholl, and J. K. Howard, "Novel method for determining the anisotropy constant of MnFe in a NiFe/MnFe sandwich," *Journal of Applied Physics*, vol. 62, no. 7, pp. 2929–2932, aug 1987. [Online]. Available: https://doi.org/10.1063/1.339374

[73] M. Tsunoda, Y. Tsuchiya, M. Konoto, and M. Takahashi, "Microstructure of antiferromagnetic layer affecting on magnetic exchange coupling in trilayered Ni-Fe/25 at% Ni-Mn/Ni-Fe films," *Journal of Magnetism and Magnetic Materials*, vol. 171, no. 1-2, pp. 29–44, jul 1997.

[74] C. Tsang, N. Heiman, and K. Lee, "Exchange induced unidirectional anisotropy at FeMn-Ni80Fe 20 interfaces," *Journal of Applied Physics*, vol. 52, no. 3, pp. 2471–2473, aug 1981. [Online]. Available: https://doi.org/10.1063/1.328970

[75] W. Stoecklein, S. S. Parkin, and J. C. Scott, "Ferromagnetic resonance studies of exchange-biased Permalloy thin films," *Physical Review B*, vol. 38, no. 10, pp. 6847–6854, oct 1988. [Online]. Available: https://journals.aps.org/prb/abstract/10.1103/PhysRevB.38.6847

[76] R. Jungblut, R. Coehoorn, M. T. Johnson, J. Aan De Stegge, and A. Reinders, "Orientational dependence of the exchange biasing in molecular-beam-epitaxy- grown ni80fe20/fe50mn50 bilayers (invited)," *Journal of Applied Physics*, vol. 75, no. 10, pp. 6659–6664, aug 1994. [Online]. Available: https://aip.scitation.org/doi/abs/10.1063/1.356888

[77] M. Ali, C. H. Marrows, M. Al-Jawad, B. J. Hickey, A. Misra, U. Nowak, and K. D. Usadel, "Antiferromagnetic layer thickness dependence of the IrMn/Co exchange-bias system," *Physical Review B - Condensed Matter and Materials Physics*, vol. 68, no. 21, p. 214420, dec 2003. [Online]. Available: https://journals.aps.org/prb/abstract/10.1103/PhysRevB.68.214420

[78] M. Ali, C. H. Marrows, and B. J. Hickey, "Onset of exchange bias in ultrathin antiferromagnetic layers," *Physical Review B - Condensed Matter and Materials Physics*, vol. 67, no. 17, p. 172405, may 2003. [Online]. Available: https://journals.aps.org/prb/abstract/10.1103/PhysRevB.67.172405

[79] M. S. Lund, W. A. Macedo, K. Liu, J. Nogués, I. K. Schuller, and C. Leighton, "Effect of anisotropy on the critical antiferromagnet thickness in exchange-biased bilayers," *Physical Review B - Condensed Matter and Materials Physics*, vol. 66, no. 5, pp. 544 221–544 227, aug 2002. [Online]. Available: https://journals.aps.org/prb/abstract/10.1103/PhysRevB.66.054422

[80] H. Xi and R. M. White, "Antiferromagnetic thickness dependence of exchange biasing," *Physical Review B - Condensed Matter and Materials Physics*, vol. 61, no. 1, pp. 80–83, jan 2000. [Online]. Available: https://journals.aps.org/prb/abstract/10.1103/PhysRevB.61.80

[81] R. Nakatani, H. Hoshiya, K. Hoshino, and Y. Sugita, "Exchange coupling of (Mn-Ir, Fe-Mn)/Ni-Fe-Co and Ni-Fe-Co/(Mn-Ir, Fe-Mn) films formed by ion beam sputtering," *IEEE Transactions on Magnetics*, vol. 33, no. 5 PART 2, pp. 3682–3684, 1997.

[82] A. P. Malozemoff, "Heisenberg-to-Ising crossover in a random-field model with uniaxial anisotropy," *Physical Review B*, vol. 37, no. 13, pp. 7673–7679, may 1988. [Online]. Available: https://journals.aps.org/prb/abstract/10.1103/PhysRevB.37.7673

[83] P. J. van der Zaag, R. M. Wolf, A. R. Ball, C. Bordel, L. F. Feiner, and R. Jungblut, "A study of the magnitude of exchange biasing in [111] Fe3O4/CoO bilayers," *Journal of Magnetism and Magnetic Materials*, vol. 148, no. 1-2, pp. 346–348, jul 1995.

[84] Y. Ijiri, J. A. Borchers, R. W. Erwin, S. H. Lee, P. J. Van Der Zaag, and R. M. Wolf, "Perpendicular coupling in exchange-biased Fe3O4/CoO superlattices," *Physical Review Letters*, vol. 80, no. 3, pp. 608–611, jan 1998. [Online]. Available: https://journals.aps.org/prl/abstract/10.1103/PhysRevLett.80.608

[85] J. X. Shen and M. T. Kief, "Exchange coupling between Nip and NiFe thin films," *Journal of Applied Physics*, vol. 79, no. 8 PART 2A, pp. 5008–5010, apr 1996. [Online]. Available: https://doi.org/10.1063/1.361556

[86] D. H. Han, J. G. Zhu, J. H. Judy, and J. M. Sivertsen, "Texture and surface/interface topological effects on the exchange and coercive fields of NiFe/NiO bilayers," *Journal of Applied Physics*, vol. 81, no. 1, pp. 340–343, jan 1997. [Online]. Available: https://doi.org/10.1063/1.364116

[87] S. S. Lee, D. G. Hwang, C. M. Park, K. A. Lee, and J. R. Rhee, "Effects of crystal texture on exchange anisotropy in NiO spin valves," *Journal of Applied Physics*, vol. 81, no. 8 PART 2B, pp. 5298–5300, apr 1997. [Online]. Available: https://doi.org/10.1063/1.364948

[88] J. Nogués, D. Lederman, T. J. Moran, and I. K. Schuller, "Positive exchange bias in FeF2-Fe bilayers," *Physical Review Letters*, vol. 76, no. 24, pp. 4624–4627, jun 1996. [Online]. Available: https://journals.aps.org/prl/abstract/10.1103/PhysRevLett.76.4624

[89] D. Lederman, J. Nogués, and I. K. Schuller, "Exchange anisotropy and the antiferromagnetic surface order parameter," *Physical Review B - Condensed Matter and Materials Physics*, vol. 56, no. 5, pp. 2332–2335, aug 1997. [Online]. Available: https://ui.adsabs.harvard.edu/abs/1997PhRvB..56.2332L/abstracthttps://journals.aps.org/prb/abstract/10.1103/PhysRevB.56.2332

[90] C. M. Park, K. I. Min, and K. H. Shin, "Effects of surface topology and texture on exchange anisotropy in NiFe/Cu/NiFe/FeMn spin valves," *Journal of Applied Physics*, vol. 79, no. 8 PART 2B, pp. 6228–6230, apr 1996. [Online]. Available: https://doi.org/10.1063/1.361891

[91] R. Jungblut, R. Coehoorn, M. T. Johnson, C. Sauer, P. J. van der Zaag, A. R. Ball, T. G. Rijks, J. aan de Stegge, and A. Reinders, "Exchange biasing in MBE-grown Ni80Fe20/Fe50Mn50 bilayers," *Journal of Magnetism and Magnetic Materials*, vol. 148, no. 1-2, pp. 300–306, jul 1995.

[92] J. Nogués, T. J. Moran, D. Lederman, I. K. Schuller, K. V. Rao, and K. V. Rao, "Role of interfacial structure on exchange-biased FeF2 - Fe," *Physical Review B - Condensed Matter and Materials Physics*, vol. 59, no. 10, pp. 6984–6993, mar 1999. [Online]. Available: https://journals.aps.org/prb/abstract/10.1103/PhysRevB.59.6984

[93] S. M. Zhou, L. Sun, P. C. Searson, and C. L. Chien, "Perpendicular exchange bias and magnetic anisotropy in CoO/permalloy multilayers," *Physical Review B - Condensed Matter and Materials Physics*, vol. 69, no. 2, pp. 1–5, 2004.

[94] L. Sun, S. M. Zhou, P. C. Searson, and C. L. Chien, "Longitudinal and perpendicular exchange bias in FeMn/(FeNi/FeMn)n multilayers," *Journal of Applied Physics*, vol. 93, no. 10 2, pp. 6841–6843, 2003.

[95] Z. Y. Liu and S. Adenwalla, "Oscillatory Interlayer Exchange Coupling and Its Temperature Dependence in [Formula presented] Multilayers with Perpendicular Anisotropy," *Physical Review Letters*, vol. 91, no. 3, pp. 1–4, 2003.

[96] J. Y. Chen, N. Thiyagarajah, H. J. Xu, and J. M. Coey, "Perpendicular exchange bias effect in sputter-deposited CoFe/IrMn bilayers," *Applied Physics Letters*, vol. 104, no. 15, 2014.

[97] A. M. Choukh, "Effect of interface on exchange coupling in nife/femn system," *IEEE Transactions on Magnetics*, vol. 33, no. 5 PART 2, pp. 3676–3678, 1997.

[98] D. H. Han, J. G. Zhu, and J. H. Judy, "NiFe/NiO bilayers with high exchange coupling and low coercive fields," *Journal of Applied Physics*, vol. 81, no. 8 PART 2B, pp. 4996–4998, apr 1997. [Online]. Available: https://doi.org/10.1063/1.364964

[99] S. F. Cheng, J. P. Teter, P. Lubitz, M. M. Miller, L. Hoines, J. J. Krebs, D. M. Schaefer, and G. A. Prinz, "Factors affecting performance of NiO biased giant - Magnetoresistance structures," *Journal of Applied Physics*, vol. 79, no. 8 PART 2B, pp. 6234–6236, apr 1996. [Online]. Available: https://doi.org/10.1063/1.362079

[100] C. H. Lai, T. C. Anthony, E. Iwamura, and L. Robert, "The effect of microstructure and interface conditions on the anisotropie exchange fields of NiO/NiFe," *IEEE Transactions on Magnetics*, vol. 32, no. 5 PART 1, pp. 3419–3421, 1996.

[101] B. Y. Wong, C. Mitsumata, S. Prakash, D. E. Laughlin, and T. Kobayashi, "Structural origin of magnetic biased field in NiMn/NiFe exchange coupled films," *Journal of Applied Physics*, vol. 79, no. 10, pp. 7896–7904, may 1996. [Online]. Available: https://doi.org/10.1063/1.362401

[102] H. Fujiwara, K. Nishioka, C. Hou, M. R. Parker, S. Gangopadhyay, and R. Metzger, "Temperature dependence of the pinning field and coercivity of NiFe layers coupled with an antiferromagnetic FeMn layer," *Journal of Applied Physics*, vol. 79, no. 8 PART 2B, pp. 6286–6288, apr 1996. [Online]. Available: https://doi.org/10.1063/1.362039

[103] R. Nakatani, K. Hoshino, S. Noguchi, and Y. Sugita, "Magnetoresistance and preferred orientation in fe-mn/ni-fe/cu/ni-fe sandwiches with various buffer layer materials," *Japanese Journal of Applied Physics*, vol. 33, no. 1R, p. 133, jan 1994. [Online]. Available: https://iopscience.iop.org/article/10.1143/JJAP.33.133https://iopscience.iop.org/article/10.1143/JJAP.33.133/meta

[104] G. Choe and S. Gupta, "NiFe underlayer effects on exchange coupling field and coercivity in nife/femn films," *IEEE Transactions on Magnetics*, vol. 33, no. 5 PART 2, pp. 3691–3693, 1997.

[105] A. J. Devasahayam and M. H. Kryder, "The Effect of Sputtering Conditions on the Exchange Fields of CoxNi1−xO and NiFe," *IEEE Transactions on Magnetics*, vol. 31, no. 6, pp. 3820–3822, 1995.

[106] W. E. Bailey, N. C. Zhu, R. Sinclair, and S. X. Wang, "Structural comparisons of ion beam and dc magnetron sputtered spin valves by high-resolution transmission electron microscopy," pp. 6393–6395, apr 1996. [Online]. Available: https://doi.org/10.1063/1.362009

[107] P. Bayle-Guillemaud, A. K. Petford-Long, T. C. Anthony, and J. A. Brug, "HREM study of Co/Cu/Co/MnFe spin valves," *IEEE Transactions on Magnetics*, vol. 32, no. 5 PART 2, pp. 4627–4629, 1996.

[108] S. X. Wang, W. E. Bailey, and C. Sürgers, "Ion beam deposition and structural characterization of GMR spin valves," *IEEE Transactions on Magnetics*, vol. 33, no. 3, pp. 2369–2374, 1997.

[109] X. Portier and A. K. Petford-Long, "HREM study of spin valves with mnni pinning layer," *IEEE Transactions on Magnetics*, vol. 33, no. 5 PART 2, pp. 3679–3681, 1997.

[110] R. P. Michel, A. Chaiken, Y. K. Kim, and L. E. Johnson, "NiO Exchange Bias Layers Grown by Direct Ion Beam Sputtering of a Nickel Oxide Target," *IEEE Transactions on Magnetics*, vol. 32, no. 5 PART 2, pp. 4651–4653, 1996.

[111] D. Guarisco, "In situ and Ex situ Observation of Spin Valves Obtained by Ion-Beam Deposition," *IEEE Transactions on Magnetics*, vol. 33, no. 5 PART 2, pp. 3595–3597, 1997.

[112] L. Tang, D. E. Laughlin, and S. Gangopadhyay, "Microstructural study of ion-beam deposited giant magnetoresistive spin valves," *Journal of Applied Physics*, vol. 81, no. 8, pp. 4906–4908, apr 1997. [Online]. Available: https://doi.org/10.1063/1.364891

[113] H. Uyama, Y. Otani, K. Fukamichi, O. Kitakami, Y. Shimada, and J. I. Echigoya, "Effect of antiferromagnetic grain size on exchange-coupling field of Cr70Al30/Fe19Ni81 bilayers," *Applied Physics Letters*, vol. 71, no. 9, pp. 1258–1260, sep 1997. [Online]. Available: https://doi.org/10.1063/1.119866

[114] K. Takano, R. H. Kodama, A. E. Berkowitz, W. Cao, and G. Thomas, "Interfacial uncompensated antiferromagnetic spins: Role in unidirectional anisotropy in polycrystalline Ni81Fe19/CoO bilayers," *Physical Review Letters*, vol. 79, no. 6, pp. 1130–1133, jan 1997. [Online]. Available: https://journals.aps.org/prl/abstract/10.1103/PhysRevLett.79.1130

[115] C. H. Lai, H. Matsuyama, R. L. White, T. C. Anthony, and H. Matsuyama, "Anisotropic Exchange for NiFe Films Grown on Epitaxial NiO," *IEEE Transactions on Magnetics*, vol. 31, no. 6, pp. 2609–2611, 1995.

[116] M. A. Russak, S. M. Rossnagel, S. L. Cohen, T. R. McGuire, G. J. Scilla, C. V. Jahnes, J. M. Baker, J. J. Cuomo, and C. Hwang, "MnFe and NiFe Thin Films and Magnetic Exchange Bilayers," *Journal of The Electrochemical Society*, vol. 136, no. 6, jun 1989. [Online]. Available: https://iopscience.iop.org/article/10.1149/1.2097014https://iopscience.iop.org/article/10.1149/1.2097014/meta

[117] K. Uneyama, M. Tsunoda, and M. Takahashi, "Influence of gas adsorption at the interface on the exchange coupling field of Ni-Fe/25at%Ni-Mn/Ni-fe films," *IEEE Transactions on Magnetics*, vol. 33, no. 5 PART 2, pp. 3685–3687, 1997.

[118] H. D. Chopra, B. J. Hockey, P. J. Chen, R. D. McMichael, and W. F. Egelhoff, "Nanostructure, interfaces, and magnetic properties in giant magnetoresistive NiO-Co-Cu-based spin valves," *Journal of Applied Physics*, vol. 81, no. 8 PART 2A, pp. 4017–4019, apr 1997. [Online]. Available: https://doi.org/10.1063/1.365273

[119] N. J. Gökemeijer, T. Ambrose, C. L. Chien, N. Wang, and K. K. Fung, "Long-range exchange coupling between a ferromagnet and an antiferromagnet across a nonmagnetic spacer layer," *Journal of Applied Physics*, vol. 81, no. 8 PART 2B, pp. 4999–5001, apr 1997. [Online]. Available: https://doi.org/10.1063/1.364965

[120] N. J. Gökemeijer, T. Ambrose, and C. L. Chien, "Long-Range exchange bias across a spacer layer," *Physical Review Letters*, vol. 79, no. 21, pp. 4270–4273, nov 1997. [Online]. Available: https://journals.aps.org/prl/abstract/10.1103/PhysRevLett.79.4270

[121] T. J. Moran and I. K. Schuller, "Effects of cooling field strength on exchange anisotropy at permalloy/CoO interfaces," *Journal of Applied Physics*, vol. 79, no. 8 PART 2A, pp. 5109–5111, apr 1996. [Online]. Available: https://doi.org/10.1063/1.361317

[122] T. J. Moran, J. Nogués, D. Lederman, and I. K. Schuller, "Perpendicular coupling at Fe-FeF2 interfaces," *Applied Physics Letters*, vol. 72, no. 5, pp. 617–619, jun 1998. [Online]. Available: https://aip.scitation.org/doi/abs/10.1063/1.120823

[123] N. C. Koon, "Calculations of Exchange Bias in Thin Films with Ferromagnetic/Antiferromagnetic Interfaces," *Physical Review Letters*, vol. 78, no. 25, pp. 4865–4868, jun 1997. [Online]. Available: https://journals.aps.org/prl/abstract/10.1103/PhysRevLett.78.4865

[124] W. H. Meiklejohn, "Exchange anisotropy - A review," *Journal of Applied Physics*, vol. 33, no. 3, pp. 1328–1335, jun 1962. [Online]. Available: https://doi.org/10.1063/1.1728716

[125] N. K. (Author), *Selected Works of Louis Neel*, 1st ed. CRC Press, 1988. [Online]. Available: http://gen.lib.rus.ec/book/index.php?md5=6FAE4A29235BF8685F6E0C6BDFE9D969

[126] A. P. Malozemoff, "Random-field model of exchange anisotropy at rough ferromagnetic- antiferromagnetic interfaces," *Physical Review B*, vol. 35, no. 7, pp. 3679–3682, mar 1987. [Online]. Available: https://journals.aps.org/prb/abstract/10.1103/PhysRevB.35.3679

[127] D. Mauri, H. C. Siegmann, P. S. Bagus, and E. Kay, "Simple model for thin ferromagnetic films exchange coupled to an antiferromagnetic substrate," *Journal of Applied Physics*, vol. 62, no. 7, pp. 3047–3049, aug 1987. [Online]. Available: https://doi.org/10.1063/1.339367

[128] J. Nogués, C. Leighton, and I. K. Schuller, "Correlation between antiferromagnetic interface coupling and positive exchange bias," *Physical Review B - Condensed Matter and Materials Physics*, vol. 61, no. 2, pp. 1315–1317, jan 2000. [Online]. Available: https://journals.aps.org/prb/abstract/10.1103/PhysRevB.61.1315

[129] A. R. Ball, A. J. Leenaers, P. J. Van Der Zaag, K. A. Shaw, B. Singer, D. M. Lind, H. Frederikze, and M. T. Rekveldt, "Polarized neutron reflectometry study of an exchange biased Fe3O4/NiO multilayer," *Applied Physics Letters*, vol. 69, no. 10, pp. 1489–1491, sep 1996. [Online]. Available: https://doi.org/10.1063/1.116917

[130] V. Ström, B. J. Jönsson, K. V. Rao, and D. Dahlberg, "Determination of exchange anisotropy by means of ac susceptometry in Co/CoO bilayers," *Journal of Applied Physics*, vol. 81, no. 8 PART 2B, pp. 5003–5005, apr 1997. [Online]. Available: https://doi.org/10.1063/1.364967

[131] E. D. Dahlberg, B. Miller, B. Hill, B. J. Jonsson, V. Strom, K. V. Rao, J. Nogues, and I. K. Schuller, "Measurements of the ferromagnetic/antiferromagnetic interface exchange energy in CO/CoO and Fe/FeF2 layers (invited)," *Journal of Applied Physics*, vol. 83, no. 11, pp. 6893–6895, oct 1998. [Online]. Available: https://aip.scitation.org/doi/abs/10.1063/1.367938

[132] E. E. Fullerton, J. Jiang, M. Grimsditch, C. Sowers, and S. Bader, "Exchange-spring behavior in epitaxial hard/soft magnetic bilayers," *Physical Review B - Condensed Matter and Materials Physics*, vol. 58, no. 18, pp. 12 193–12 200, nov 1998. [Online]. Available: https://journals.aps.org/prb/abstract/10.1103/PhysRevB.58.12193

[133] T. C. Schulthess and W. H. Butler, "Consequences of Spin-Flop Coupling in Exchange Biased Films," *Physical Review Letters*, vol. 81, no. 20, pp. 4516–4519, nov 1998. [Online]. Available: https://journals.aps.org/prl/abstract/10.1103/PhysRevLett.81.4516

[134] ——, "Coupling mechanisms in exchange biased films (invited)," *Journal of Applied Physics*, vol. 85, no. 8 II B, pp. 5510–5515, apr 1999. [Online]. Available: https://doi.org/10.1063/1.369878

[135] S. Zhang, D. V. Dimitrov, G. C. Hadjipanayis, J. W. Cai, and C. L. Chien, "Coercivity induced by random field at ferromagnetic and antiferromagnetic interfaces," *Journal of Magnetism and Magnetic Materials*, vol. 198, pp. 468–470, jun 1999.

[136] D. Dimitrov and S. Zhang, "Effect of exchange interactions at antiferromagnetic/ferromagnetic interfaces on exchange bias and coercivity," *Physical Review B - Condensed Matter and Materials Physics*, vol. 58, no. 18, pp. 12 090–12 094, nov 1998. [Online]. Available: https://journals.aps.org/prb/abstract/10.1103/PhysRevB.58.12090

[137] J. C. Slonczewski, "Fluctuation mechanism for biquadratic exchange coupling in magnetic multilayers," *Physical Review Letters*, vol. 67, no. 22, pp. 3172–3175, nov 1991. [Online]. Available: https://journals.aps.org/prl/abstract/10.1103/PhysRevLett.67.3172

[138] M. Kiwi, J. Mejía-López, R. D. Portugal, and R. Ramírez, "Exchange-bias systems with compensated interfaces," *Applied Physics Letters*, vol. 75, no. 25, pp. 3995–3997, dec 1999. [Online]. Available: https://doi.org/10.1063/1.12551775,3995

[139] ——, "Positive exchange bias model: Fe/FeF2 and Fe/MnF2 bilayers," *Solid State Communications*, vol. 116, no. 6, pp. 315–319, oct 2000.

[140] M. D. Stiles and R. D. McMichael, "Model for exchange bias in polycrystalline ferromagnet-antiferromagnet bilayers," *Physical Review B - Condensed Matter and Materials Physics*, vol. 59, no. 5, pp. 3722–3733, feb 1999. [Online]. Available: https://journals.aps.org/prb/abstract/10.1103/PhysRevB.59.3722

[141] A. S. Carriço, R. E. Camley, and R. L. Stamps, "Phase diagram of thin antiferromagnetic films in strong magnetic fields," *Physical Review B*, vol. 50, no. 18, pp. 13 453–13 460, nov 1994. [Online]. Available: https://journals.aps.org/prb/abstract/10.1103/PhysRevB.50.13453

[142] R. E. Camley, "Surface spin reorientation in thin Gd films on Fe in an applied magnetic field," *Physical Review B*, vol. 35, no. 7, pp. 3608–3611, mar 1987. [Online]. Available: https://journals.aps.org/prb/abstract/10.1103/PhysRevB.35.3608

[143] R. E. Camley and D. R. Tilley, "Phase transitions in magnetic superlattices," *Physical Review B*, vol. 37, no. 7, pp. 3413–3421, mar 1988. [Online]. Available: https://journals.aps.org/prb/abstract/10.1103/PhysRevB.37.3413

[144] F. Nolting, A. Scholl, J. Stöhr, J. W. Seo, J. Fompeyrine, H. Siegwart, J. P. Locquet, S. Anders, J. Lüning, E. E. Fullerton, M. F. Toney, M. R. Scheinfein, and H. A. Padmore, "Direct observation of the alignment of ferromagnetic spins by antiferromagnetic spins," *Nature*, vol. 405, no. 6788, pp. 767–769, jun 2000. [Online]. Available: https://www.nature.com/articles/35015515

[145] H. Matsuyama, C. Haginoya, and K. Koike, "Microscopic imaging of Fe magnetic domains exchange coupled with those in a NiO(001) surface," *Physical Review Letters*, vol. 85, no. 3, pp. 646–649, jul 2000. [Online]. Available: https://journals.aps.org/prl/abstract/10.1103/PhysRevLett.85.646

[146] U. Nowak, K. D. Usadel, J. Keller, P. Miltényi, B. Beschoten, and G. Güntherodt, "Domain state model for exchange bias. I. Theory," *Physical Review B - Condensed Matter and Materials Physics*, vol. 66, no. 1, pp. 1–9, 2002.

[147] Y. Imry and S. K. Ma, "Random-field instability of the ordered state of continuous symmetry," *Physical Review Letters*, vol. 35, no. 21, pp. 1399–1401, 1975. [Online]. Available: https://ui.adsabs.harvard.edu/abs/1975PhRvL..35.1399I/abstract

[148] S. J. Han, D. P. Belanger, W. Kleemann, and U. Nowak, "Relaxation of the excess magnetization of random-field-induced metastable domains in Fe0.47Zn0.53F2," *Physical Review B*, vol. 45, no. 17, pp. 9728–9735, 1992.

[149] U. Nowak, J. Esser, and K. D. Usadel, "Dynamics of domains in diluted antiferromagnets," *Physica A: Statistical Mechanics and its Applications*, vol. 232, no. 1-2, pp. 40–50, oct 1996.

[150] M. Staats, U. Nowak, and K. D. Usadel, "Non-exponential relaxation in dilute antiferromagnets," *Phase Transitions*, vol. 65, no. 1-4, pp. 159–167, 1998. [Online]. Available: https://www.tandfonline.com/action/journalInformation?journalCode=gpht20

[151] J. Keller, P. Miltényi, B. Beschoten, G. Güntherodt, U. Nowak, and K. D. Usadel, "Domain state model for exchange bias. II. Experiments," *Physical Review B - Condensed Matter and Materials Physics*, vol. 66, no. 1, pp. 1–11, 2002.

[152] P. J. Kelly and R. D. Arnell, "Magnetron sputtering: A review of recent developments and applications," pp. 159–172, mar 2000.

[153] I. Suzuki, Y. Hamasaki, M. Itoh, and T. Taniyama, "Controllable exchange bias in Fe/metamagnetic FeRh bilayers," *Applied Physics Letters*, vol. 105, no. 17, p. 172401, oct 2014. [Online]. Available: https://doi.org/10.1063/1.4900619

[154] S. Maat, J. U. Thiele, and E. E. Fullerton, "Temperature and field hysteresis of the antiferromagnetic-to-ferromagnetic phase transition in epitaxial FeRh films," *Physical Review B - Condensed Matter and Materials Physics*, vol. 72, no. 21, p. 214432, dec 2005. [Online]. Available: https://journals.aps.org/prb/abstract/10.1103/PhysRevB.72.214432

[155] K. Aikoh, S. Kosugi, T. Matsui, and A. Iwase, "Quantitative control of magnetic ordering in FeRh thin films using 30 keV Ga ion irradiation from a focused ion beam system," in *Journal of Applied Physics*, vol. 109, no. 7. American Institute of PhysicsAIP, apr 2011, pp. 7–311. [Online]. Available: https://doi.org/10.1063/1.3549440

[156] A. Tohki, K. Aikoh, A. Iwase, K. Yoneda, S. Kosugi, K. Kume, T. Batchuluun, R. Ishigami, and T. Matsui, "Effect of high temperature annealing on ion-irradiation induced magnetization in FeRh thin films," in *Journal of Applied Physics*, vol. 111, no. 7. American Institute of PhysicsAIP, apr 2012, pp. 7–742. [Online]. Available: https://doi.org/10.1063/1.3687133

[157] J. Nogués, J. Sort, V. Langlais, V. Skumryev, S. Suriñach, J. S. Muñoz, and M. D. Baró, "Exchange bias in nanostructures," pp. 65–117, dec 2005.

[158] A. Migliorini, B. Kuerbanjiang, T. Huminiuc, D. Kepaptsoglou, M. Muñoz, J. L. Cuñado, J. Camarero, C. Aroca, G. Vallejo-Fernández, V. K. Lazarov, and J. L. Prieto, "Spontaneous exchange bias formation driven by a structural phase transition in the antiferromagnetic material," *Nature Materials*, vol. 17, no. 1, pp. 28–34, jan 2018. [Online]. Available: www.nature.com/naturematerials

[159] V. Uhlíř, J. A. Arregi, and E. E. Fullerton, "Colossal magnetic phase transition asymmetry in mesoscale FeRh stripes," *Nature Communications*, vol. 7, no. 1, p. 20018, oct 2016. [Online]. Available: www.nature.com/naturecommunications

[160] X. Marti, I. Fina, C. Frontera, J. Liu, P. Wadley, Q. He, R. J. Paull, J. D. Clarkson, J. Kudrnovský, I. Turek, J. Kuneš, D. Yi, J. H. Chu, C. T. Nelson, L. You, E. Arenholz, S. Salahuddin, J. Fontcuberta, T. Jungwirth, and R. Ramesh, "Room-temperature antiferromagnetic memory resistor," *Nature Materials*, vol. 13, no. 4, pp. 367–374, jan 2014. [Online]. Available: www.nature.com/naturematerials

[161] J. A. Arregi, M. Horký, K. Fabianová, R. Tolley, E. E. Fullerton, and V. Uhlíř, "Magnetization reversal and confinement effects across the metamagnetic phase transition in mesoscale FeRh structures," *Journal of Physics D: Applied Physics*, vol. 51, no. 10, p. 105001, feb 2018. [Online]. Available: https://doi.org/10.1088/1361-6463/aaaa5a

[162] C. Bordel, J. Juraszek, D. W. Cooke, C. Baldasseroni, S. Mankovsky, J. Minár, H. Ebert, S. Moyerman, E. E. Fullerton, and F. Hellman, "Fe spin reorientation across the metamagnetic transition in strained FeRh thin films," *Physical Review Letters*, vol. 109, no. 11, p. 117201, sep 2012. [Online]. Available: https://journals.aps.org/prl/abstract/10.1103/PhysRevLett.109.117201